Manual IndoQCT

Version 22a

IndoQCT

Choirul Anam
Ariij Naufal
Wahyu S Budi
Heri Sutanto
Freddy Haryanto
Geoff Dougherty

IndoQCT

Version 22a

Software for evaluating the quality of computed tomography images

Manual-English

Developed by:

Choirul Anam (Diponegoro University)
Ariij Naufal (Diponegoro University)
Wahyu S. Budi (Diponegoro University)
Heri Sutanto (Diponegoro University)
Freddy Haryanto (Bandung Institute of Technology)
Geoff Dougherty (California State University Channel Islands)

UNDIP PRESS publishing

2023

IndoQCT

Version 22a

CONTACT

Ariij Naufal
Department of Physics,
Faculty of Sciences and Mathematics,
Diponegoro University,
Indonesia
ariij.2019@fisika.fsm.undip.ac.id

ISBN : 978-623-417-106-8

diterbitkan oleh
UNDIP PRESS
publishing

Anggota APPTI
003.151.1.3.2022
Anggota IKAPI 246/Anggota Luar Biasa/JTE/2022

MANUAL BOOK

English

This software evaluates various image quality parameters for the following phantoms:

1. AAPM CT performance phantom
2. ACR CT accreditation phantom
3. Catphan® phantom
4. GE CT QA phantom
5. Canon TOS phantom
6. Siemens CT phantom
7. Philips CT QA phantom
8. Neusoft CT phantom
9. Hitachi CT phantom
10. Computational phantom

DISCLAIMER:

This publication is based on sources and information believed to be reliable, but the authors disclaim any warranty or liability based on or relating to the contents of this publication. IndoQCT is intended for research purposes, not for clinical applications.

PREFACE

Computed tomography (CT) is an excellent tool for modern medical imaging. It is available in almost all hospitals throughout the world. CT produces 3D images with excellent image quality for patient diagnosis purposes. CT imaging is carried out very fast, in just a few minutes.

However, CT uses X-rays, which are ionizing radiation, so its use can cause harm to the human body. In addition, the CT system is very complex so there are the potential errors from each stage that can produce images leading to mis-diagnosis. To minimize this, CT must always be monitored so that it is always performing to standard. This monitoring is done by a complex procedure known as Quality Control or QC.

The QC procedure consists of daily, monthly, and annual tasks. Each procedure is time-consuming. Manual QC can take many hours. Manual measurement of image quality parameters can also lead to a bias due to the subjectivity of examiners. IndoQCT answers these needs by being automatic, fast, objective, and accurate. IndoQCT originated from comprehensive research published in reputable international journals.

Unlike some existing software that can only be used on one type of phantom and with limited parameters, IndoQCT can be used to evaluate CT image quality using various phantoms and numerous parameters. IndoQCT can also measure some image quality metrics directly from the patient's clinical image for easier and more objective dose optimization.

IndoQCT can be utilized by various groups: clinical medical physicists, researchers, lecturers, students, or for those who want to learn about CT. It provides convenience, efficiency, measurement objectivity, universality, and portability. IndoQCT can be downloaded from the website www.indosect.com.

This manual book explains technical use of IndoQCT, starting from the initial explanation about IndoQCT, its features, how to install it, and how to use it. It should be noted that the manual is

a cook book so anyone who wants to understand the details of various parameters can refer to text-books or journals on CT. Because many parameters from many phantoms can be measured using IndoQCT, detailed explanations for all phantoms require hundreds of pages. In this manual book, we only explain the measurement of various parameters from the AAPM CT performance phantom. Meanwhile for other phantoms, we only show examples of the images used and their results.

IndoQCT and its manual book would never have existed without supports and contributions from many colleagues and partners. We would like to explicitly acknowledge supports and funding from the Diponegoro University (UNDIP) for providing research grant. We would like to thank especially Prof. Djarwani (University of Indonesia, UI), Prof. Idam Arif (Bandung Institute of Technology, ITB), Dr. Rena Widita (ITB), Prof. Muhammad Nur (UNDIP), Prof. Toshioh Fujibuchi (Kyushu University), Dr. Eko Hidayanto (UNDIP), Dr. Pandji Triadyaksa (UNDIP), Zaenal Arifin, M.Sc (Undip), Zaenul Muhlisin, M.Sc (UNDIP), Evi Setiawati, M.Sc (UNDIP), Dr. Mohd Hanafi Ali (Qaiwan International University), Dr. Noor Diyana Osman (Universiti Sains Malaysia), clinical medical physicists who have provided axial phantom CT images, all members of Indonesian Association of Physicist in Medicine (AFISMI), all colleagues from many universities, all students who have helped us tirelessly to make IndoQCT happens. It is not possible to mention all those by name who have contributed directly or indirectly to develop IndoQCT.

CONTENTS

Preface iii
Contents v
Recommended System Requirements ix

I. INTRODUCTION 1
1.1. About IndoQCT 1
1.2. Features 2
1.2.1. Main features of IndoQCT 2
1.2.2. Additional features 5
1.2.3. More features 6
1.3. Developers 7
1.4. Publication list 7
1.5. Information 10
II. INSTALLATION OF INDOQCT 11
2.1. Installation process 11
2.2. Uninstall the IndoQCT 16
III. MAIN PARTS OF INDOQCT 17
3.1. Main tabs 18
3.2. Main viewer 20
3.3. Toolbars 21
IV. OVERVIEW ON THE INDOQCT WORKFLOW 26
4.1. Opening the images 26
4.2. Workflow 27
4.3. Standard / Evaluation section 29
4.4. Database and analysis section 31
V. MEASUREMENTS OF IMAGE QUALITY ON AAPM PHANTOM 34
5.1. CT# accuracy 34
5.2. CT# uniformity 35

5.3. CT# homogeneity 36
5.4. CT# histogram 37
5.5. CT# profile 38
5.6. Noise accuracy 38
5.7. Noise uniformity 39
5.8. Noise power spectrum (NPS) 39
5.9. CT number linearity 40
5.10. Visual spatial resolution 41
5.11. Point MTF 42
5.12. Edge MTF 43
5.13. Task Transfer Function (TTF) 44
5.14. Slice thickness 45
5.15. Visual low contrast 46
5.16. CNR 48
5.17. SD-LCD 48
5.18. Alignment 49
5.19. Gantry tilt 50
5.20. Phantom diameter 51
5.21. Distance between slices 53
5.22. Distance accuracy 54
VI. EXAMPLE MEASUREMENTS ON ACR PHANTOM 57
VII. EXAMPLE MEASUREMENTS ON CATPHAN PHANTOM 65
VIII. EXAMPLE MEASUREMENTS ON GE PHANTOM 73
IX. EXAMPLE MEASUREMENTS ON CANON PHANTOM 83
X. EXAMPLE MEASUREMENTS ON SIEMENS PHANTOM 89
XI. EXAMPLE MEASUREMENTS ON PHILIPS PHANTOM 95

XII. EXAMPLE MEASUREMENTS ON NEUSOFT PHANTOM 103
XIII. EXAMPLE MEASUREMENTS ON HITACHI PHANTOM 109
XIV. EXAMPLE MEASUREMENTS ON COMPUTATIONAL PHANTOM 115
XV. EXAMPLE MEASUREMENTS ON ANTHROPOMORPHIC PHANTOM / PATIENT 121

Author Biographies 123

Recommended System Requirements

The system requirements below are recommended based on the software development device specifications. Specifications that differ from the following recommendations may cause some performance and interface differences, but do not affect the calculation results.

Components	Requirements
☐ OS	Windows 10 x64
☐ Processor	1.8 GHz Intel Core i5-8250U
☐ Memory	8 GB
☐ Storage	At least 4 GB
☐ Graphics card	Intel UHD Graphics 620 with 4 GB VRAM
☐ Display mode	1366 x 768 (32 bit, 60 Hz)
☐ Input	Keyboard and mouse

I. INTRODUCTION

1.1. About IndoQCT

The main feature of the IndoQCT software is to evaluate CT image quality. In the CT quality control (QC) procedure, generally qualified examiners or medical staff check the CT image quality parameters manually on a phantom using available tools in the control panel. The QC procedure consists of daily, monthly, and annual tasks. To carry out this procedure requires a lot of time, especially for the daily routine. Moreover, manual measurement of image quality parameters leads to a certain bias due to the subjectivity of examiners.

There are several other available softwares for automatic measurement of CT image quality parameters. However, they are limited to certain phantoms and certain vendors. IndoQCT presents integrated features in the form of automatic measurement of CT image quality parameters on various phantoms available in the market. Therefore, IndoQCT provides convenience in the aspects of efficiency, measurement objectivity, universality, and portability.

Besides being able to measure image quality parameters on the phantom, IndoQCT can also measure some image quality metrics directly from the patient's clinical image. This is useful for easier and more objective dose optimization processes. In addition, IndoQCT is also equipped with several additional features, such as texture analysis, several noise reductions, several window options (including multiple-windows blending in the form of red-green-blue (RGB) images), and image reformatting on sagittal, coronal, oblique, and irregular planes, and several other features. In IndoQCT, all image quality measurement parameters can be directly stored in the database, which can be analyzed.

Reports can also be automatically generated in pdf file from the database.

IndoQCT has been developed since 2018 using the Matlab programming language. In 2021, it was redeveloped using the Python programming language to facilitate easy distribution.

1.2. Features

The summary of IndoQCT features is shown in Figure 1. Basically, the features in IndoQCT are divided into two categories, namely main and additional features.

1.2.1. Main features of IndoQCT

In accordance with IndoQCT's initial vision, the main features presented are the automation of CT image quality measurements on various types of phantoms using a user-friendly Graphical User Interface (GUI). In version 22a, the covered phantoms are as follows:

- AAPM CT performance phantom (model 610, CIRS Inc, VA, USA)
- ACR CT accreditation phantom (Gammex Inc, Middleton, WI, USA)
- Catphan® phantom (Catphan 500, 504, 604, The Phantom Lab, NY, USA)
- GE CT QA phantom (GE Healthcare, Milwaukee, WI, USA)
- Canon TOS phantom (Canon Medical System, CA, USA)
- Siemens CT phantom (Siemens Healthcare, Erlangen, Germany)
- Philips CT QA phantom (Philips Medical System, Cleveland, OH, USA)
- Neusoft CT phantom (Neusoft Medical System, Shenyang, China)

- Hitachi CT phantom (Hitachi Ltd., Tokyo, Japan)

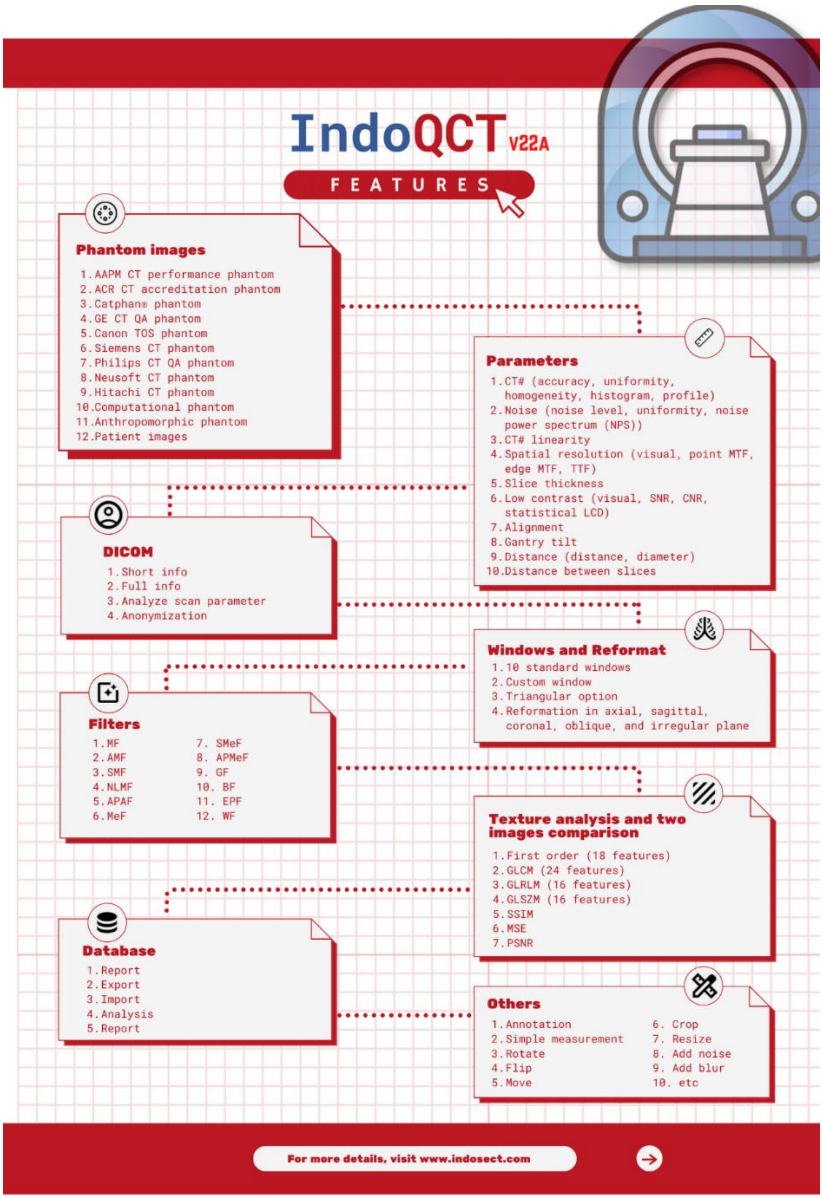

Figure 1. Features of IndoQCT.

In addition to commercial phantoms already on the market and factory default phantoms, IndoQCT can also generate synthetic images using a computational approach. We call this as a computational phantom. This phantom is useful for educational purposes.

The image quality parameters presented in the main features of IndoQCT include parameters that are already known and standardized by many international agencies, as well as those that are still relatively new, as follows:

- **CT number**
    1. CT number accuracy
    2. CT number uniformity
    3. CT number homogeneity
    4. CT number histogram
    5. CT number profile
- **Noise**
    1. Noise accuracy
    2. Noise uniformity
    3. Noise power spectrum (NPS)
- **CT number linearity**
- **Spatial resolution**
    1. Visual resolution
    2. Point modulation transfer function (MTF)
    3. Edge MTF
    4. Task transfer function (TTF)
- **Slice thickness**
- **Low contrast**
    1. Visual observation
    2. Signal-to-noise ratio (SNR)
    3. Contrast-to-noise ratio (CNR)
    4. Statistically-defined low contrast detectability (SD-LCD)

- **Alignment**
- **Gantry tilt**
- **Distance**
    1. Distance accuracy
    2. Diameter accuracy
- **Distance between slices**

In addition to phantom image quality, IndoQCT has included several patient image quality parameters that can be tested, which include the following:

1. Patient CT number
2. Patient noise calculation (see publications no. 5, 8, 10)
3. Patient low contrast
4. Patient alignment (See publication no 14)
5. Patient diameter

1.2.2. Additional features

In addition to the main features, IndoQCT has additional features that are useful for activities other than quality control, which are as follows:

1. Multiple-windows blending in color domain (see Publication no. 6).
2. Images reformation in sagittal and coronal planes, with image interpolation and data slicing to oblique and irregular reconstructions.
3. Generation of computational phantoms with various designs and parameter settings (see Publications no. 8, 11, and 13).
4. Modification of DICOM images for educational and research purposes includes: move, flip, rotate, resize, crop, add noise and blur, DICOM anonymization, and modified DICOM storage.

5. Noise reduction with various options of algorithm (see Publications no. 4, 12, 17, 20, and 23).
6. Image comparison with various parameters, such as mean squared error (MSE), peak signal-to-noise ratio (PSNR), and structural similarity (SSIM).
7. Texture analysis in the first order, gray level co-occurrence matrix (GLCM), gray level run length matrix (GLRLM), and gray level size zone matrix (GLZM).

1.2.3. More features

In order to provide convenience for users and practitioners, IndoQCT includes the following features:

1. Connection to the Picture Archiving and Communication System (PACS), to facilitate users in collecting images directly from the DICOM server.
2. Storage to an integrated local database that is useful for recording all measurements that have been made. This storage has been facilitated with an export tool to save data in Microsoft Excel document format (*.xlxs).
3. Analyze various measurements of image quality. This is useful for viewing measurement trends on a certain parameter according to what the user needs, both chronologically and analytically.
4. Generation of measurement reports in portable document file (PDF) format. This feature can help users to quickly and easily create measurement reports for documentation purposes.
5. Evaluation of image quality measurements based on standards. IndoQCT implements automatic evaluations based on standards set by nuclear regulatory agencies including Bapeten, IAEA, ACR, AAPM, as well as user-customized ones that can be flexibly modified.

6. Sorting datasets with multiple sequence configurations that make it easy for users to sort mixed images in one folder.
7. Image annotation, ROI, and saving to common images to facilitate research publications and education.

1.3. Developers

- Choirul Anam (Diponegoro University)
- Ariij Naufal (Diponegoro University)
- Wahyu S. Budi (Diponegoro University)
- Heri Sutanto (Diponegoro University)
- Freddy Haryanto (Bandung Institute of Technology)
- Geoff Dougherty (California State University Channel Islands)

1.4. Publication list

For those who are interested in understanding more about the scientific aspects of IndoQCT, please refer to the following publications:

1. Anam C, Naufal A, Fujibuchi T, Matsubara K, Dougherty G. Automated development of the contrast-detail curve based on statistical low-contrast detectability in CT images. *J Appl Clin Med Phys*. 2022;23(9):e13719.
2. Anam C, Fujibuchi T, Budi WS, Haryanto F, Dougherty G. An algorithm for automated modulation transfer function measurement using an edge of a PMMA phantom: Impact of field of view on spatial resolution of CT images. *J Appl Clin Med Phys*. 2018;19(6):244-252.
3. Lasiyah N, Anam C, Hidayanto E, Dougherty G. Automated procedure for slice thickness verification of computed tomography images: Variations of slice thickness, position from iso-center, and reconstruction filter. *J Appl Clin Med Phys*. 2021;22(7):313-321.

4. Anam C, Naufal A, Sutanto H, Adi K, Dougherty G. Impact of iterative bilateral filtering on the noise power spectrum of computed tomography images. *Algorithms*. 2022;15(10):374.
5. Anam C, Budi WS, Adi K, Sutanto H, Haryanto F, Ali MH, Fujibuchi T, Dougherty G. Assessment of patient dose and noise level of clinical CT images: automated measurements. *J Radiol Prot*. 2019;39:783–793.
6. Anam C, Budi WS, Haryanto F, Fujibuchi T, Dougherty G. A novel multiple-windows blending of CT images in red-green-blue (RGB) color space: Phantoms study. *Scientific Visualization*. 2019;11(5):56-69.
7. Anam C, Fujibuchi T, Haryanto F, Budi WS, Sutanto H, Adi K, Muhlisin Z, Dougherty G. Automated MTF measurement in CT images with a simple wire phantom. *Pol J Med Phys Eng.* 2019;25(3):179-187.
8. Anam C, Sutanto H, Adi K, Budi WS, Muhlisin Z, Haryanto F, Matsubara K, Fujibuchi T, Dougherty G. Development of a computational phantom for validation of automated noise measurement in CT images. *Biomed Phys Eng Express*. 2020;6(6):065001.
9. Anam C, Amilia R, Naufal A, Budi WS, Maya AT, Dougherty G. Automated measurement of CT number linearity using an ACR accreditation phantom. *Biomed Phys Eng Express*. 2023;9(1):017002
10. Anam C, Arif I, Haryanto F, Lestari FP, Widita R, Budi WS, Sutanto H, Adi K, Fujibuchi T, Dougherty G. An improved method of automated noise measurement system in CT images. *J Biomed Phys Eng*. 2021;11(2):163-174.
11. Anam C, Triadyaksa P, Naufal A, Arifin Z, Muhlisin Z, Setiawati E, Budi WS. Impact of ROI size on the accuracy of

noise measurement in CT on computational and ACR phantoms. *J Biomed Phys Eng*. 2022;12(4):359-368.
12. Anam C, Adi K, Sutanto H, Arifin Z, Budi WS, Fujibuchi T, Dougherty G. Noise reduction in CT images using a selective mean filter. *J Biomed Phys Eng*. 2020;10(5):623-634.
13. Anam C, Naufal A, Sutanto H, Dougherty G. Computational phantoms for investigating impact of noise magnitude on modulation transfer function. *Indonesian J Elec Eng Comp Sci*. 2022;27(3):1428-1437.
14. Anam C, Amilia R, Naufal A, Adi K, Sutanto H, Budi WS, Arifin Z, Dougherty G. Automated patient centering of computed tomography images and its implementation to evaluate clinical practices in three hospitals in Indonesia. *Pol J Med Phys Eng*. 2022;28(4):207-2014.
15. Noviliawati R, Anam C, Sutanto H, Dougherty G, Mak'ruf MR. Automatic validation of the gantry tilt in a computed tomography scanner using a head polymethyl methacrylate phantom. *Pol J Med Phys Eng*. 2021;27(1):57-62.
16. Ximenes AD, Anam C, Hidayanto E, Naufal A, Rukmana DA, Dougherty G. Automation of slice thickness measurements in computed tomography images of AAPM CT performance phantom using a non-rotational method. *Pol J Med Phys Eng*. 2022;28(3):133-138.
17. Zahro UM, Anam C, Budi WS, Triadyaksa P, Saragih JH, Rukmana DA. Investigation of noise level and spatial resolution of CT images filtered with a selective mean filter and its comparison to an adaptive statistical iterative reconstruction. *Iran J Med Phys*. 2021;18(5):376-383.
18. Sofiyatun S, Anam C, Zahro UM, Rukmana DA, Dougherty G. An automated measurement of image slice thickness of computed tomography. *Atom Indonesia*. 2021;47(2):121-128.

19. Widyanti ER, Anam C, Hidayanto E, Naufal A, Haekal M. An evaluation of automated measurement of slice sensitivity profile of computed tomography image: Field of view variations. *Indonesian J Elec Eng Comp Sci*. 2022;29(3):1430-1437.
20. Saragih JH, Anam C, Budi WS, Simarmata TI, Dougherty G. Implementation of a selective mean filter algorithm to reduce noise in computed radiography images. *AIP Conf Proc*. 2021;2346(1):040006.
21. Ainurrofik N, Anam C, Sutanto H, Dougherty G. An automation of radial modulation transfer function (MTF) measurement on a head polymethyl methacrylate (PMMA) phantom. *AIP Conf Proc*. 2021;2346(1):040009.
22. Hak EZ, Anam C, Budi WS, Dougherty G. An improvement in automatic MTF measurement in CT images using an edge of the PMMA phantom. *J Phys: Conf Ser*. 2020;1505(1):012039.
23. Mukmin A, Anam C, Widodo CE, Naufal A, Arisyi FR. Implementation of a Selective Median Filter in Computed Tomography for Image Quality Enhancement. *Int J Sci Res Sci Tech*. 2022;9(4):545-551.
24. Setiawati E, Anam C, Widyasari W, Dougherty G. The quantitative effect of noise and object diameter on low-contrast detectability of AAPM CT performance phantom images. *Atom Indonesia*. 2022. Accepted.

1.5. Information

For further information about IndoQCT, please contact email: ariij.2019@fisika.fsm.undip.ac.id or anam@fisika.fsm.undip.ac.id

II. INSTALLATION OF INDOQCT

2.1. Installation process

Before installing IndoQCT, please make sure you have the IndoQCT installation file on your computer. To get the ID and key needed to access its features, you can contact the email listed in the information section (Chapter I). Make sure the installation file is the original officially released file. The file is around 260 MB in size. Figure 1 shows the installation files on the Windows operating system.

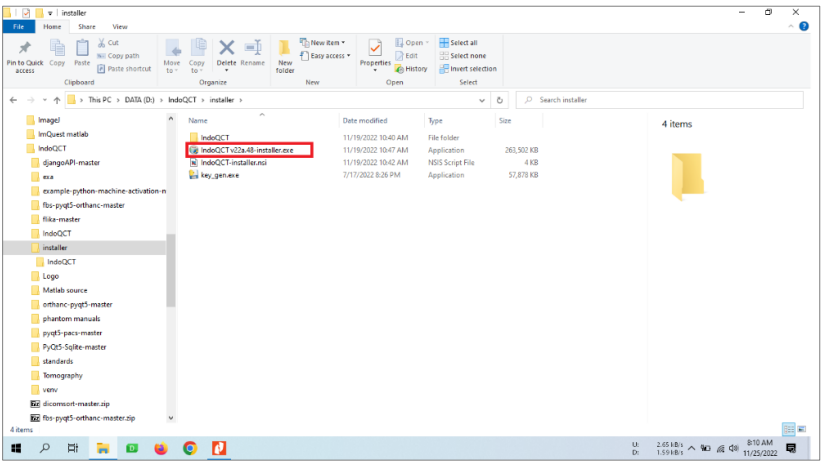

Figure 1. IndoQCT file installation.

To install, please double click the installation file until a user admin control warning appears as shown in Figure 2. Click Yes to approve the installation.

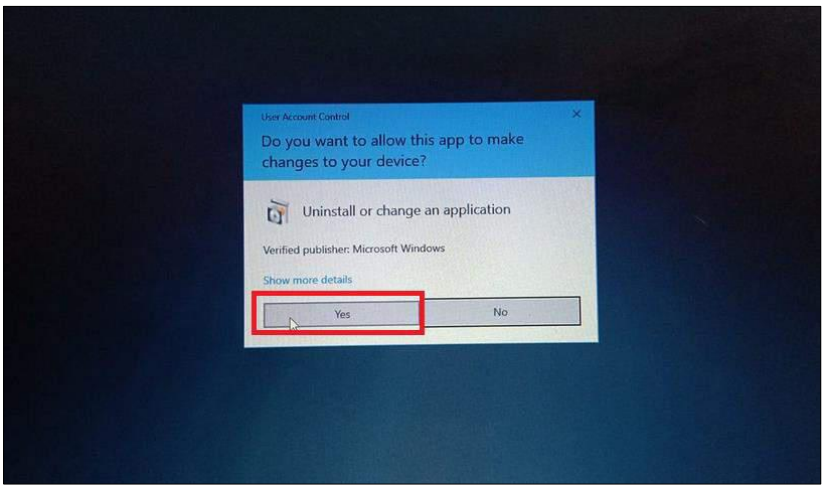

Figure 2. User admin control when opening the installation file.

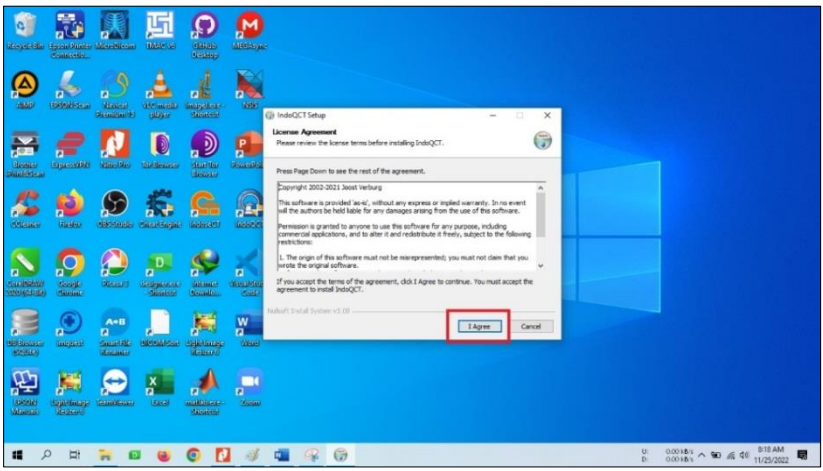

Figure 3. Click “I agree” to continue the installation.

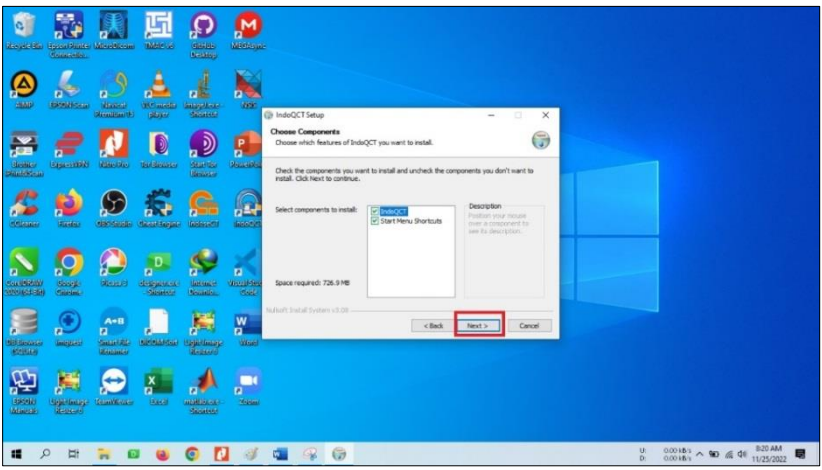

Figure 4. Click “Next” to continue the installation.

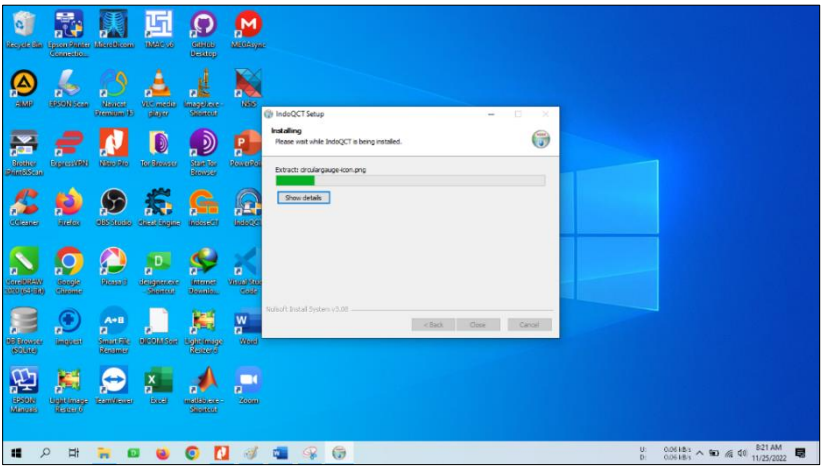

Figure 5. Installation is in progress.

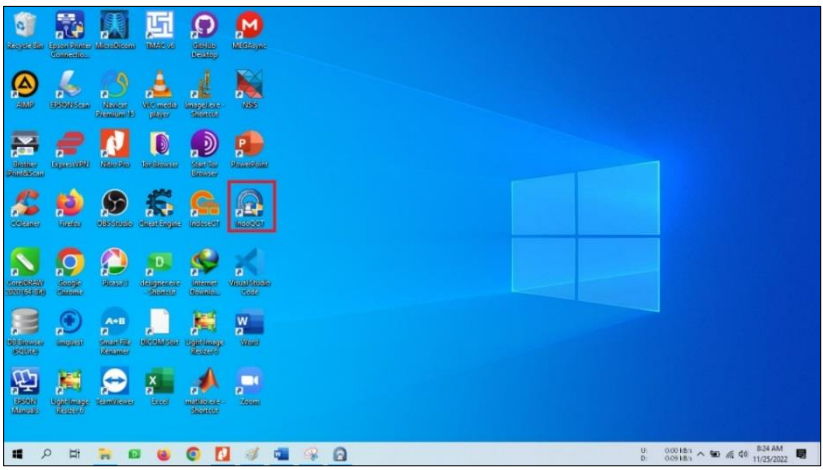

Figure 6. IndoQCT shortcut on the desktop.

After installation, open IndoQCT via the shortcut on the desktop. The user will be asked to enter the “ID” and “key” during the activation process. Figure 7 shows the ID and key filling.

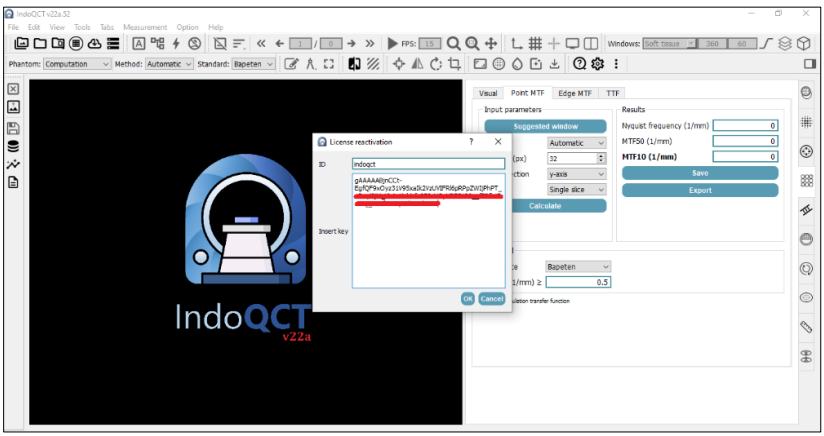

Figure 7. IndoQCT activation process.

Copy and paste the installation “ID” and “key” in the form provided. If the “ID” and “key” are valid, an active period will appear, as shown in Figure 8.

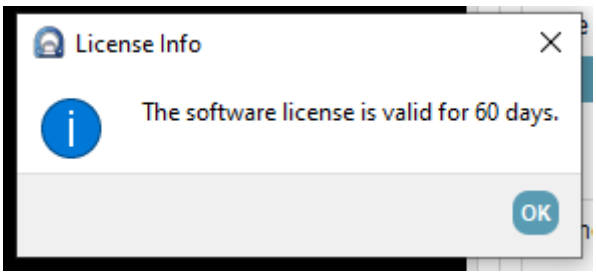

Figure 8. Active period after activating IndoQCT.

After activation, IndoQCT is ready to use. Figure 9 shows the initial view of IndoQCT.

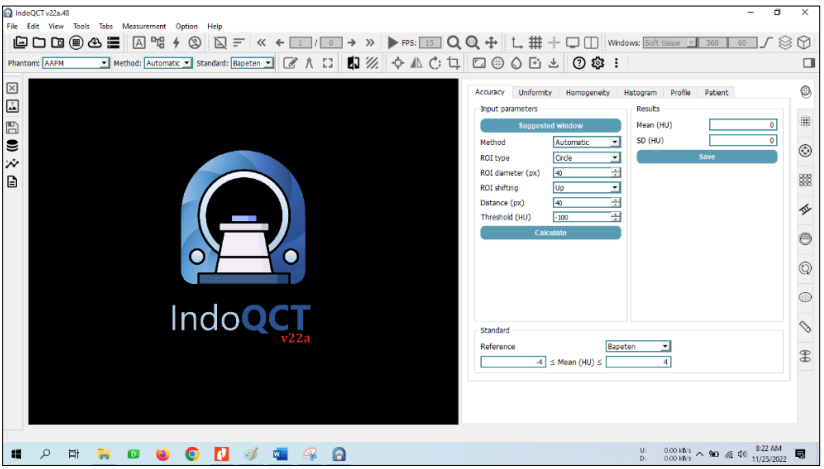

Figure 9. After installation, double click the shortcut on the Desktop to open the initial GUI.

2.2. Uninstall the IndoQCT

To uninstall IndoQCT, you can access the uninstall icon on the Start Menu, as shown in Figure 10.

Figure 10. Shortcut to uninstall IndoQCT.

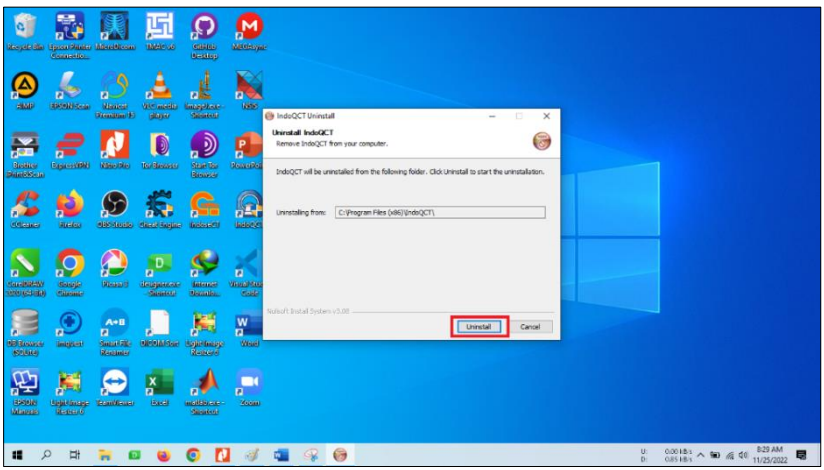

Figure 11. Uninstall dialog on IndoQCT. Click Install to continue.

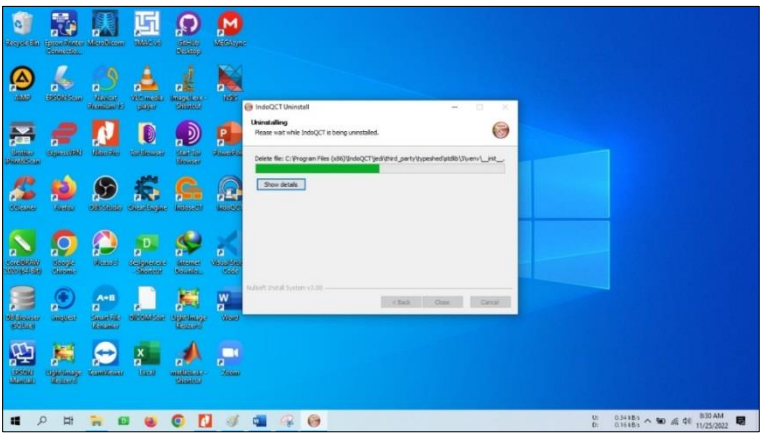

Figure 12. The uninstall process is running.

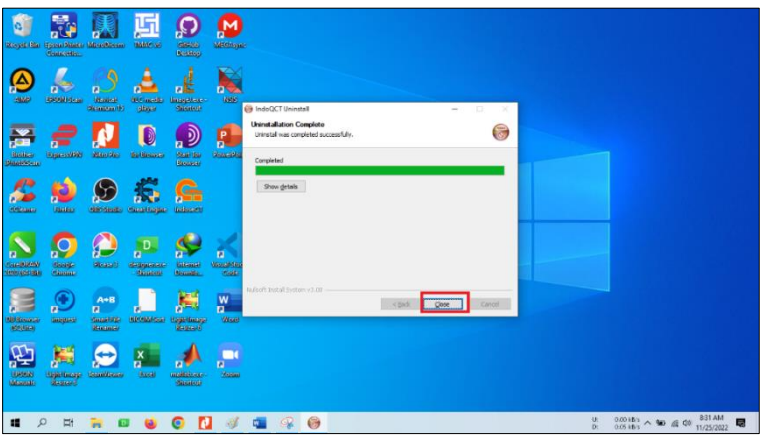

Figure 13. Uninstall notification has been completed.

III. MAIN PARTS OF INDOQCT

In the previous section, we discussed how to install IndoQCT. In this section, some of the main parts of IndoQCT will be explained. The initial appearance of IndoQCT can be seen in Figure 9. It can be seen that there are several main sections with different functions.

3.1. Main tabs

The first part of IndoQCT is the tab section which contains the main features for evaluating the quality of CT images (Figure 14). This section consists of 11 main tabs, namely (from top to bottom): CT#, Noise, CT# linearity, Spatial resolution, Slice thickness, Low contrast, Alignment, Gantry tilt, Distance, and Distance between slices. Tabs can consist of several sub tabs, which contain interfaces for various purposes.

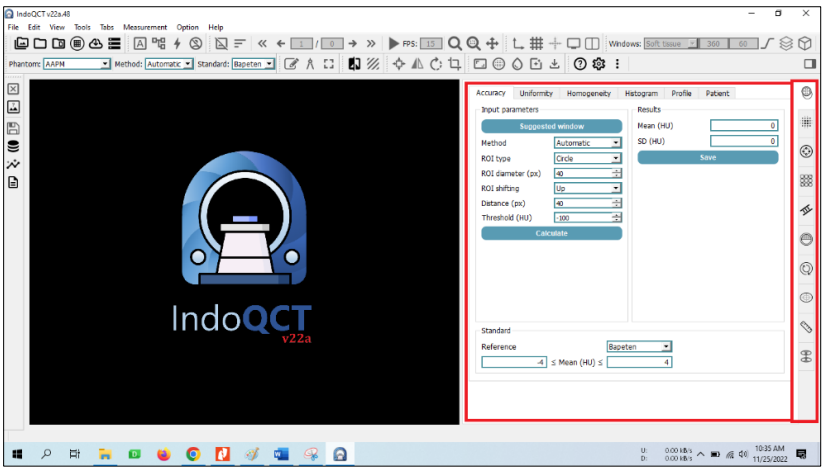

Figure 14. Main tabs on IndoQCT.

The CT# tab is a section for calculating CT# related parameters, including accuracy, uniformity, homogeneity, histogram, profile, and patient CT#.

The Noise tab is a section for calculating noise in the image. These include accuracy noise, uniformity, NPS, and patient noise.

The CT# linearity tab is specifically intended to measure CT# linearity on various types of phantoms. In this tab, there are several methods for testing CT# linearity, along with the manual method.

The Spatial resolution tab includes several ways to describe spatial resolution, namely through visual observation, Point MTF, Edge MTF, and TTF.

The Slice thickness tab is useful for evaluating slice thickness in images, either by measuring the geometry of objects manually or automatically. Several methods are provided and adapted to the phantom design.

The Low contrast tab is a section for evaluating low contrast detectability in CT images. This includes visual observation, CNR calculations, statistically-defined low contrast detectability (SD-LCD) calculations, and patient low contrast measurements.

The Alignment tab is a section for evaluating the accuracy of laser alignment. This can be done manually or automatically, both in phantom and patient images.

The Gantry tilt tab simply evaluates the gantry tilt of a phantom image.

The Distance tab evaluates the parameters related to the distance in the image. This includes the defined distance, the phantom diameter, as well as the patient diameter.

The Distance between slices tab evaluates a relatively new parameter, namely the distance that exists between two slices with different locations.

Detailed discussion of each tab will be discussed in the next chapter.

3.2. Main viewer

The second part of IndoQCT is the main viewer, which displays DICOM images (Figure 15). This screen can be zoomed, full screen, grid, axes, display DICOM info, and several other interactive functions.

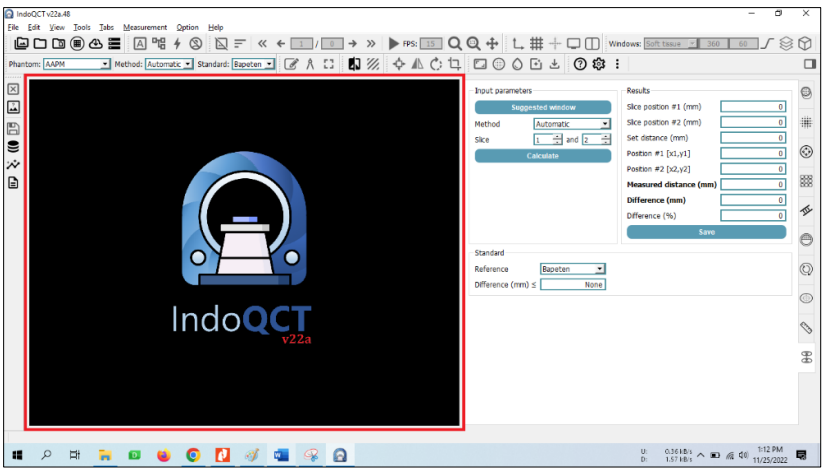

Figure 15. Main viewer from IndoQCT.

3.3. Toolbars

Another part of IndoQCT are the toolbars with various uses. Figure 16 displays the toolbar area of IndoQCT. Most toolbars are active when an image is open.

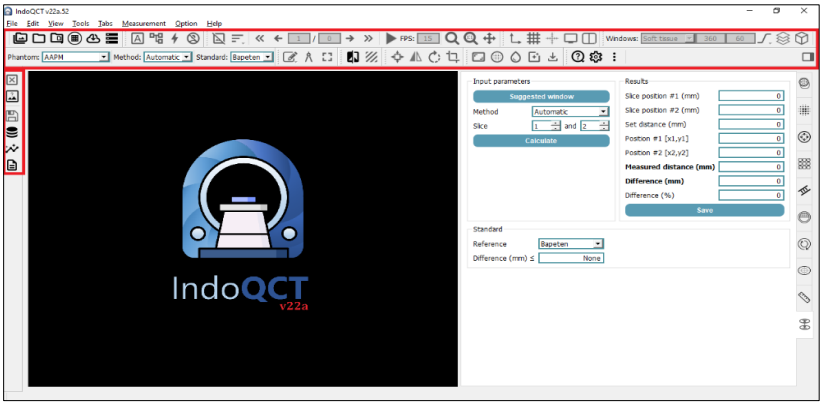

Figure 16. The toolbar area in IndoQCT.

From the most left on the Images toolbar, namely:

Open file ➔ for opening DICOM files,

Open folder ➔ for opening directory contains DICOM files,

Open sample ➔ for opening sample images,

Create computational phantom ➔ for generating computational phantom,

Connect to PACS ➔ to connect to PACS, if any,

Open storage ➔ to open DICOM storage once there are downloaded ones from PACS.

On the DICOM control toolbar, namely:

Short info ➔ used for displaying short info from the opened image,

DICOM info ➔ used for displaying all DICOM info/headers,

Analyze scan parameter ➔ to analyze the tube current and voltage in the dataset,

Anonymize DICOM ➔ used for anonymizing DICOM files.

On the Image control toolbar, namely:

Close image ➔ to close the opened dataset,

Sort image ➔ to sort the images according to slice location, acquisition time, series number, etc,

Previous series ➔ to go to the previous series, if multiple series are detected,

Previous slice ➔ to go to the previous slice,

Current slice / total slice ➔ shows the open slice positions and the total slices in the opened dataset,

Next slice ➔ to go to next slice,

Next series, to go to the next series, if multiple series are detected,

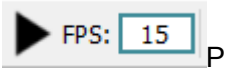

Play/pause ➔ to run movie mode with adjustable frames-per-second (FPS),

Zoom, View 1:1, Pan mode ➔ to adjust the scale of the image displayed in the main viewer.

Next on the View toolbar, namely:

Axis ➔ to display the axis in the main viewer,

Grid ➔ to display the grid in the main viewer with adjustable scale,

Central axis ➔ to display the central axis in the main viewer with adjustable ticks,

Fullscreen ➔ change the main viewer to full screen,

Splitscreen ➔ change the layout of the main viewer into a split screen with various split modes.

On the Windows toolbar, namely:

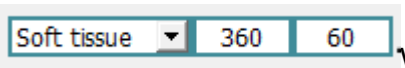

Window type, width, level ➔ contains windowing settings,

Window option ➔ windowing options with linear or triangular,

Multi windows ➔ to open the multiple windows blending feature with 3 types of windows at once,

Reformatting ➔ to open reformatting features in axial, sagittal, coronal, oblique, and irregular planes.

On the Measurement toolbar, there are several combo boxes, namely: 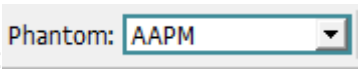

Phantom combo box ➔ to set the phantom type to be used in accordance with opened image,

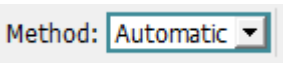

Method combo box ➔ to select the measurement method (Automatic or Manual) for all parameters,

Standard combo box ➔ to set the standard reference on image quality evaluation.

On the Annotation toolbar, namely:

Annotate ➔ to place various annotations to images opened in the main viewer,

ROIs, Show ROI summary ➔ to perform simple measurements using several types of ROI and display the results.

On the Tools toolbar, namely:

Compare images ➔ to compare 2 images in terms of SSIM, MSE, and PSNR,

Texture analysis ➔ to analyze image texture on First Order, GLCM, GLRLM, and GLSZM parameters.

On the Image manipulation toolbar, namely:

Move ➔ to shift the image in a certain direction and distance,

Flip ➔ to flip the image in a certain axis,

Rotate ➔ to rotate the image in a certain direction and angle,

Crop ➔ to crop the image.

On the Image enhancement toolbar, namely:

Resize ➔ to resize the image with multiple interpolation options,

Add noise ➔ to add noise to the image with a certain level,

Add blur ➔ to add a level of blurriness to the image,

Filter ➔ to open the filter feature with various algorithms and parameters,

Save image ➔ to save images that have been modified (in DICOM format) or annotated (in common image format).

On the More toolbar, that is:

Help ➔ to open the user guide and display the list of main features.

Settings ➔ contains configuration of IndoQCT,

More ➔ not implemented yet,

Collapse tabs ➔ to hide the main tabs.

On the Data toolbar, namely:

Close all figures ➔ to close all displayed figures,

Show example ➔ to display examples of image quality measurements according to the selected parameter and phantom,

Save records ➔ to save all the measurement results of image quality parameters,

Open records ➔ to open measurement results storage,

Analyze ➔ to analyze results with various configuration,

Create report ➔ to create a report on the results of image quality measurements.

IV. OVERVIEW ON THE INDOQCT WORKFLOW

4.1. Opening the images

The initial step for using IndoQCT is to open the CT image in DICOM format. There are several ways to open a DICOM image, one of them is by opening it via the Open file button located on the Images toolbar, as shown in Figure 17.

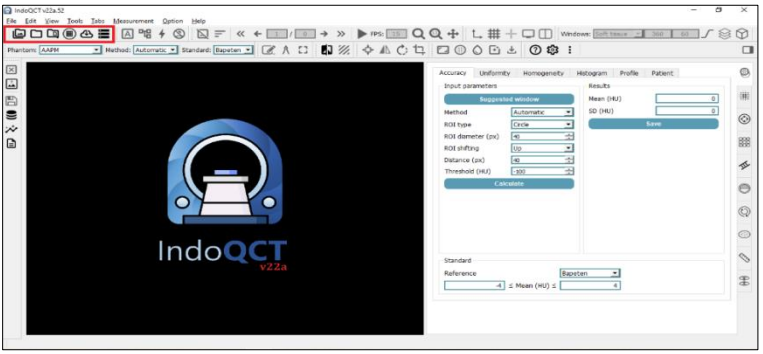

Figure 17. Toolbar Images.

Figure 18 displays the GUI on Open file. After the dialog for opening the file appears, DICOM files can be searched and selected either single or multiple.

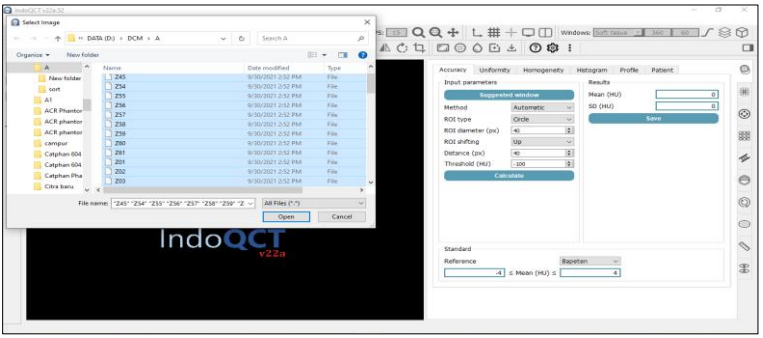

Figure 18. Open DICOM files.

Once the files are opened, the images are read and displayed in the main viewer, as shown in Figure 19. The number of opened slices is automatically updated in the image control. This slice control is used to shift the slice of the opened dataset, be it the next or the previous slice. The shortcut to activate the next slice command is the Up key, while the previous slice is the Down key. Jumping 5 slices to the next can be done by pressing the Right key, while the previous 5 slices with the Left key. In addition to slice control, there is also a series control. This series control will be active if multiple series are detected in the opened dataset.

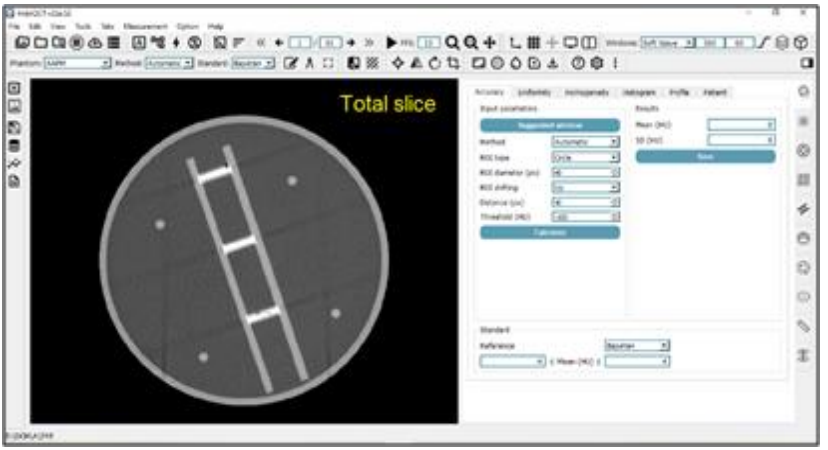

Figure 19. Phantom image opened with total slice displayed.

4.2. Workflow

In this section, we will explain the IndoQCT workflow in a simple way. The key to understanding IndoQCT's workflow in terms of QC procedures for phantom images is to always pay attention to the phantom option and parameter tab. Because each phantom has a unique design, the image quality parameters that

can be tested are also different. On parameters that cannot be tested from a given phantom, the tab will be deactivated automatically. Figure 20 shows the phantom options on one of the active parameter tabs. Meanwhile, Figure 21 shows the parameters that are not active.

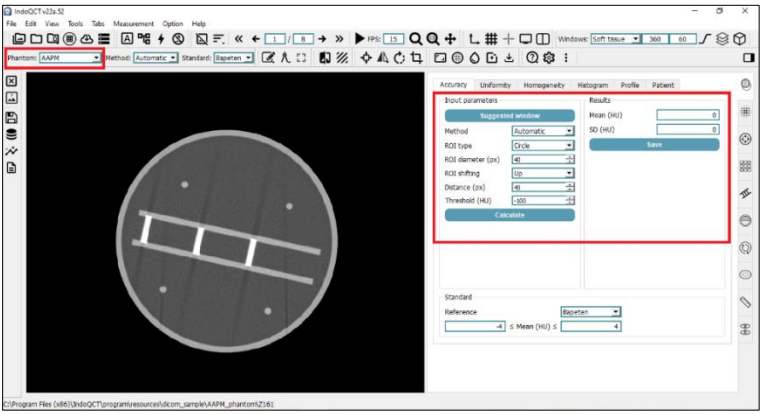

Figure 20. Options in the AAPM phantom with the CT# accuracy parameter active.

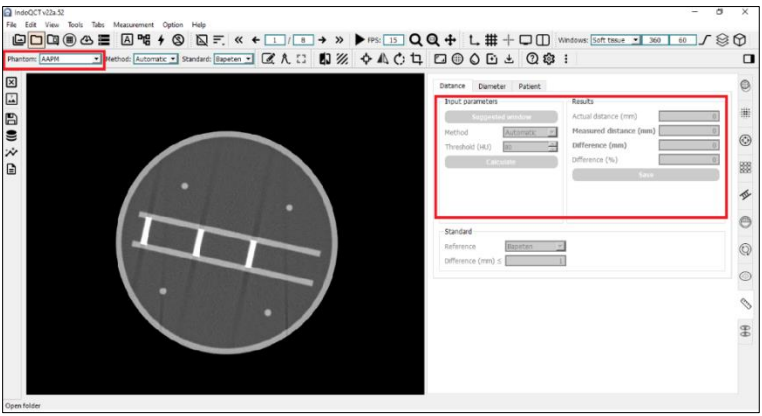

Figure 21. AAPM phantom options with the distance accuracy tab deactivated.

On the tab whose interface is active, the measurement on that tab can be performed for the selected phantom. If you press the Show example button on the toolbar, it will display an example, as shown in Figure 22.

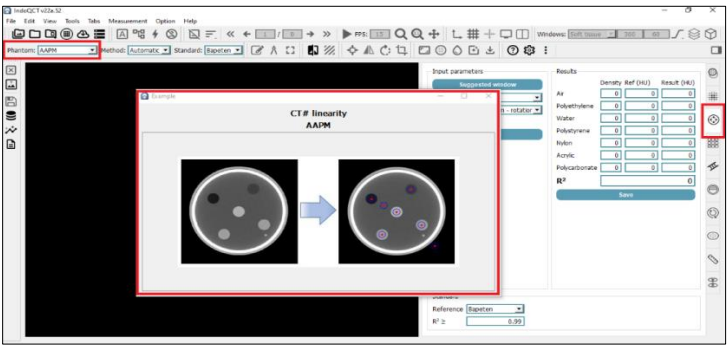

Figure 22. An example of CT# linearity measurement on an AAPM phantom.

4.3. Standard / Evaluation section

On each parameter tab, a section has been provided for evaluating the results, namely the Standard groups. Figure 23 shows one of the standard sections on IndoQCT.

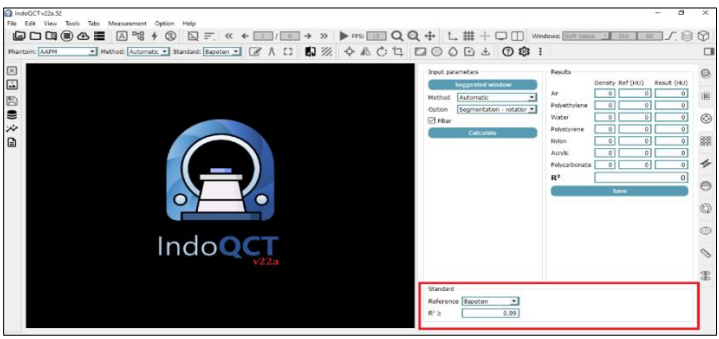

Figure 24. The Standard section on the CT# linearity tab.

After the user performs a measurement, the Standard section will evaluate the results against certain reference standardization bodies according to what has been set. Figure 25 shows an example of the evaluation results forCT# linearity measurements on the AAPM phantom. It can be seen that if the measurement results match the criteria, then the evaluation will state **Passed**. Conversely, if the measurement results do not match the criteria, then the evaluation will state **Not passed**. The results of this evaluation state whether the results of measuring the image quality parameters meet the criteria set by the selected standardization agency. Note this function will only be active if there is a value that is used as a criterion (not "None").

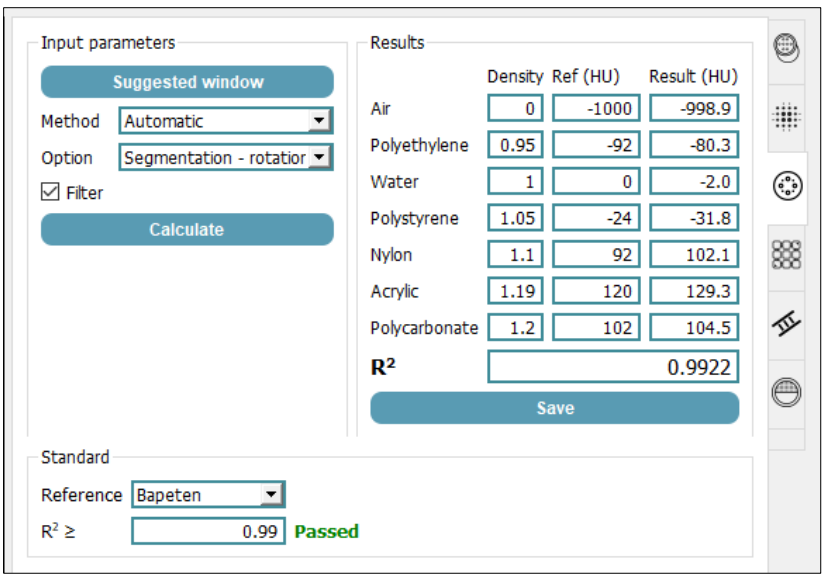

Figure 25. Example of evaluating the results of CT# linearity measurements represented by R^2.

4.4. Database and analysis section

In this section, a brief description of the storage features of measurement results and their analysis will be explained. In the complete workflow, the user will open an image dataset that will be evaluated for quality. Then the user will choose the type of phantom that matches the image, and carry out measurements on the available parameters. After all parameters are measured, the next step is to save the measurement results, either individually by pressing the Save button on each parameter tab, or collectively by pressing the Save records button on the toolbar (Figure 26).

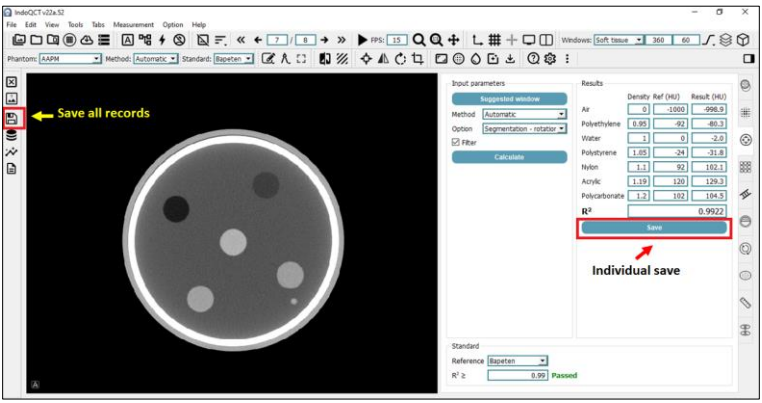

Figure 26. Save buttons on IndoQCT.

After the results are saved, the records can be viewed by pressing the Open records button. This will display a window with a collection of measurement results with tools to analyze them. The Analyze and Create report buttons also display the same window, with an additional panel on the right. Figure 27 displays the Records and Analyze window.

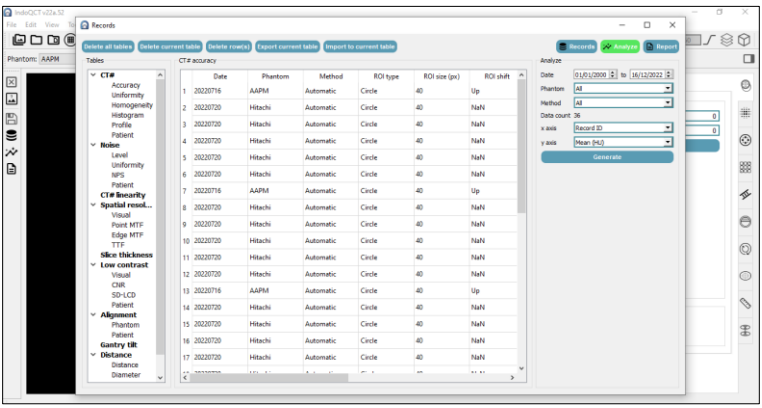

Figure 27. The Records window with the Analyze panel on the right.

Data analysis can be arranged in such a way according to the filter applied. For example, the results of the CT# accuracy measurement on the Hitachi phantom will be analyzed based on the Record ID. Thus, the phantom option in Analysis must be set to “Hitachi”. By pressing the Generate button, a figure containing CT# accuracy analysis with standard lines will appear (Figure 28).

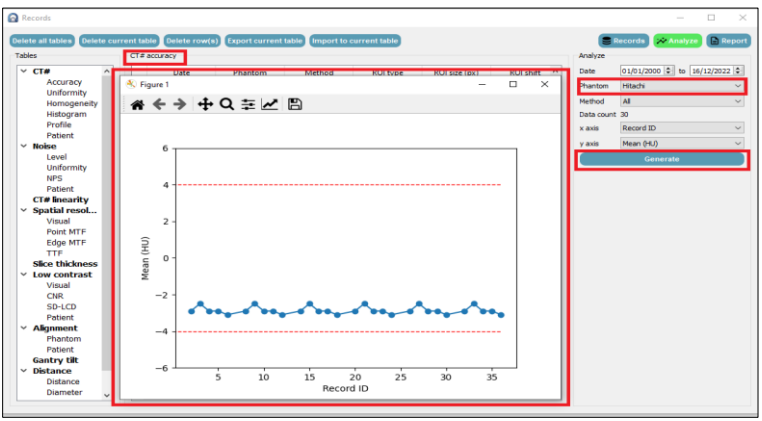

Figure 28. CT# accuracy analysis on Hitachi phantom.

The user can generate measurement results reports in PDF format. This feature can be accessed on the Create report button. For example, we want to generate a report on CT# accuracy for the first 3 entries. We can check the entries in the table, then press the "Generate" button (Figure 29). After saving, the PDF file can be accessed and printed for signature (Figure 30). Data regarding the title, operator, institution, and time for making the report can be changed as needed.

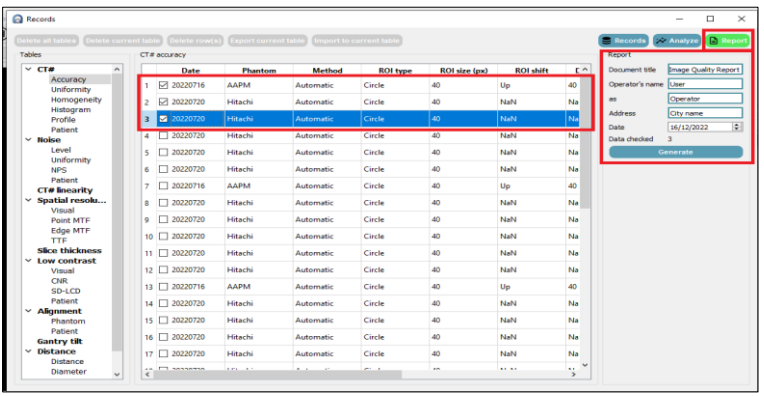

Figure 29. Generating a CT# accuracy report for the first 3 entries.

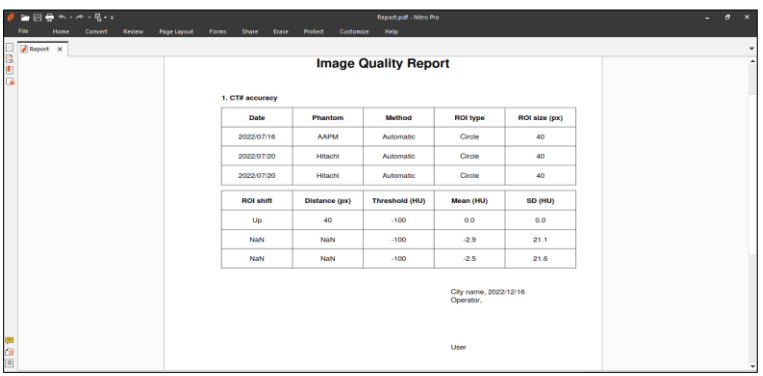

Figure 30. Report in PDF format.

V. MEASUREMENTS OF IMAGE QUALITY ON AAPM PHANTOM

5.1. CT# accuracy

CT# accuracy on the AAPM phantom is obtained from module 610-01-05 which contains homogeneous water with an object in the middle. Figure 31 shows the interface for CT# accuracy.

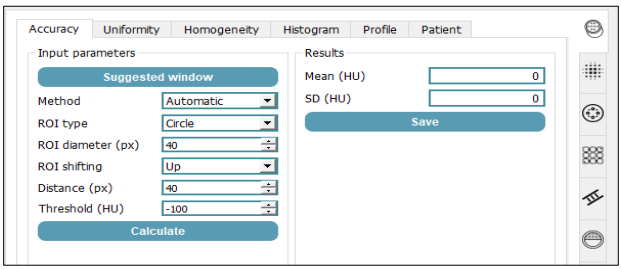

Figure 31. Interface for CT# accuracy.

By using the automatic method, circular ROI, 40 px in diameter, 40 px ROI shifting, and 100 HU threshold, will place a ROI in a homogeneous area as shown in Figure 32. ROI shifting is applied due to a non-homogeneous object in the middle of the phantom.

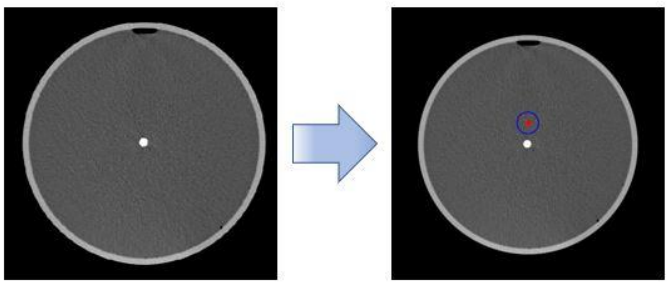

Figure 32. Automatic placement of a ROI in CT# accuracy.

5.2. CT# uniformity

CT# uniformity in the AAPM phantom is obtained from the water homogeneous module, by placing 5 ROIs at the central location, 12, 3, 9, and 6 o'clock. The interface for the automatic method can be seen in Figure 33. The distance from the edge determines how far the placement of the ROI is from the edge phantom. This process will produce 5 ROIs as shown in Figure 34. CT# uniformity is calculated based on the maximum difference of the ROIs on the edges to the central ROI.

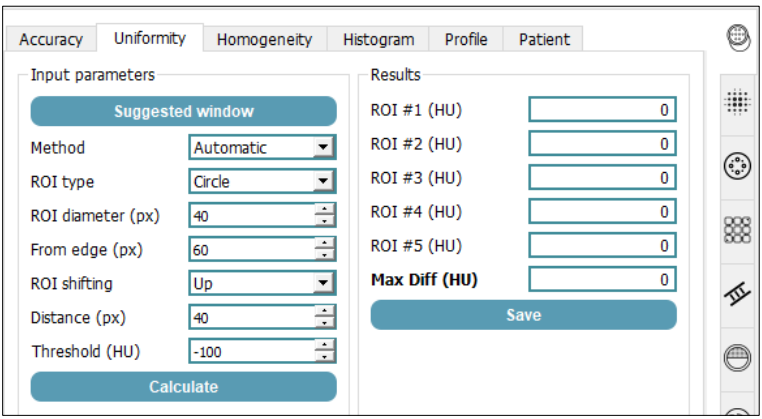

Figure 33. Interface for CT# uniformity for AAPM phantom.

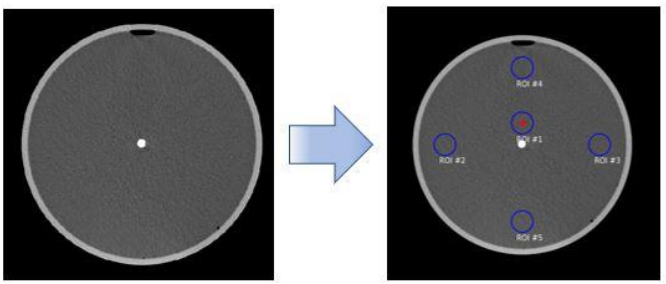

Figure 34. 5 ROIs placed to measure CT# uniformity on AAPM phantom.

5.3. CT# homogeneity

CT# homogeneity on the AAPM phantom was obtained from the homogeneous water module. This parameter is provided only by automatic methods. Figure 35 displays the interface for CT# homogeneity. In general, square-shaped ROIs are placed over all homogeneous region within a radius of 85% of the phantom radius. Especially for the AAPM phantom, the exception is the non-homogeneous object in the middle, as shown in Figure 36. Homogeneity is calculated by finding the difference between the maximum and minimum mean CT#.

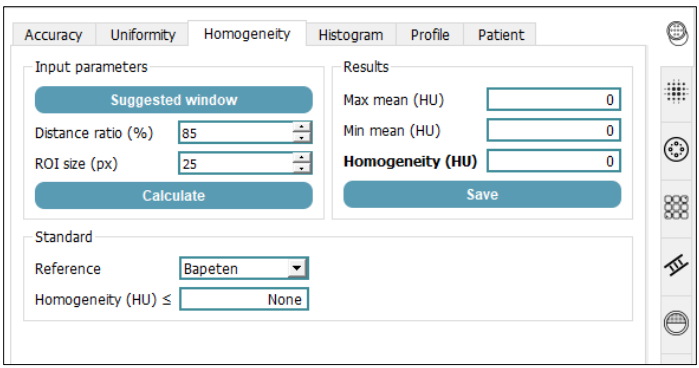

Figure 35. Interface on CT# homogeneity for the AAPM phantom.

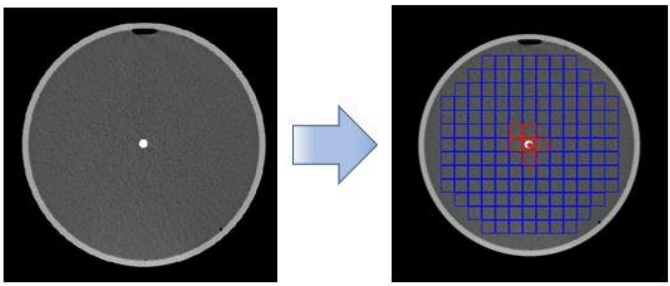

Figure 36. CT# homogeneity and its ROI placement on the AAPM phantom.

5.4. CT# histogram

The CT# histogram is obtained by placing a single ROI on a homogeneous area. Therefore, in the AAPM phantom, non-homogeneous objects in the middle are avoided. The interface for the CT# histogram can be seen in Figure 37. After pressing the Calculate button, the square-shaped ROI will be placed according to the settings and displays the histogram of CT#, as shown in Figure 38.

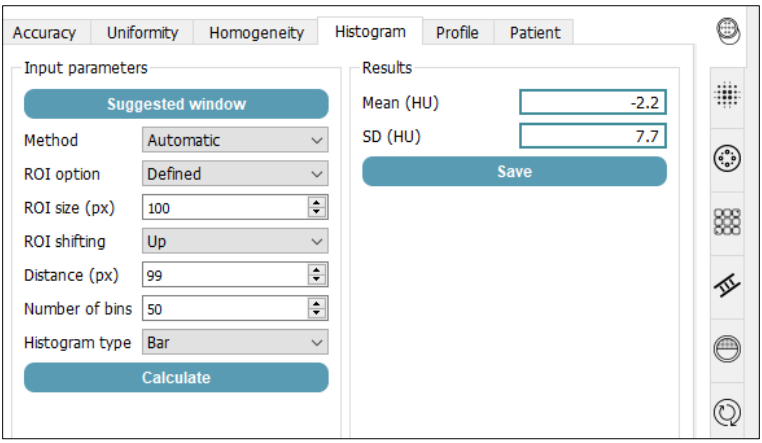

Figure 37. Interface on the CT# histogram for the AAPM phantom.

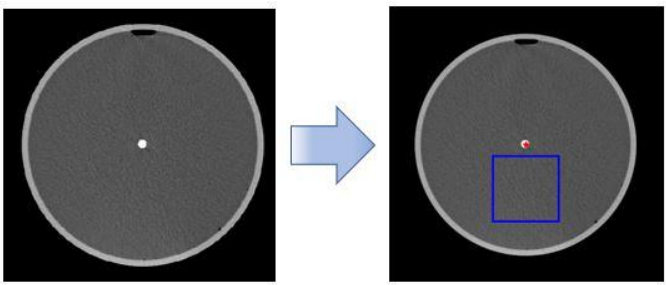

Figure 38. Placement of ROI on the CT# histogram for the AAPM phantom.

5.5. CT# profile

The CT# profile on the AAPM phantom is obtained by placing the ROI in a homogeneous area of the image. The interface for this process is shown in Figure 39, and the results of its ROI placement are shown in Figure 40.

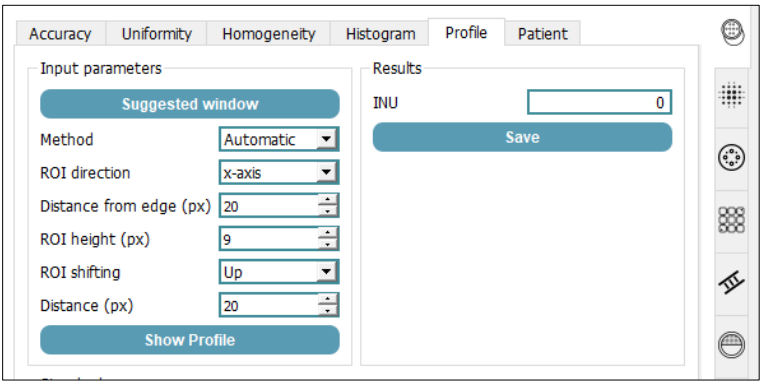

Figure 39. Interface for CT# profile for the AAPM phantom.

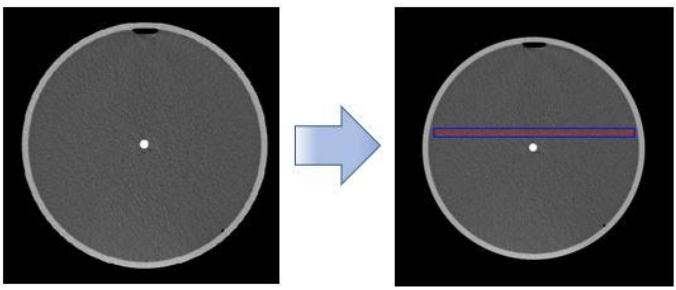

Figure 40. CT# profile forthe AAPM phantom.

5.6. Noise accuracy

Noise accuracy on the AAPM phantom is obtained by placing a single ROI in a homogeneous area. Figure 41 displays the results of automatically placing ROI to obtain noise accuracy.

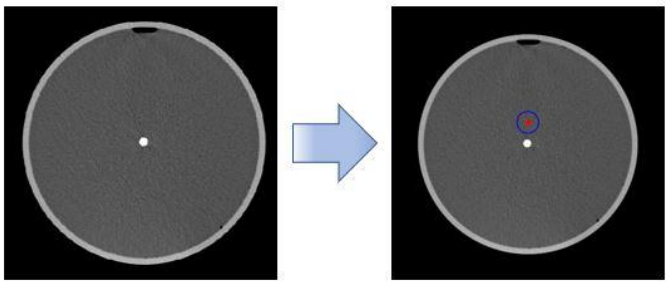

Figure 41. Noise accuracy for the AAPM phantom.

5.7. Noise uniformity

Noise uniformity for the AAPM phantom is obtained by placing 5 ROIs at the central location, at 12, 3, 9, and 6 o'clock. Figure 42 shows the locations of the five ROIs.

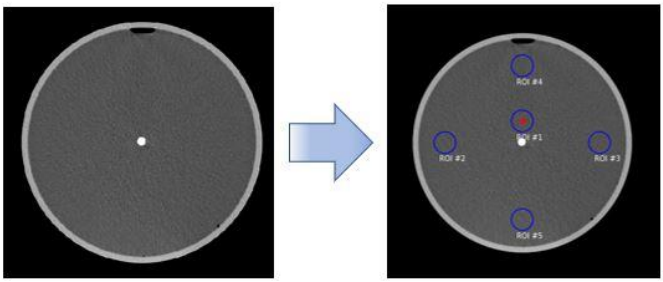

Figure 42. Noise uniformity in the AAPM phantom.

5.8. Noise power spectrum (NPS)

The NPS on the AAPM phantom is obtained by placing the desired amount of square-shaped ROIs in a homogeneous area. Figure 43 displays the interface for obtaining NPS. Figure 44 displays the placement of ROIs on NPS. The sampling angle sets the sampling interval on the radial profile to get 1D NPS. In

addition, the multiple slice option is also provided to get NPS on multiple slices at once.

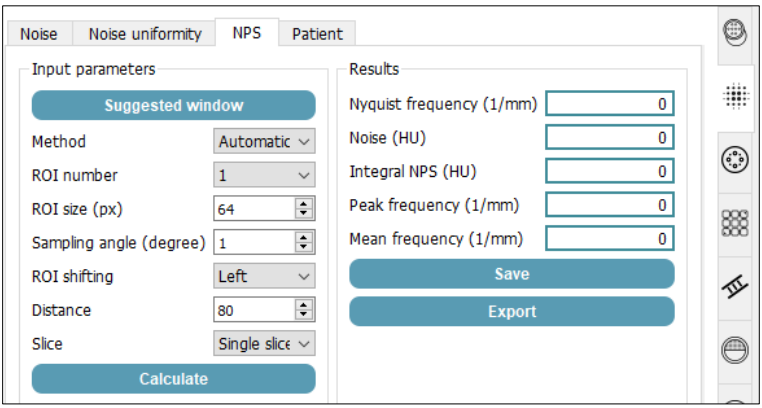

Figure 43. The interface for NPS measurement for AAPM phantom.

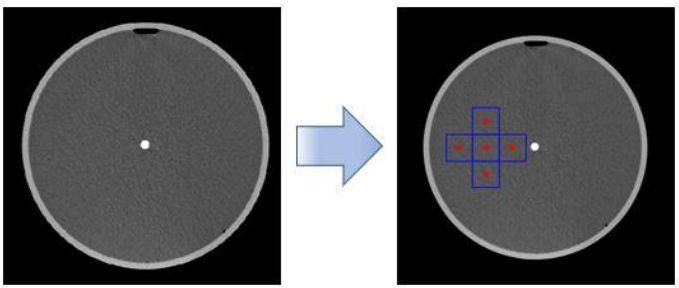

Figure 44. Placement of ROIs for NPS on the AAPM phantom.

5.9. CT number linearity

CT# linearity on the AAPM phantom is obtained by placing the ROI on the 610-02 module containing multiple pins from various materials. These materials are polyethylene, acrylic, polycarbonate, polystyrene, and nylon. Two additional materials that can be used in this module are background water and air

outside the phantom. In the automatic method, there are segmentation-rotation and full segmentation options. This option is Figure 45 displays the interface for CT# linearity, while Figure 46 displays the ROI placement results for 7 materials.

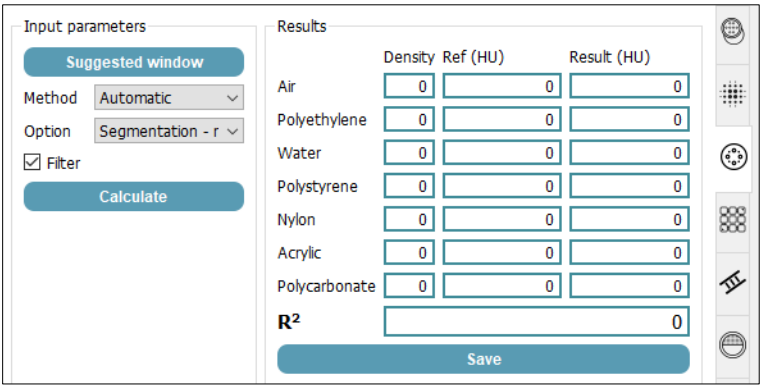

Figure 45. CT# linearity interface for the AAPM phantom.

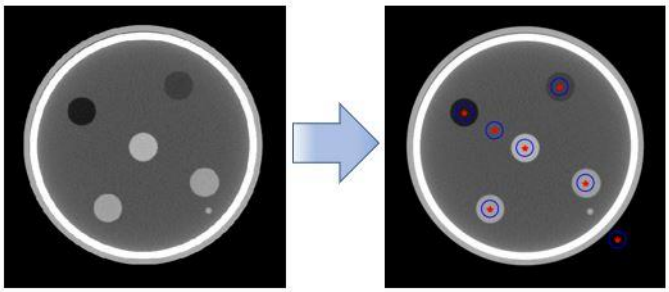

Figure 46. Placement of ROI on CT# linearity for the AAPM phantom.

5.10. Visual spatial resolution

Spatial resolution measurements using manual observations is obtained from the 610-03 module which contains hole pairs. Each pair has a different size, and is separated by a

different distance. Spatial resolution is obtained by selecting the smallest hole pair that can still be separated by eye sight. Figure 47 shows the selection of hole pairs from the largest to the smallest. Figure 48 shows the 610-03 module with hole pairs.

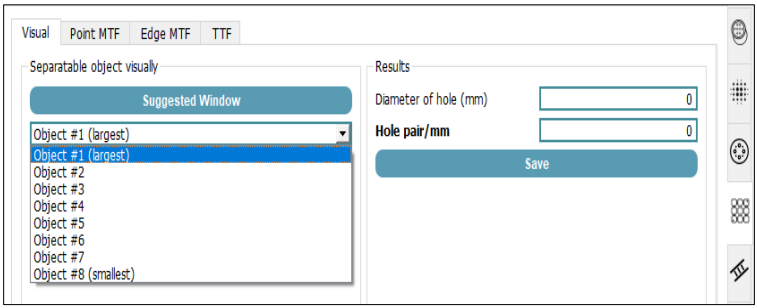

Figure 47. Interface for selecting hole pairs for visual spatial resolution in the AAPM phantom.

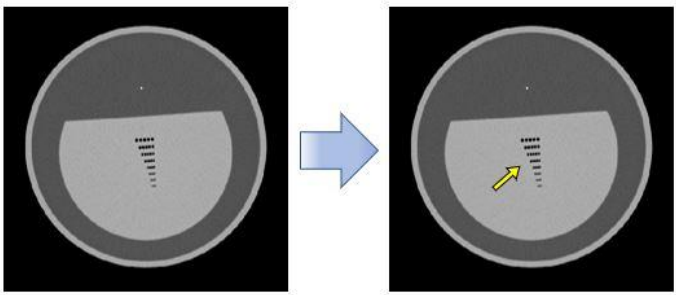

Figure 48. Hole pair objects in the AAPM phantom.

5.11. Point MTF

The MTF point on the AAPM phantom is obtained from the spatial resolution module containing the wire object. Figure 49 displays the interface at the MTF point. The segmentation process will place a ROI on the point object automatically to measure MTF, as shown in Figure 50.

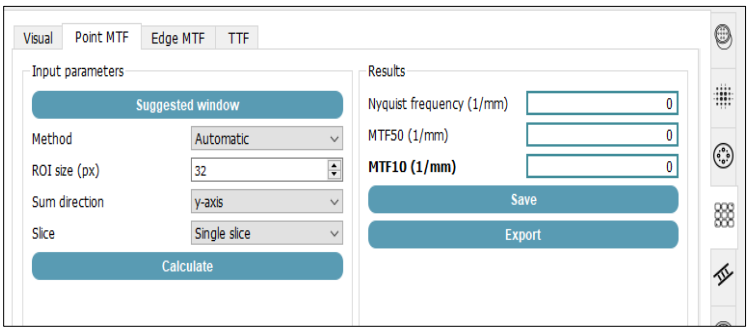

Figure 49. The interface for measuring point MTF.

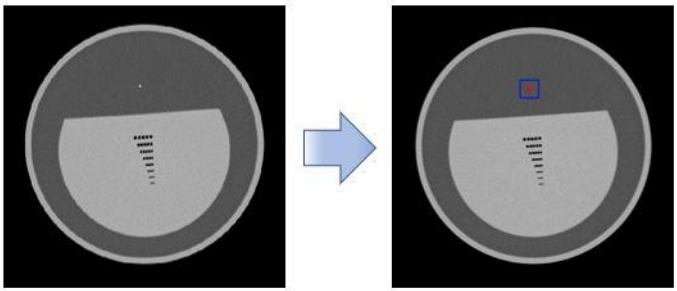

Figure 50. Point MTF measurement on the AAPM phantom.

5.12. Edge MTF

Apart from point objects, MTF can also be measured from phantom edges. Figure 51 displays the interface for MTF edge measurement. In this case, the rectangular ROI is placed on the edge of the phantom automatically. Sufficient FOV is required for this process, as shown in Figure 52.

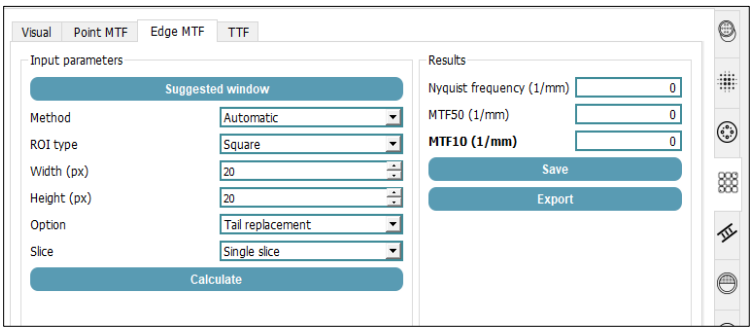

Figure 51. Interface for edge MTF measurement.

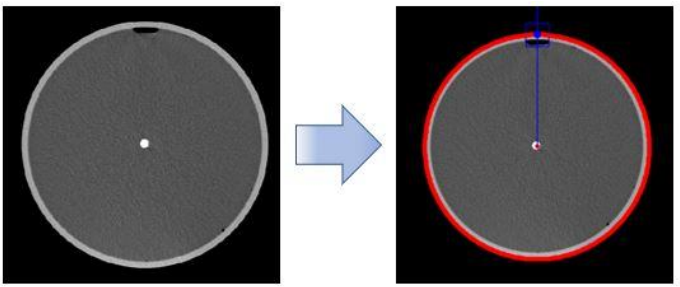

Figure 52. Rectangle ROI placement for edge MTF measurement.

5.13. Task Transfer Function (TTF)

TTF measurement on the AAPM phantom requires multiple pins with various materials. The interface for TTF measurement is shown in Figure 53. The TTF measurement process will automatically place ROIs on existing materials, then calculate the resolution along with the contrast-to-noise ratio. ROI placement for TTF measurement is shown in Figure 54.

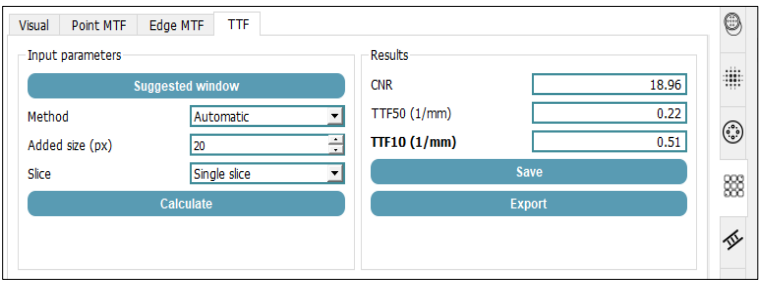

Figure 53. Interface for TTF measurement.

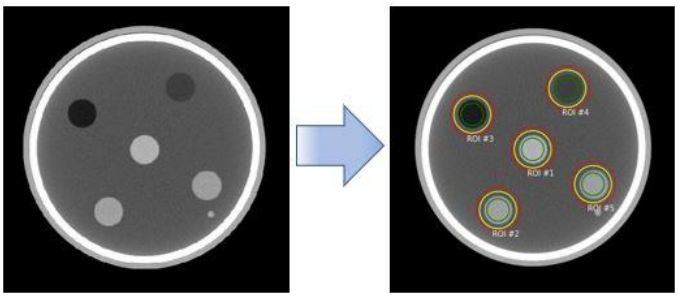

Figure 54. Placement of ROIs for TTF measurement on the AAPM phantom.

5.14. Slice thickness

Slice thickness measurement is done by measuring the thickness of the stair object. The interface for measuring slice thickness is shown in Figure 55. Automatically, there are two choices of algorithms, namely no-rotation and rotation, with the desired choice of stair object. This process places profile lines automatically, as shown in Figure 56.

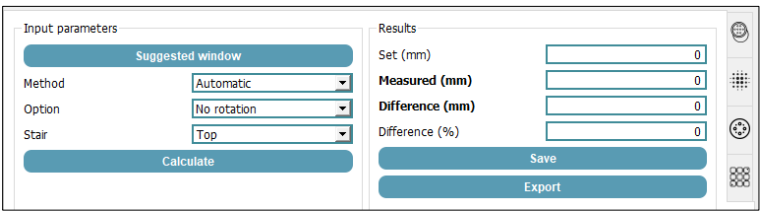

Figure 55. Interface on slice thickness measurements for the AAPM phantom.

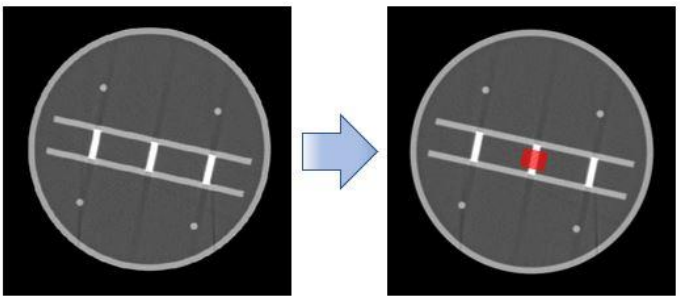

Figure 56. Measurement of slice thickness on the AAPM phantom.

5.15. Visual low contrast

Low contrast detectability (LCD) through visual observation of the AAPM phantom requires image modules 610-06 and 610-10 which contain material with a density similar to the background. LCD is determined by selecting the smallest object that can still be identified from the background. Figure 57 displays the interface for visual low contrast, and Figure 58 displays sample images.

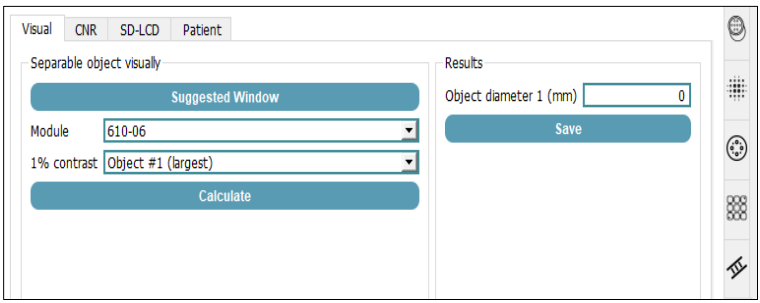

Figure 57. Interface for selecting low contrast objects for the AAPM phantom.

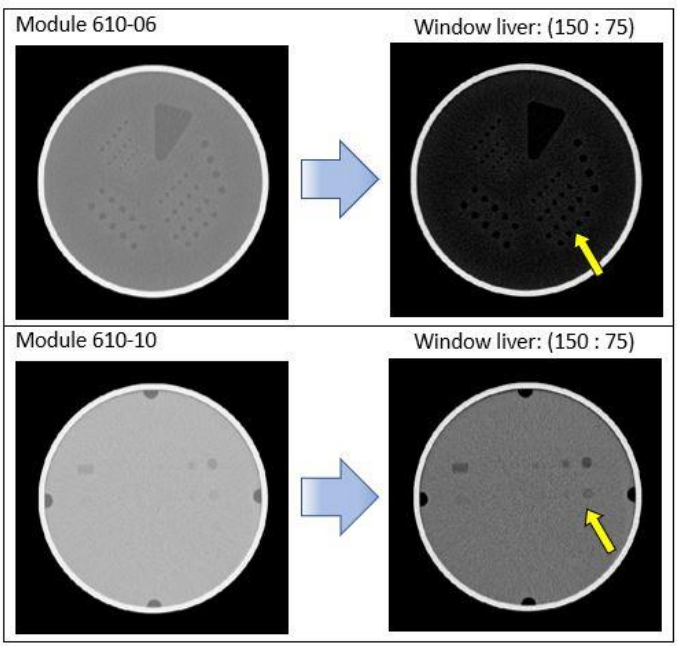

Figure 58. Two modules for visual LCD measurements on the AAPM phantom.

5.16. CNR

Contrast-to-noise ratio (CNR) on the AAPM phantom was measured using the 610-06 module. The interface for this measurement is shown in Figure 59. An option to filter the image is provided to anticipate segmentation error. Automatically, two ROIs are placed on the object and the background, as shown in Figure 60.

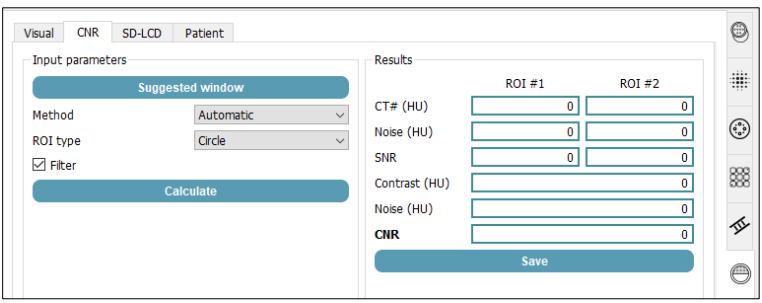

Figure 59. The interface of CNR measurement on the AAPM phantom.

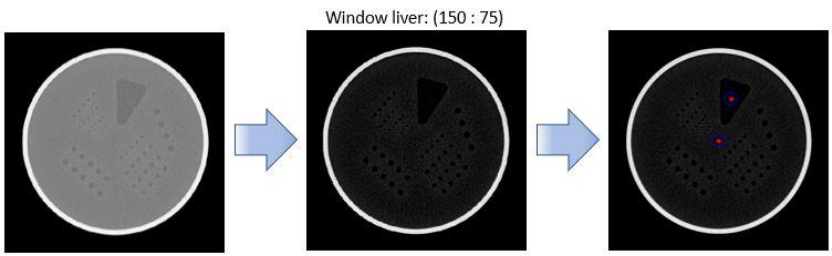

Figure 60. Automatic placement of ROI on CNR measurements for the AAPM phantom.

5.17. SD-LCD

Statistically-defined LCD on the AAPM phantom is obtained from homogeneous water images. A grid-shaped ROI is placed in a homogeneous area to obtain the minimum detectable contrast (MDC) at the set ROI size. The interface for LCD measurement is

shown in Figure 61. The placement of the ROI grid is shown in Figure 62.

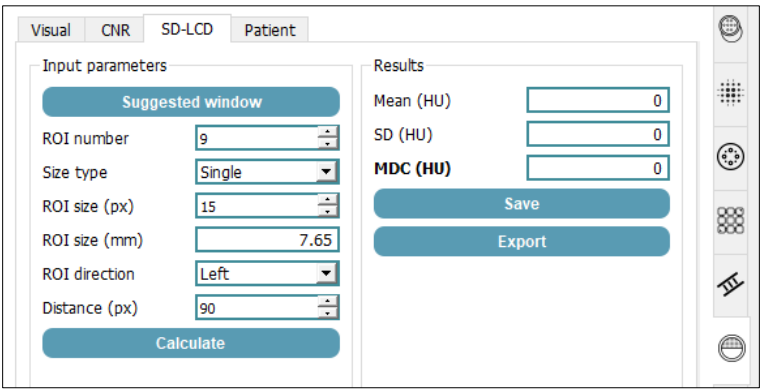

Figure 61. The interface of SD-LCD measurements for the AAPM phantom.

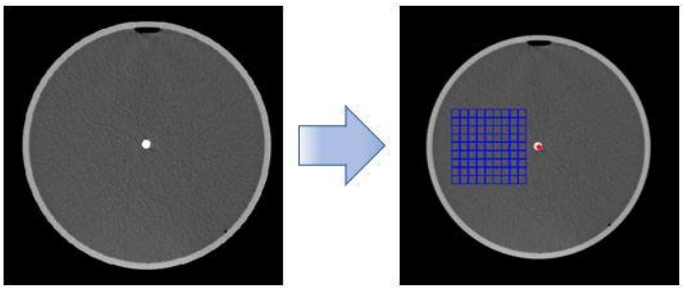

Figure 62. Grid ROI for SD-LCD measurements for the AAPM phantom.

5.18. Alignment

Testing the accuracy of the laser alignment on the AAPM phantom requires an image module 610-10 which has objects on the edges to mark the laser. Figure 63 shows the interface for measuring phantom alignment. Figure 64 shows the placement of

the ruler for alignment. In addition to testing using the edge object detection option, the accuracy of the phantom alignment can also be tested using the center option, which simply determines the centroid of the phantom relative to the center of the image.

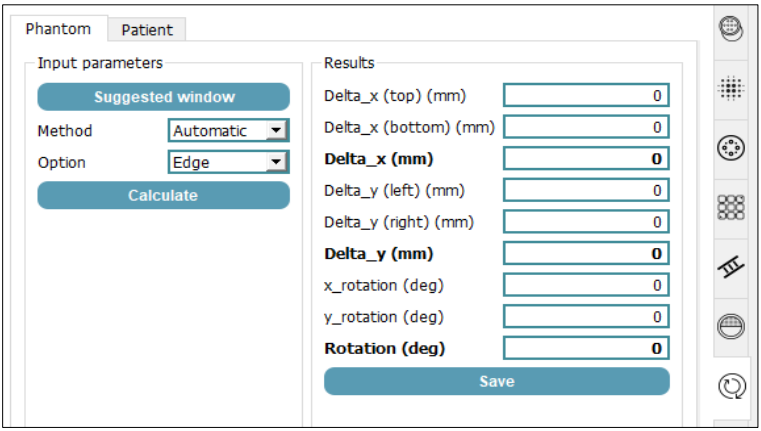

Figure 63. Interface for alignment measurements for the AAPM phantom.

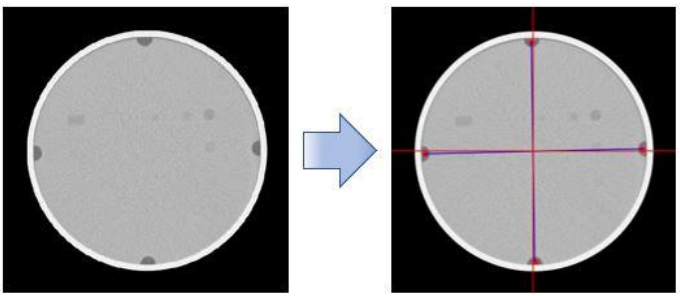

Figure 64. Alignment measurements on the AAPM phantom.

5.19. Gantry tilt

Gantry tilt evaluation can be done with any image module. The interface for this test is shown in Figure 65. In an ideal system,

a gantry tilt of 0^0 produces the same lateral and anterior-posterior diameters, as shown in Figure 66. A gantry tilt > 0^0 will produce a phantom image that looks slightly elliptical.

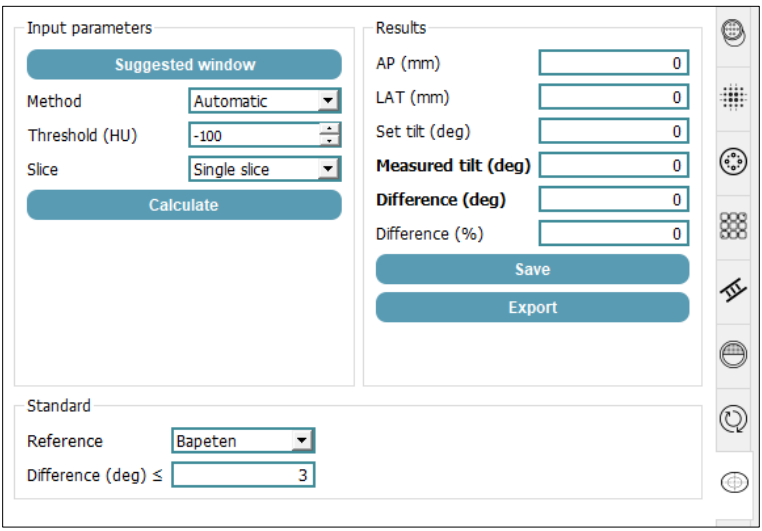

Figure 65. Interface for the gantry tilt measurement.

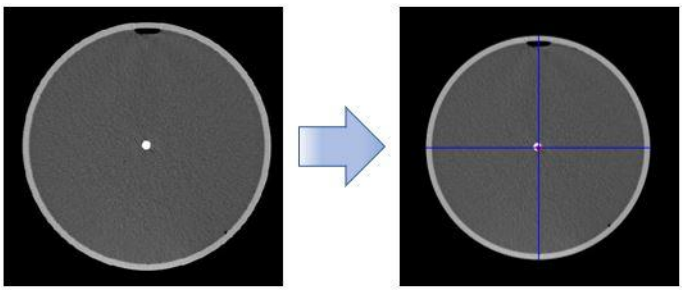

Figure 67. Gantry tilt measurement on AAPM phantom images.

5.20. Phantom diameter

The phantom diameter measurement requires a phantom image with an FOV that covers the entire phantom area, so that

the image is not truncated. The interface for measuring the phantom diameter is shown in Figure 68. Meanwhile, Figure 69 shows an example of automatic measurement.

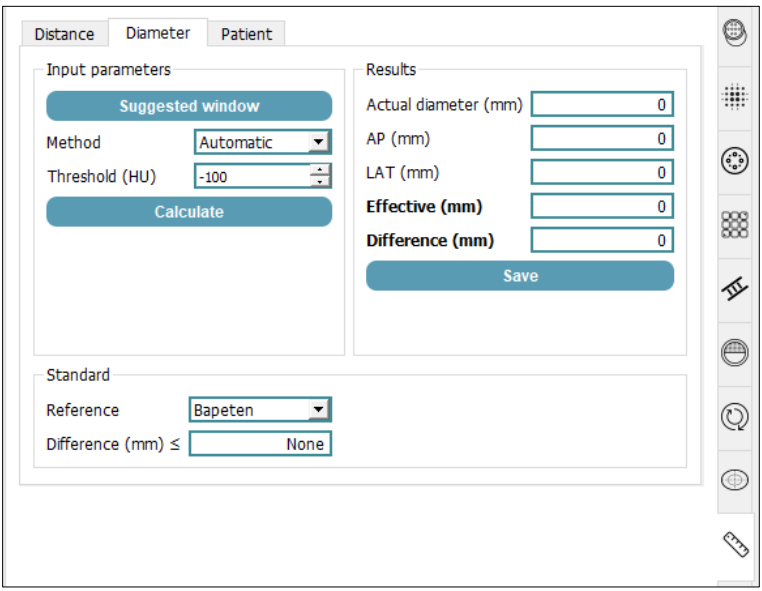

Figure 68. Interface for phantom diameter measurement.

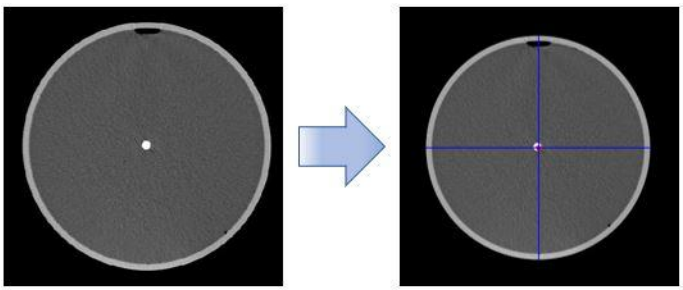

Figure 69. Measurement of the phantom diameter.

5.21. Distance between slices

The distance between slices utilizes a shift in the projection of an object that is designed to be slanted. In the AAPM phantom, objects that can be used are the stair objects from two slices with different slice locations. The interface for this purpose is shown in Figure 70. This measurement examines the distance between slices of two different slices with the reference distance being the distance between slice locations. Figure 71 displays the process of obtaining the distance between slices.

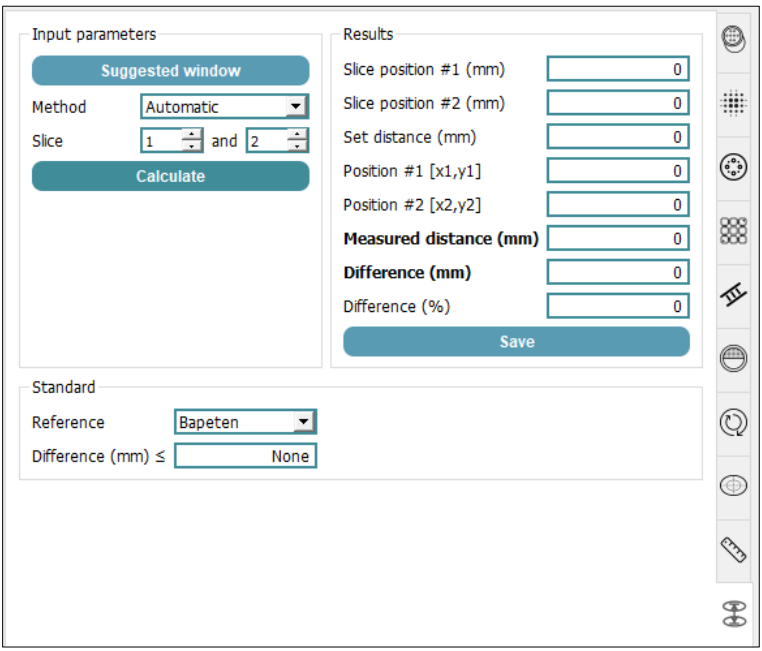

Figure 70. Interface for measuring the distance between slices.

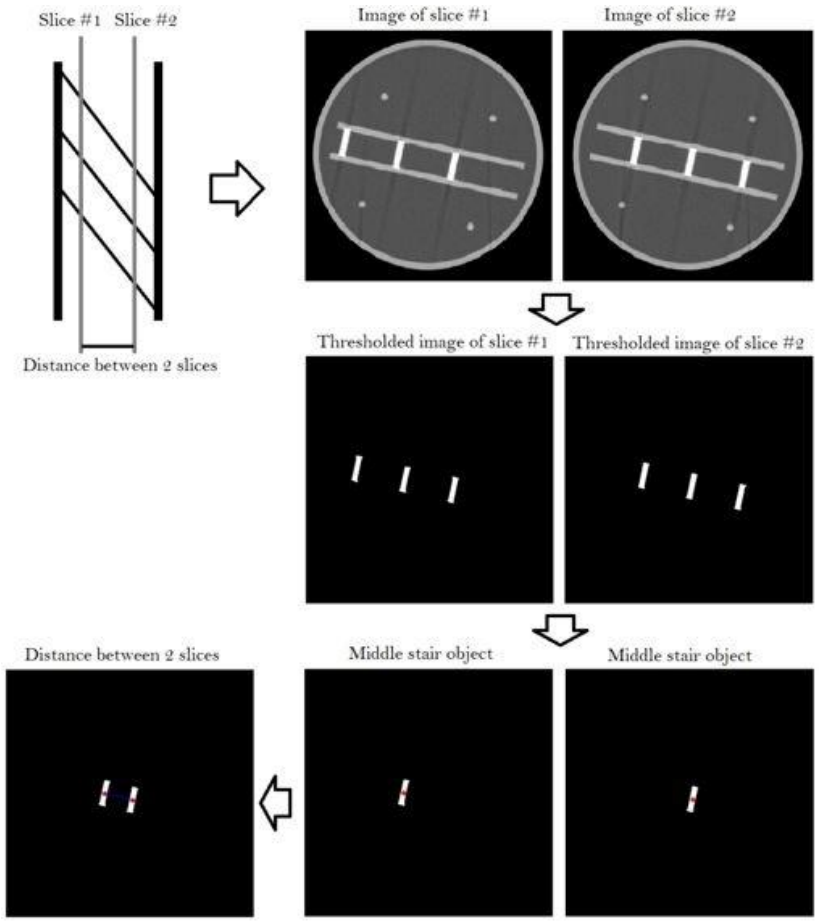

Figure 71. The process of measuring the distance between slices on the AAPM phantom.

5.22. Distance accuracy

For distance measurement, a phantom with a distance module is needed. For this, we can use the ACR phantom. The interface for measuring the distance is shown in Figure 72. Distance measurement then can be run automatically by clicking Calculate button. This process segment two separate objects with

known distance and evaluating it with the measured distance, as shown in Figure 73.

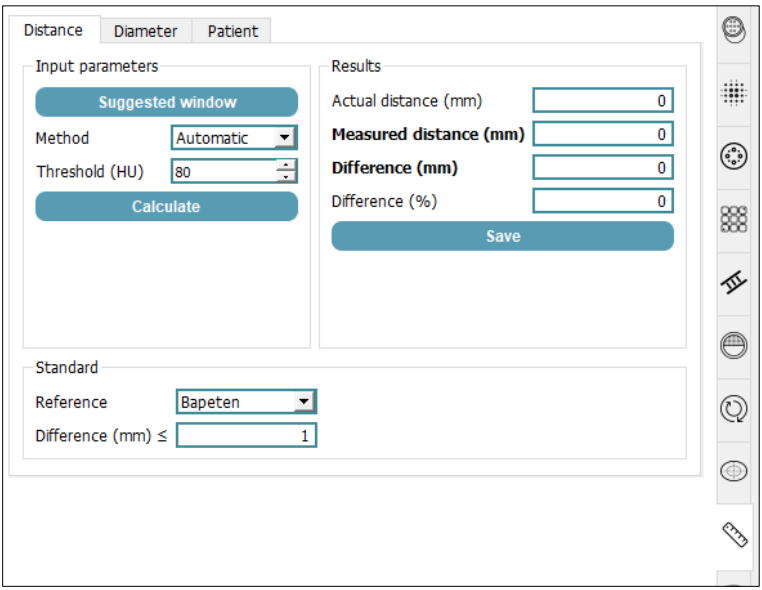

Figure 72. Interface for distance measurement.

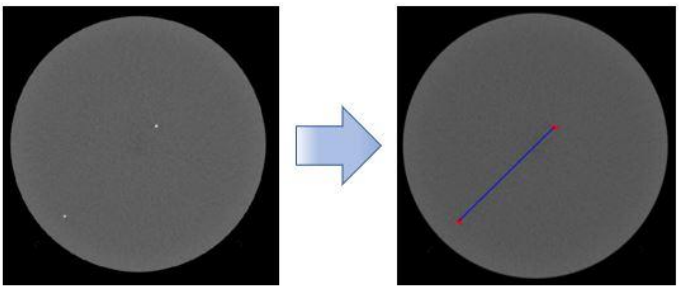

Figure 73. Distance measurement on ACR phantom.

EXAMPLE MEASUREMENTS ON ACR PHANTOM

CT number accuracy

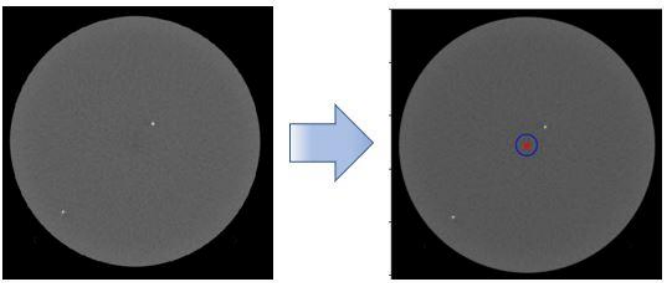

CT number uniformity

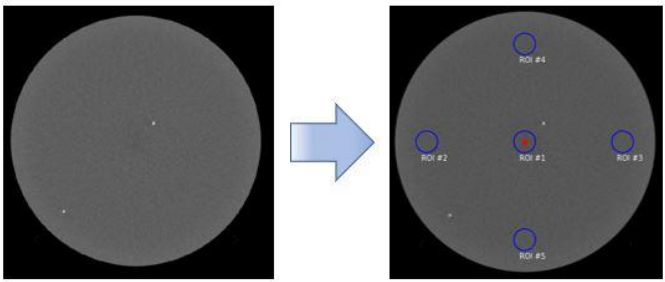

CT number homogeneity

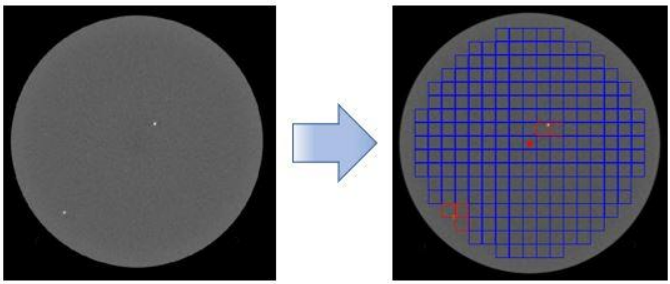

CT number histogram

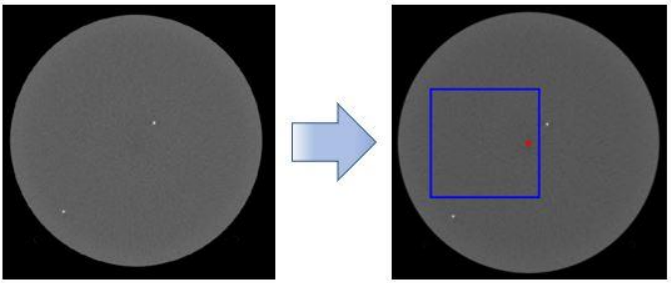

CT number profile

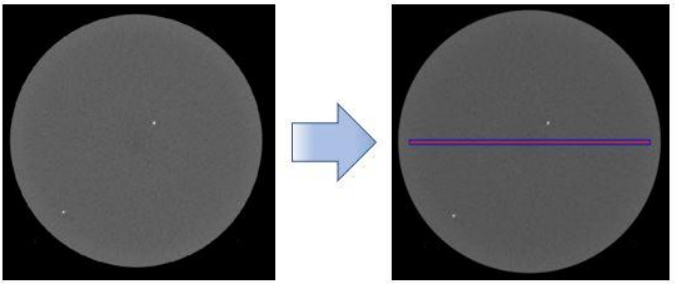

Noise accuracy

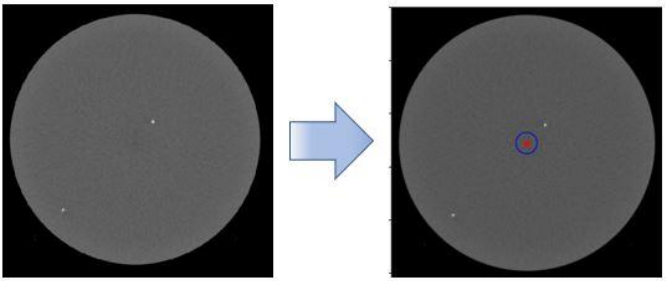

Noise uniformity

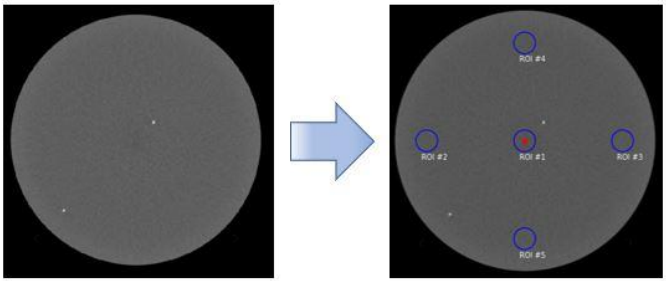

Noise power spectrum (NPS)

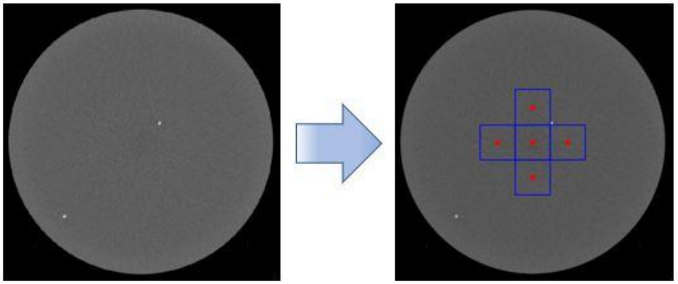

CT number linearity

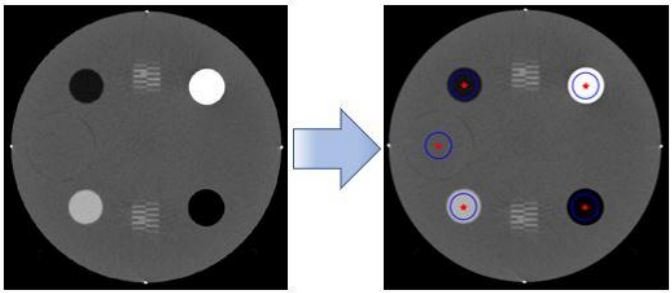

Spatial resolution
Visual resolution

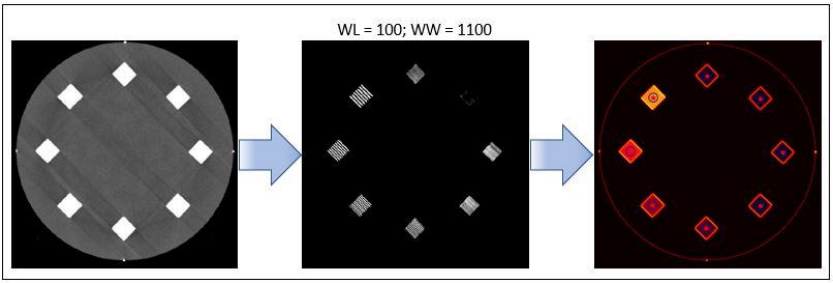

Point MTF

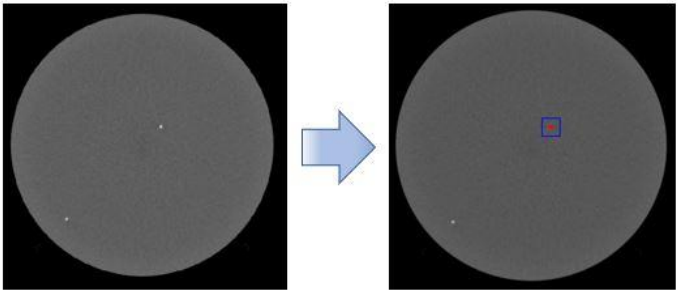

Edge MTF

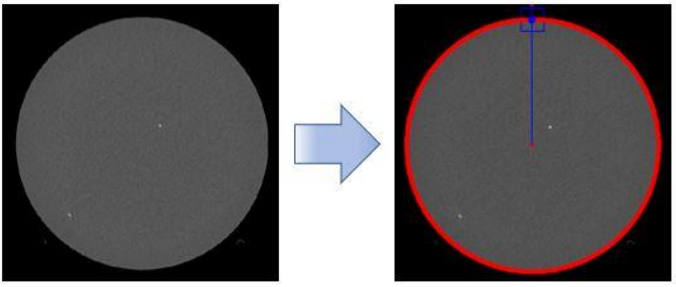

Task Transfer Function (TTF)

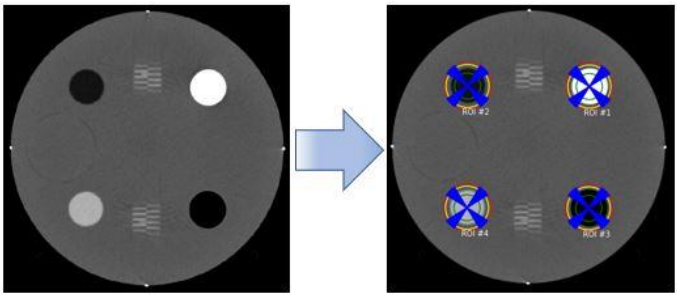

Slice thickness

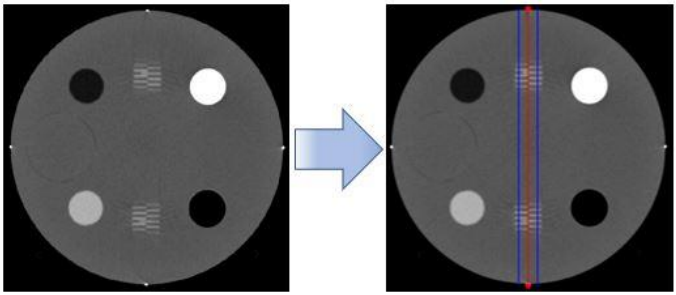

Low contrast
Smallest object

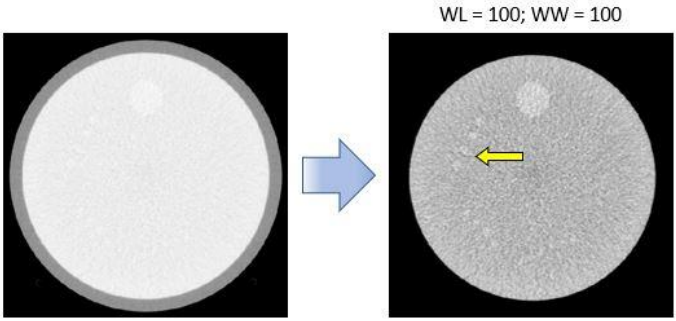

CNR

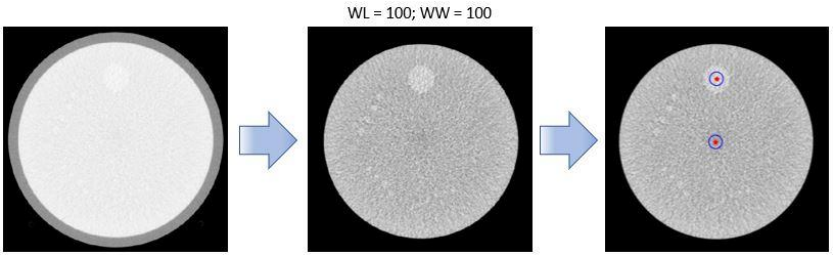

SD-LCD

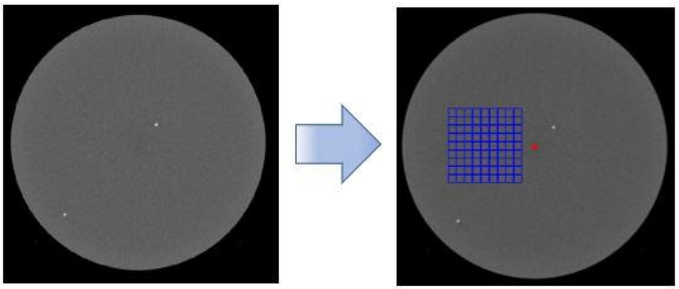

Alignment

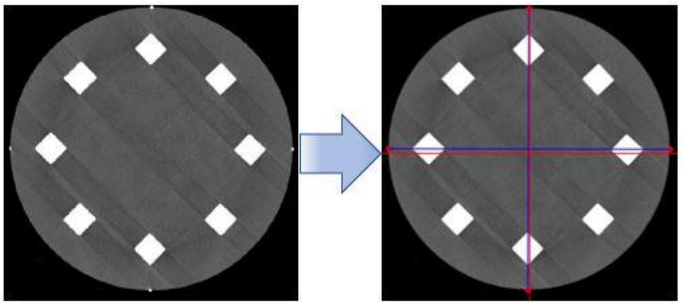

Gantry tilt

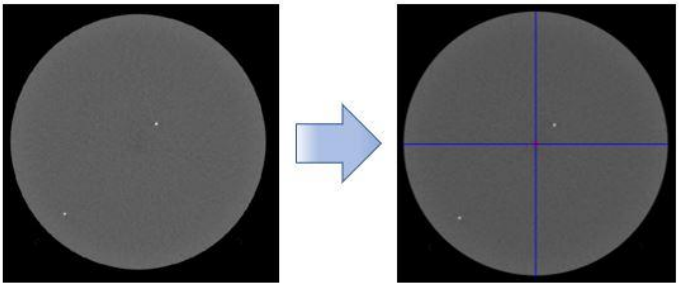

Distance

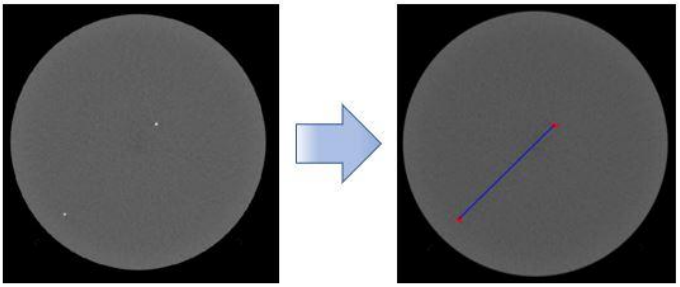

Diameter

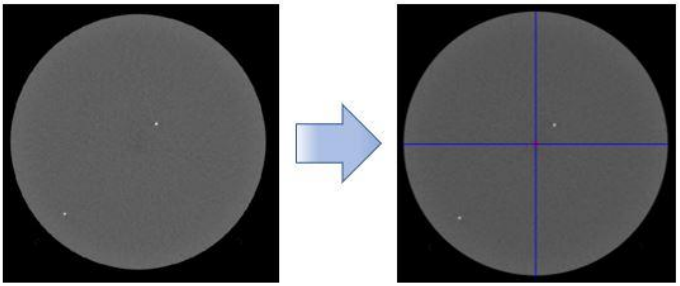

EXAMPLE MEASUREMENTS ON CATPHAN PHANTOM

CT number accuracy

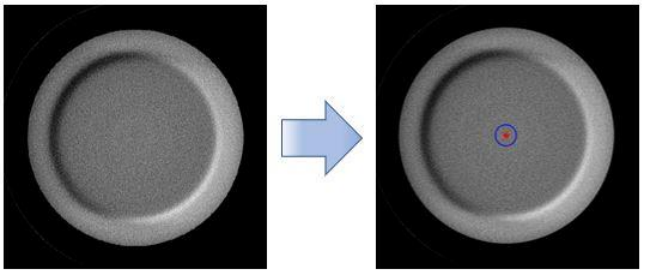

CT number uniformity

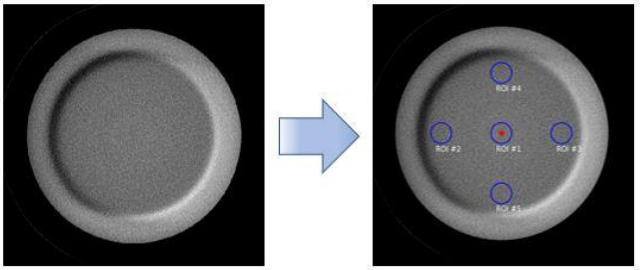

CT number homogeneity

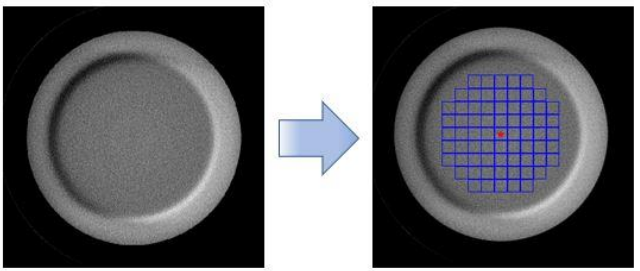

CT number histogram

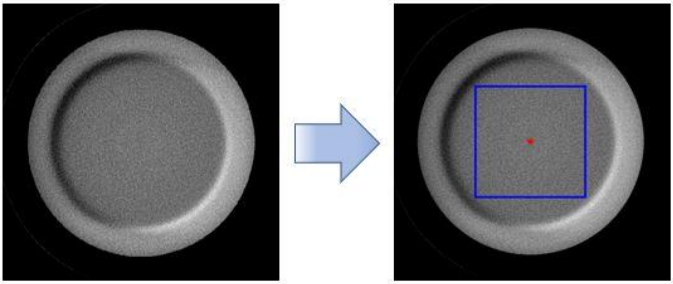

CT number profile

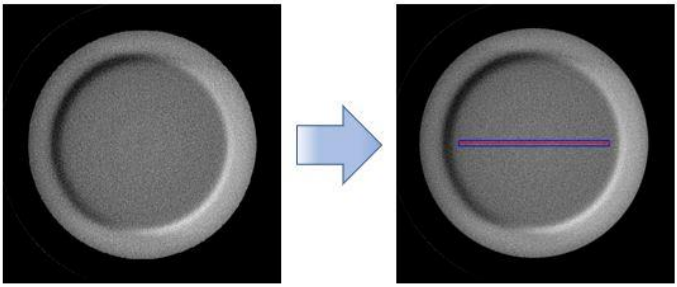

Noise accuracy

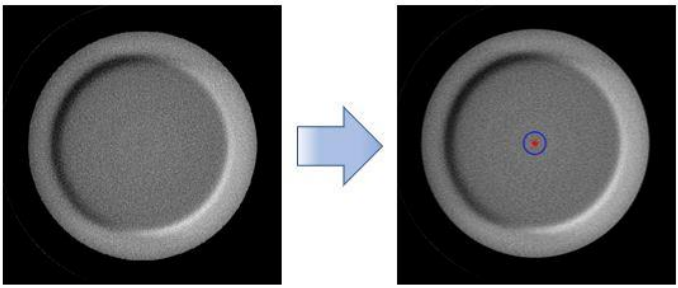

Noise uniformity

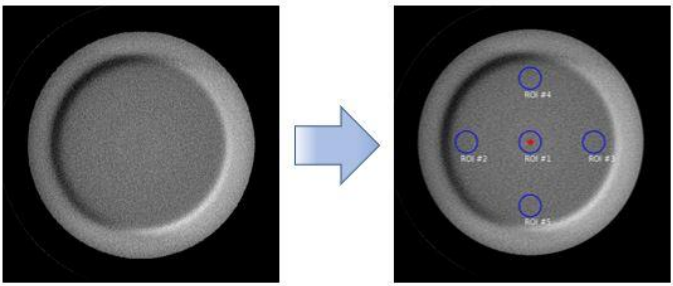

Noise power spectrum (NPS)

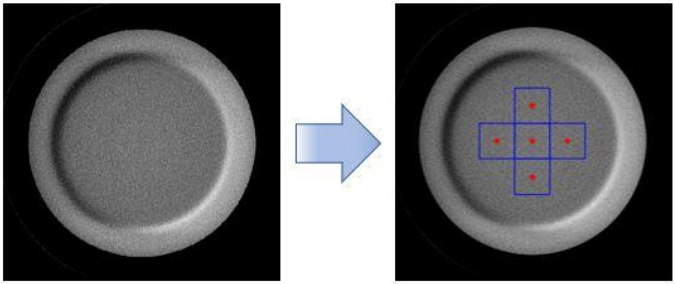

CT number linearity

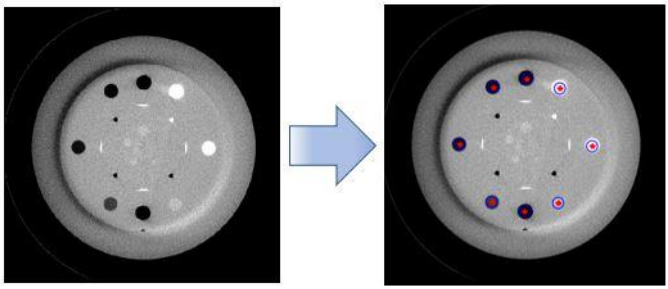

Spatial resolution

Visual

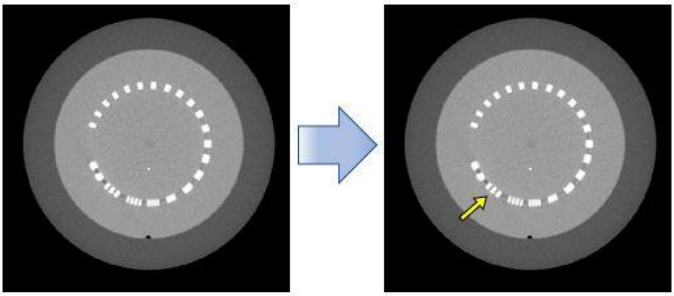

Point MTF

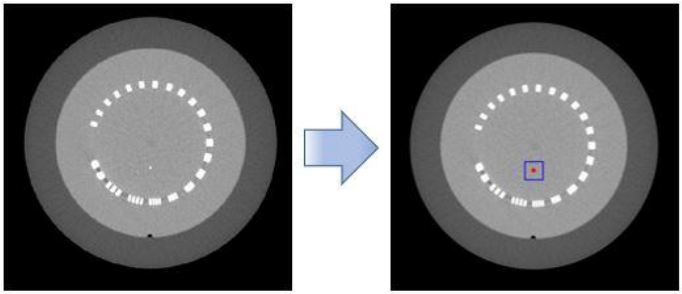

Edge MTF

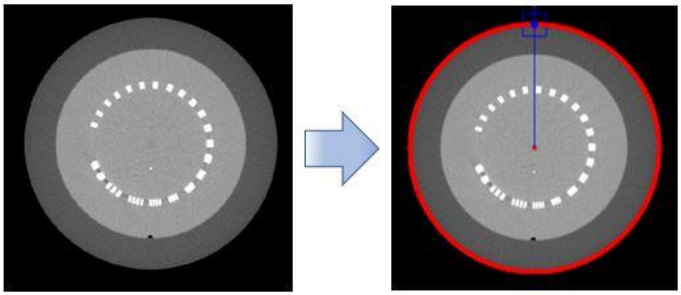

Task Transfer Function (TTF)

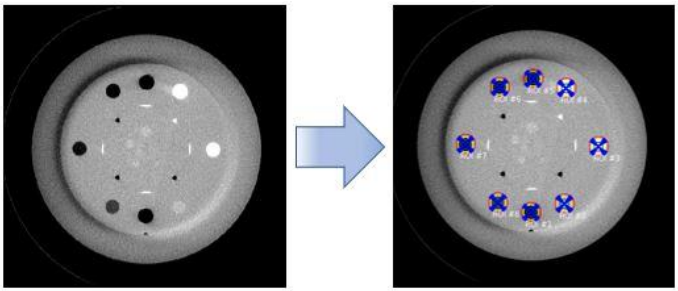

Slice thickness

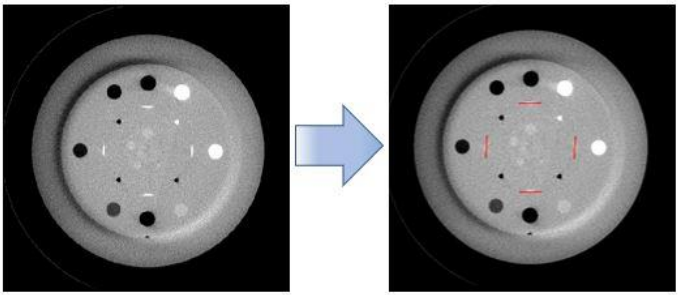

Low contrast
Smallest object

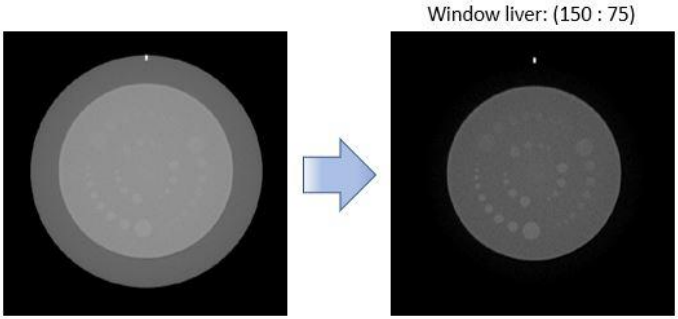

SD-LCD

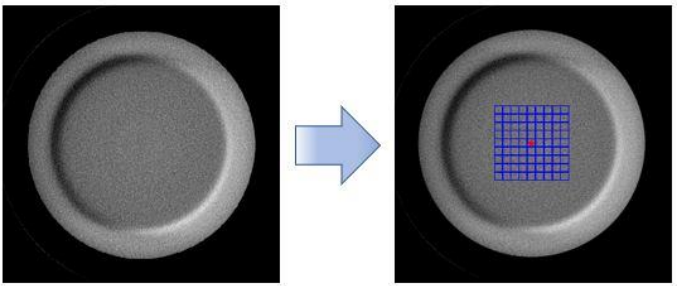

Alignment

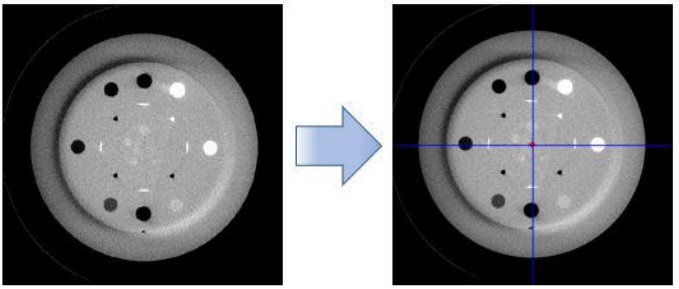

Gantry tilt

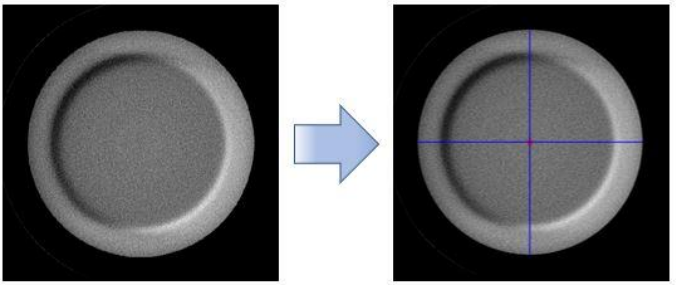

Distance

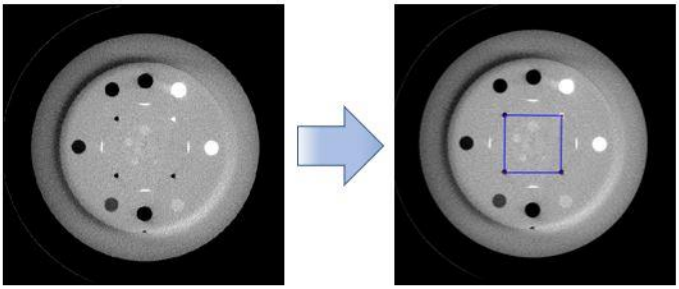

Diameter

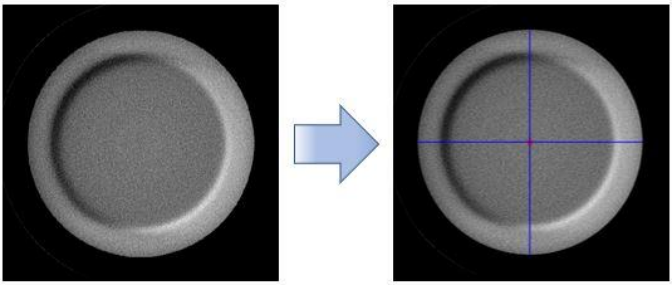

EXAMPLE MEASUREMENTS ON GE PHANTOM

CT number accuracy

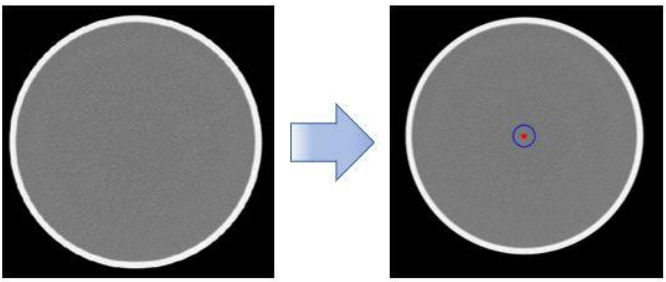

CT number uniformity

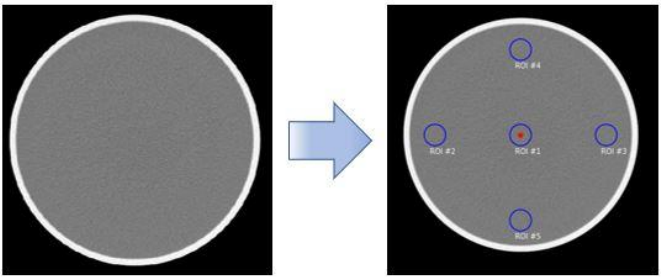

CT number homogeneity

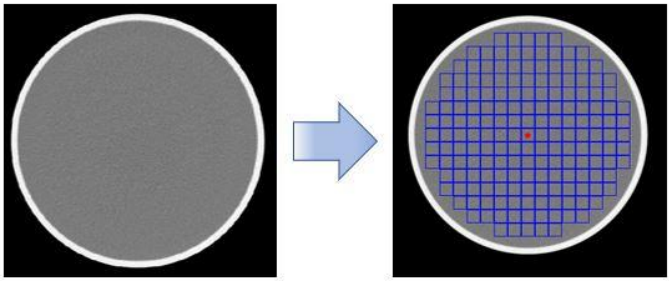

CT number histogram

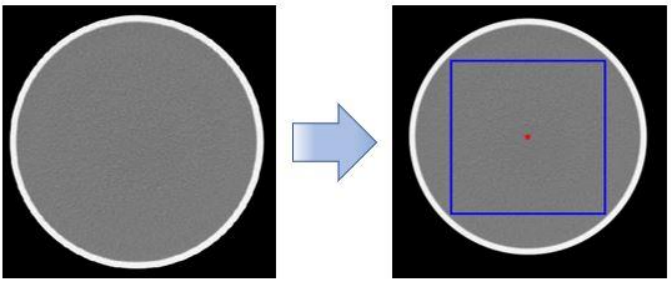

CT number profile

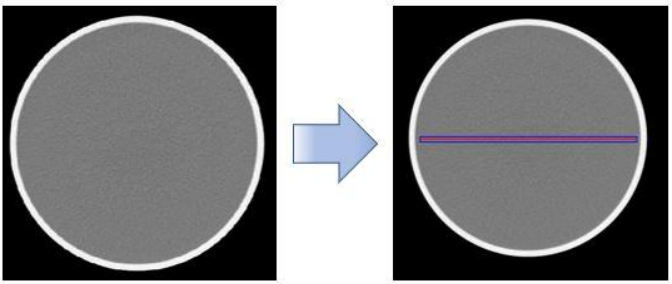

Noise accuracy

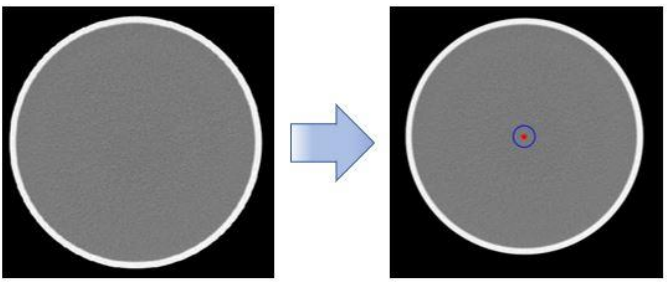

Noise uniformity

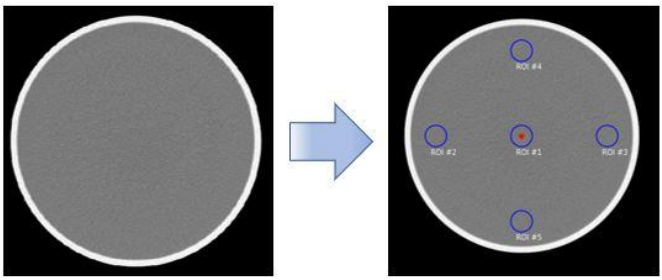

Noise power spectrum (NPS)

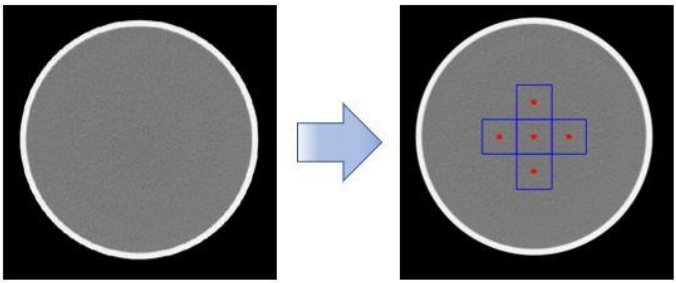

CT number linearity

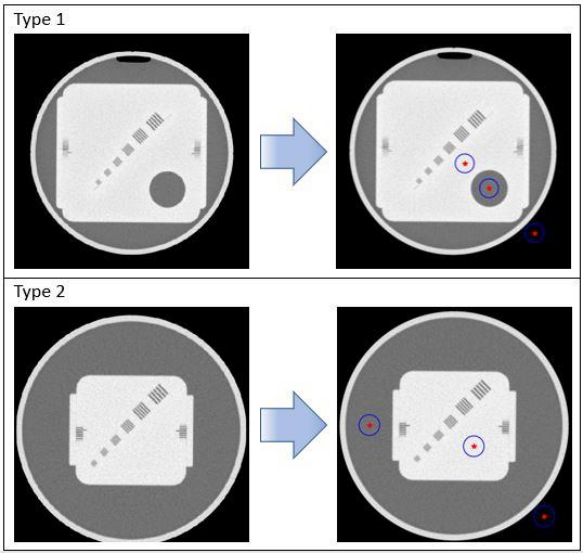

Spatial resolution
Visual resolution

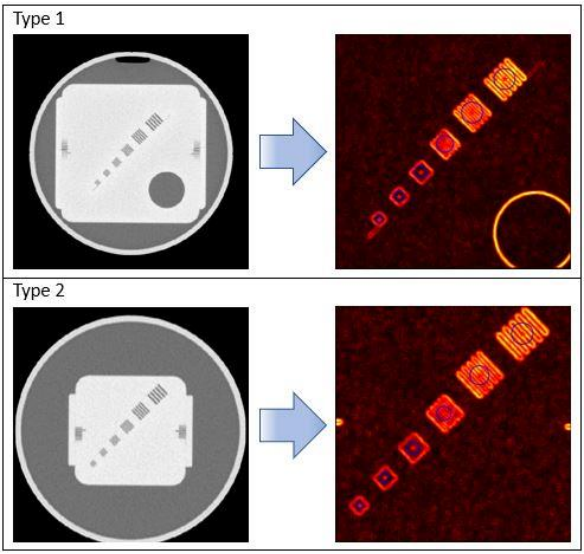

Edge MTF

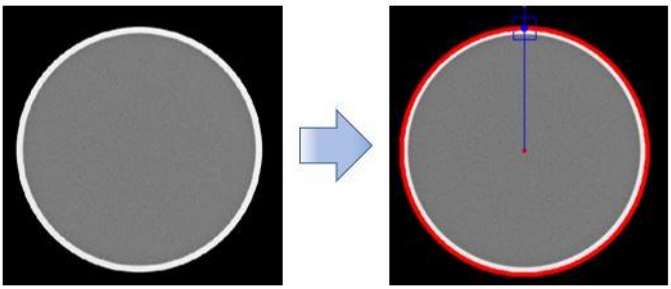

Task Transfer Function (TTF)

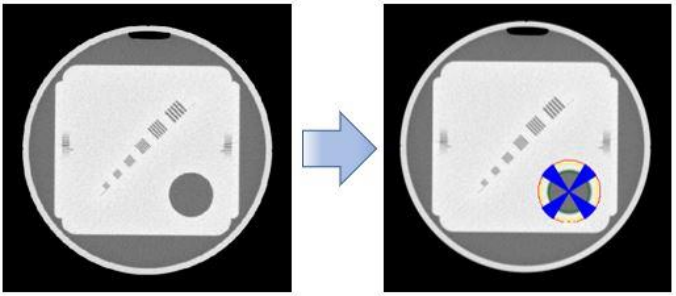

Slice thickness

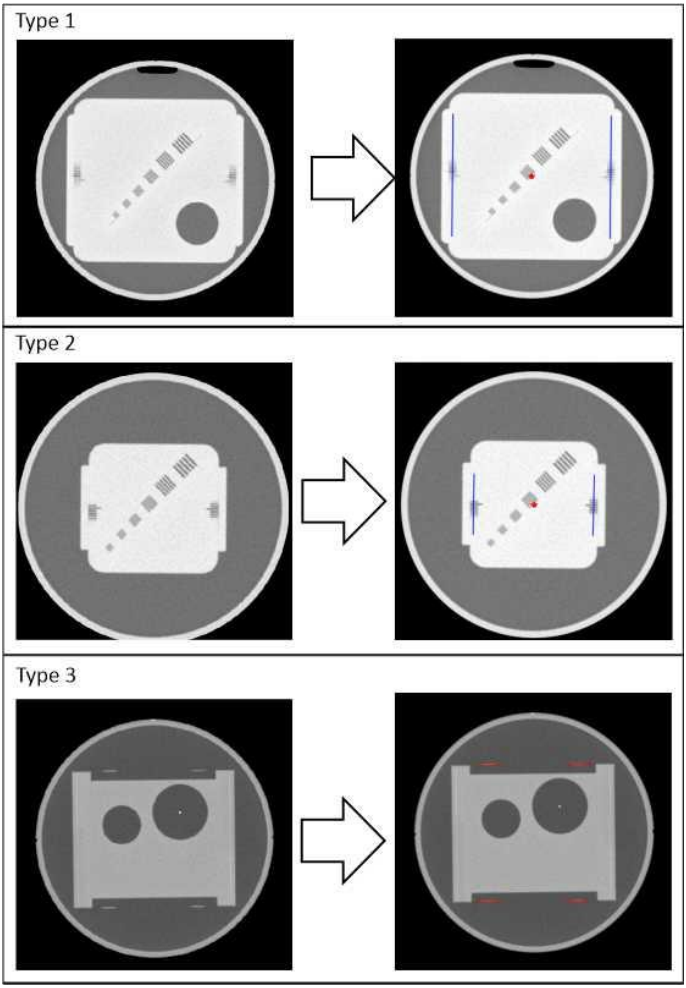

Low contrast
CNR

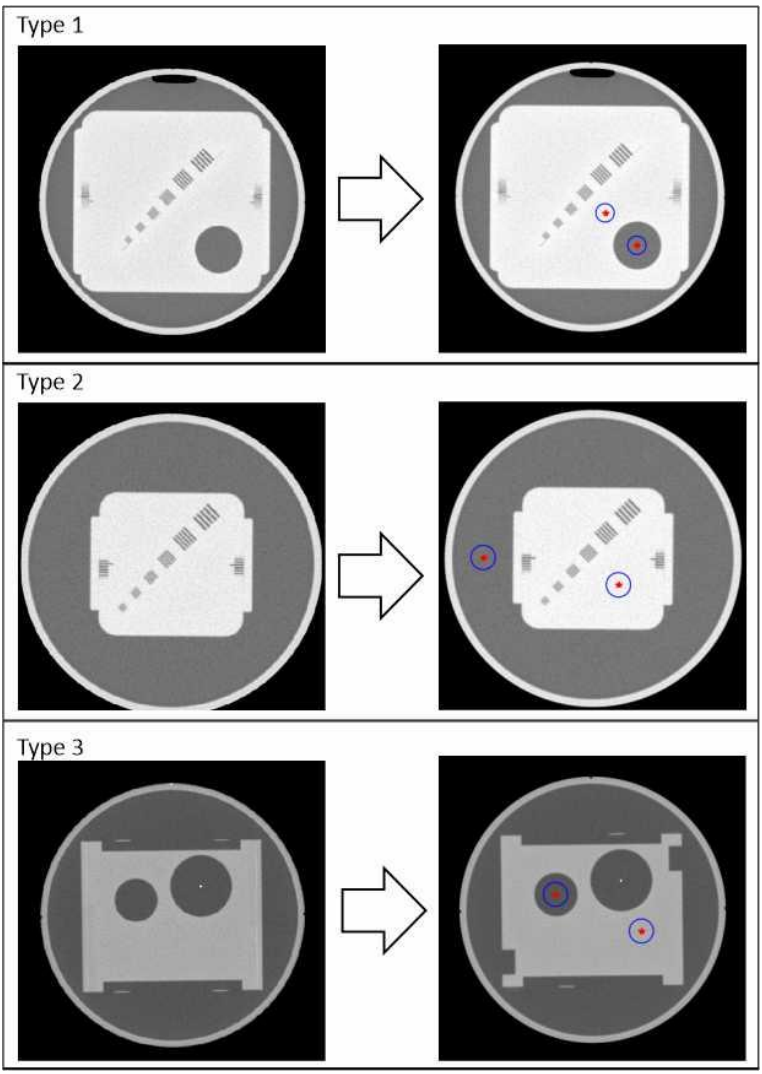

SD-LCD

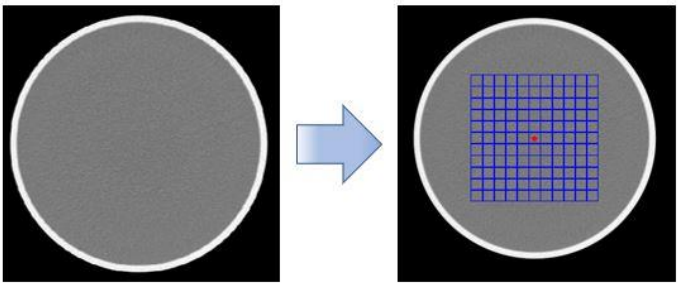

Alignment

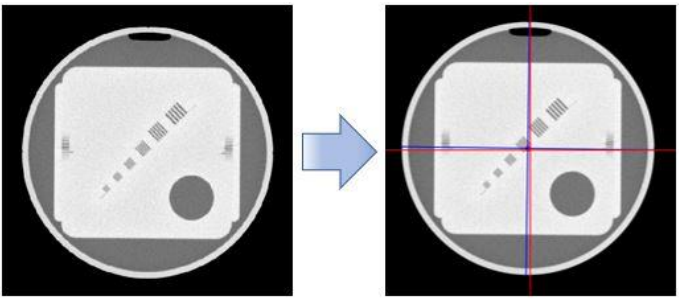

Gantry tilt

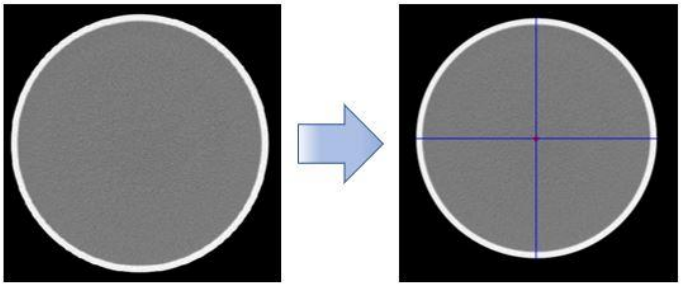

Diameter

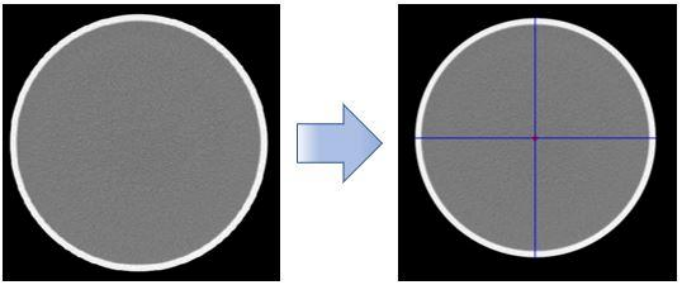

EXAMPLE MEASUREMENTS ON CANON PHANTOM

CT number accuracy

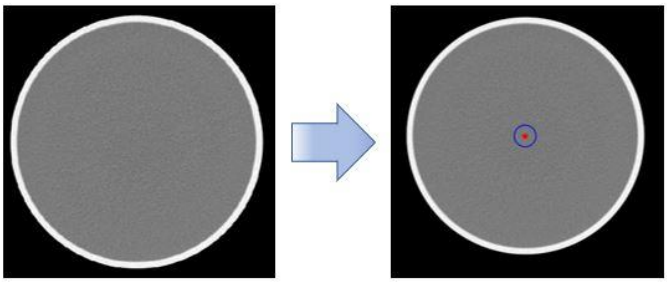

CT number uniformity

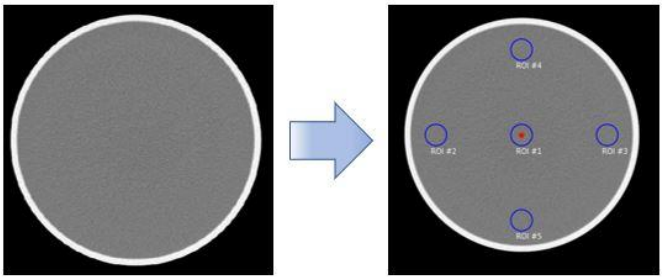

CT number homogeneity

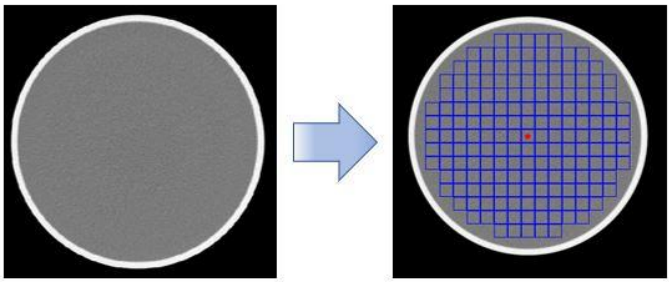

CT number histogram

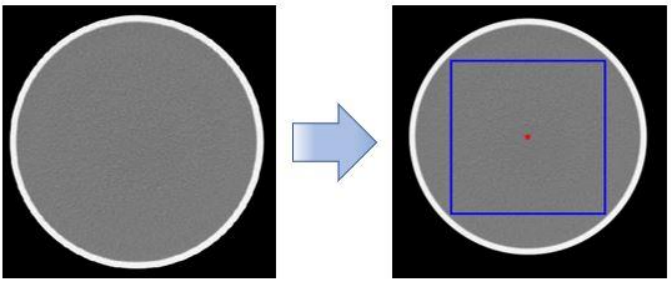

CT number profile

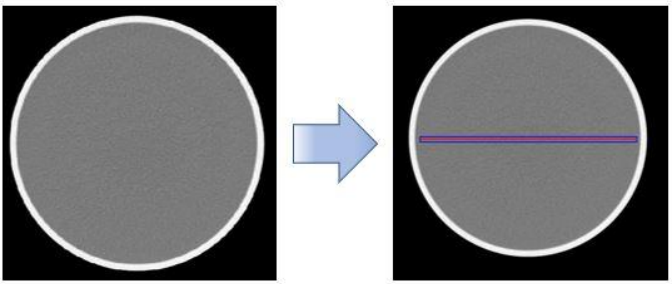

Noise accuracy

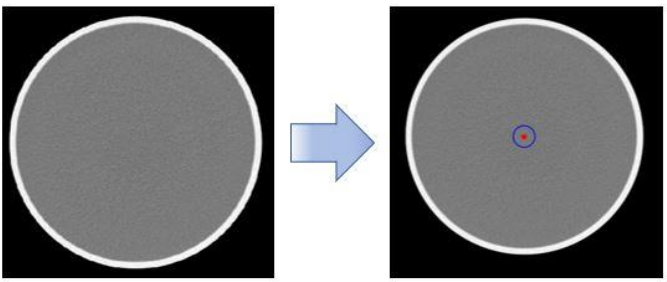

Noise uniformity

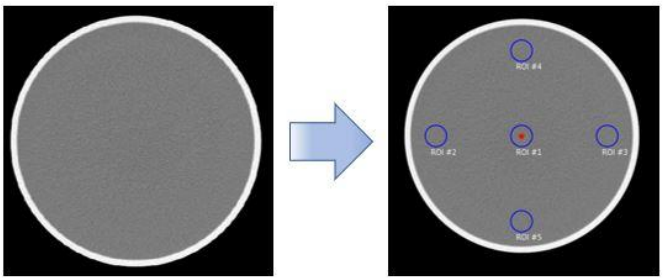

Noise power spectrum (NPS)

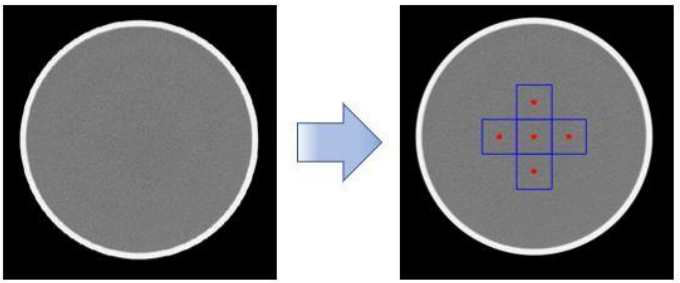

CT number linearity

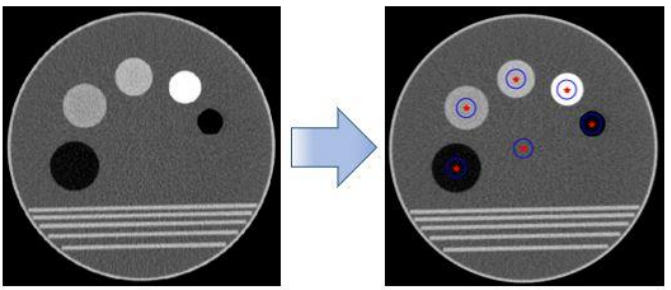

Spatial resolution
Edge MTF

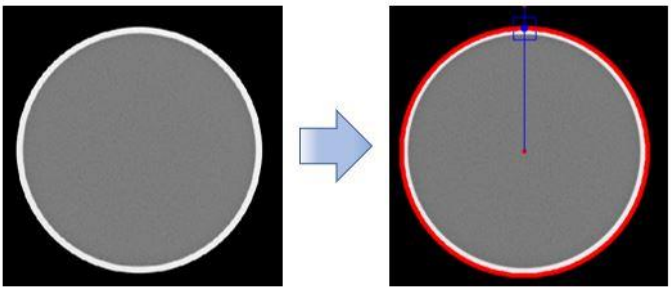

Task Transfer Function (TTF)

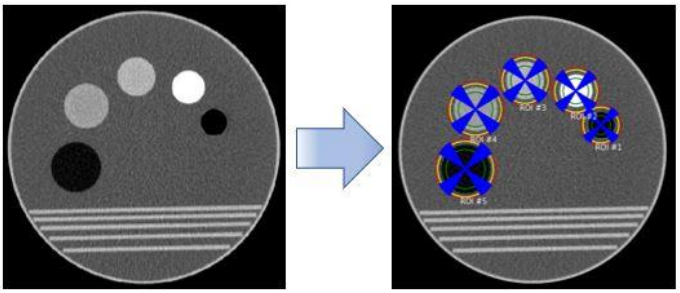

Low contrast
Smallest object

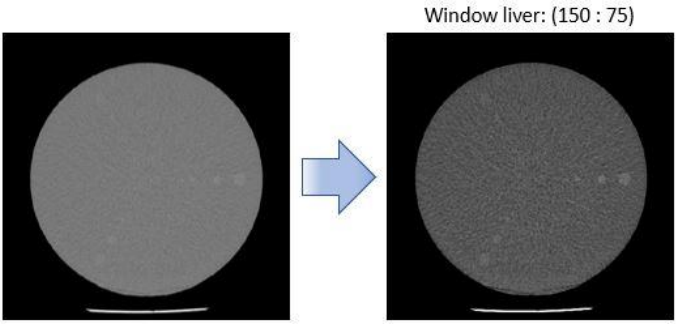

SD-LCD

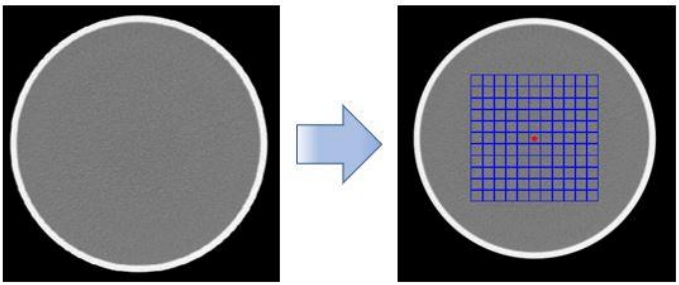

Alignment

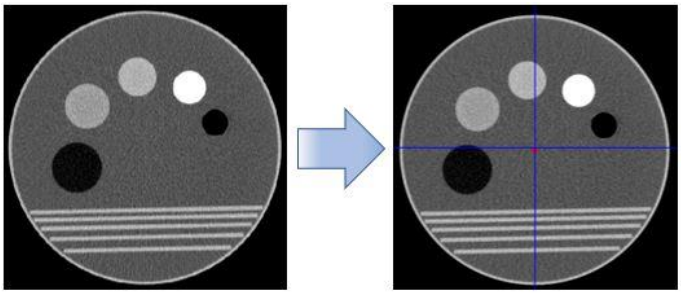

Gantry tilt

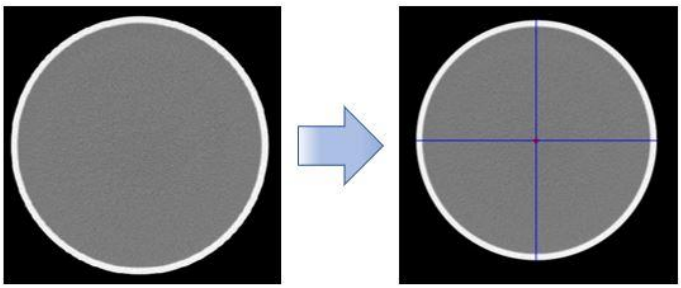

Diameter

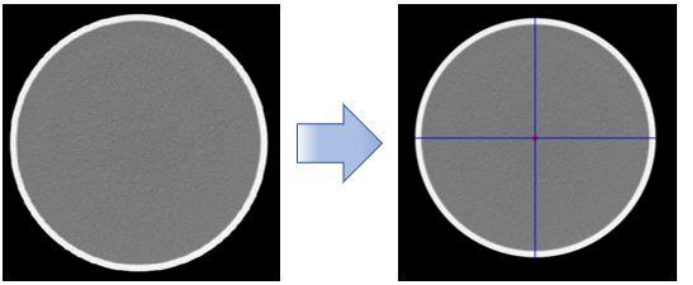

EXAMPLE MEASUREMENTS ON SIEMENS PHANTOM

CT number accuracy

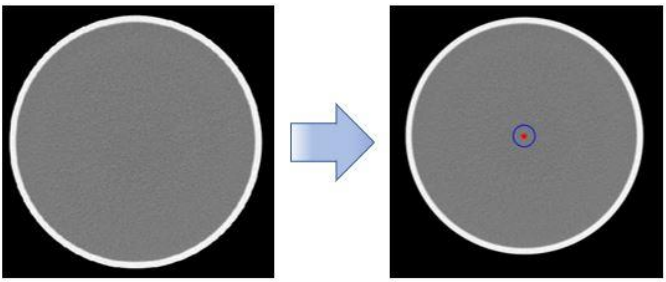

CT number uniformity

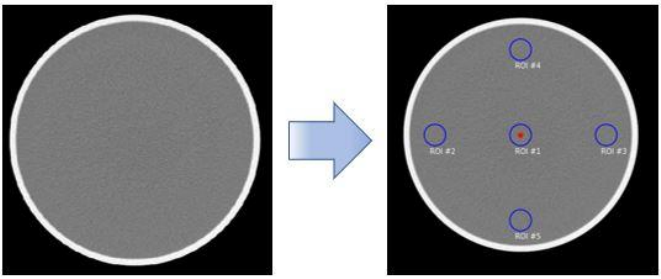

CT number homogeneity

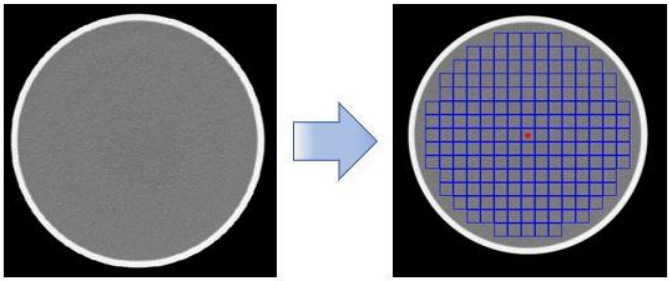

CT number histogram

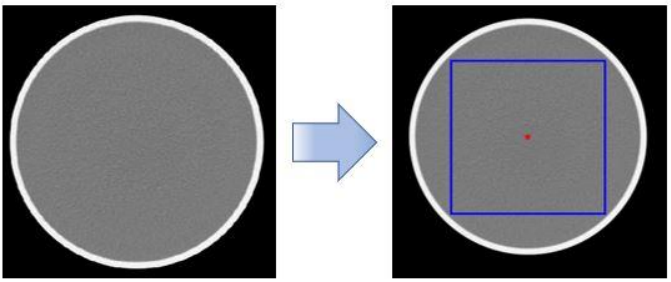

CT number profile

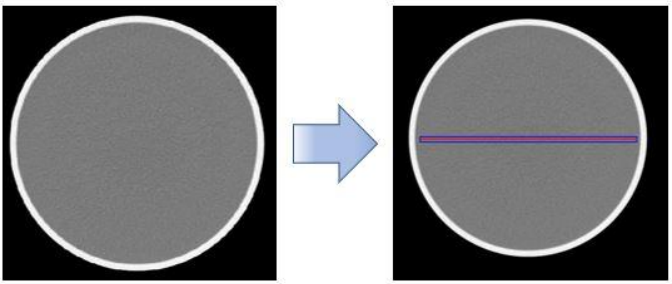

Noise accuracy

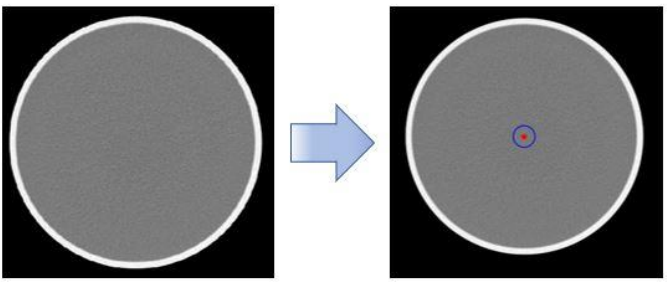

Noise uniformity

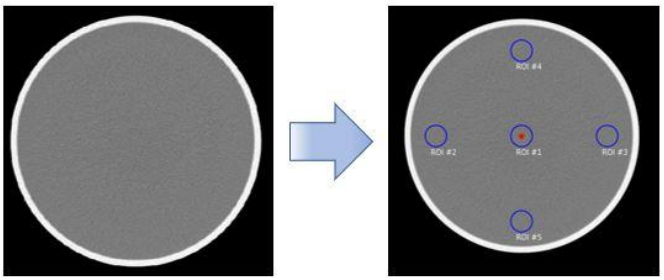

Noise power spectrum (NPS)

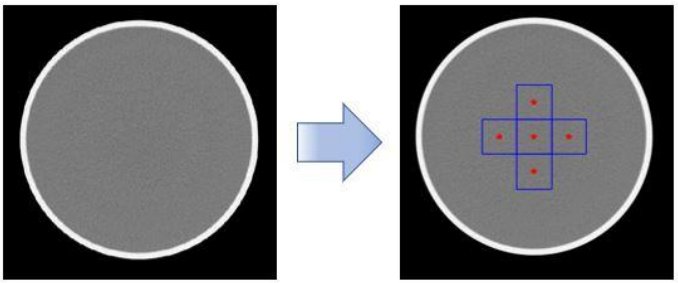

CT number linearity

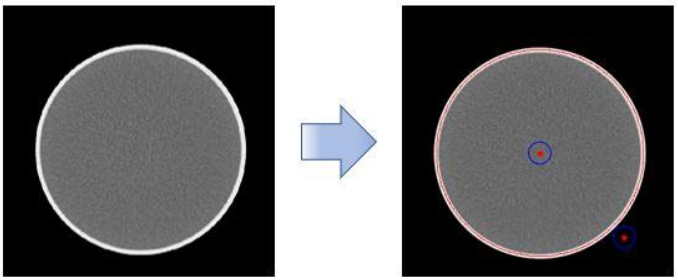

Spatial resolution

Point MTF

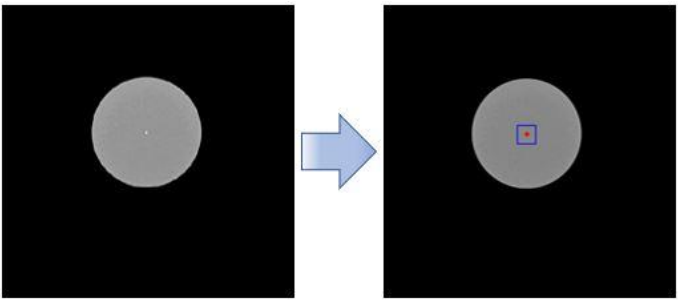

Edge MTF

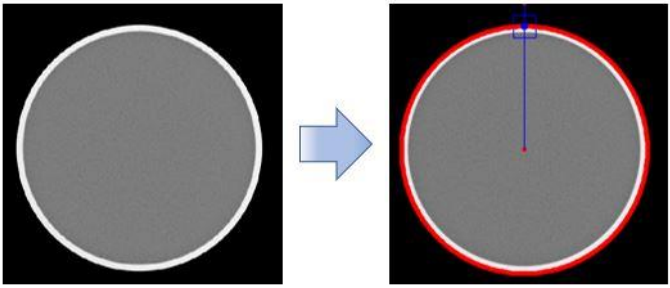

Slice thickness

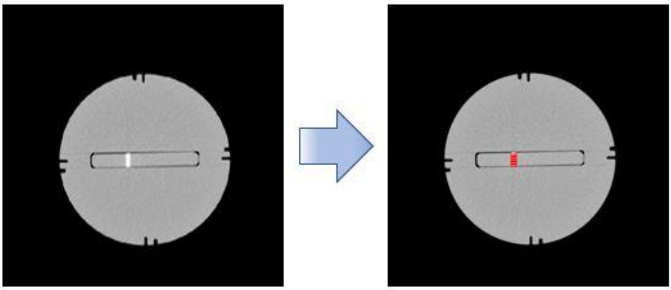

Low contrast
SD-LCD

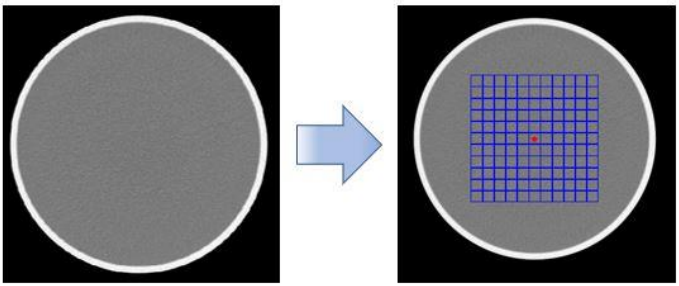

Alignment

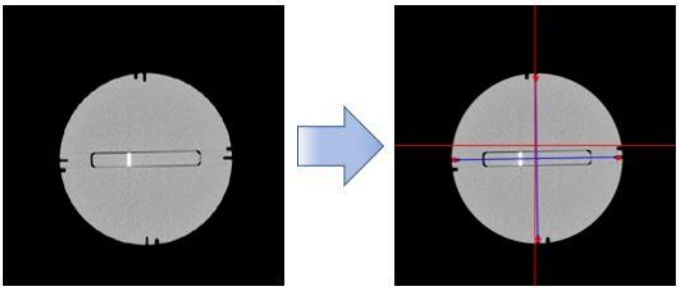

Gantry tilt

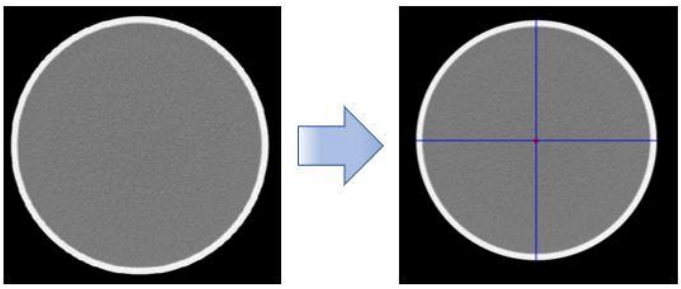

Diameter

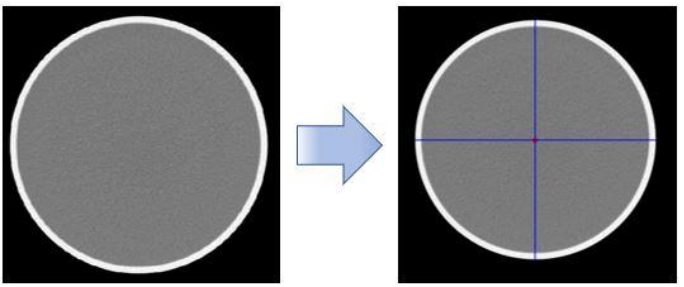

Distance between slices

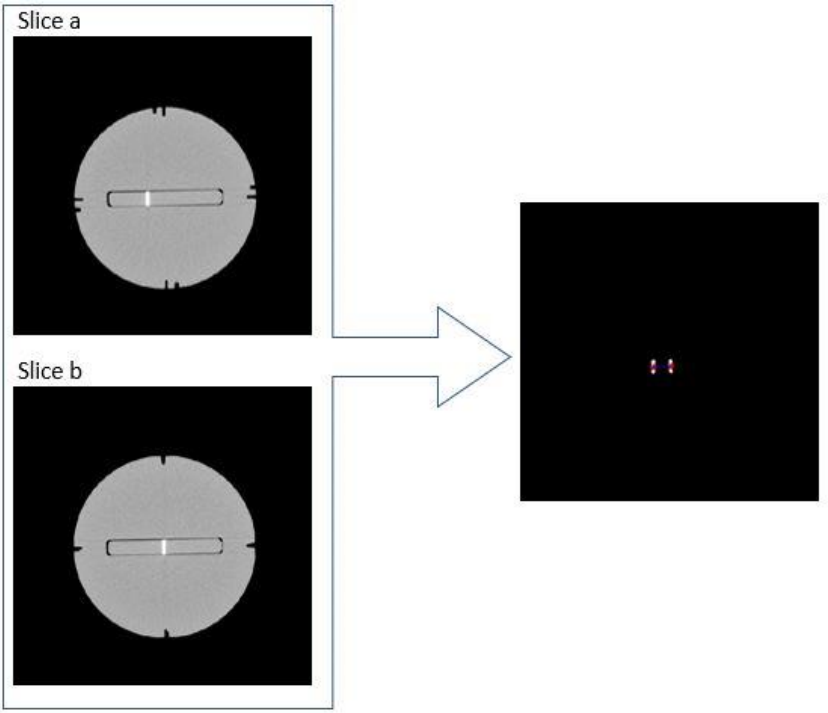

EXAMPLE MEASUREMENTS ON PHILIPS PHANTOM

CT number accuracy

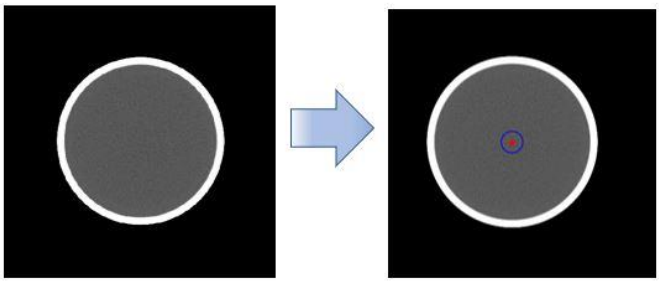

CT number uniformity

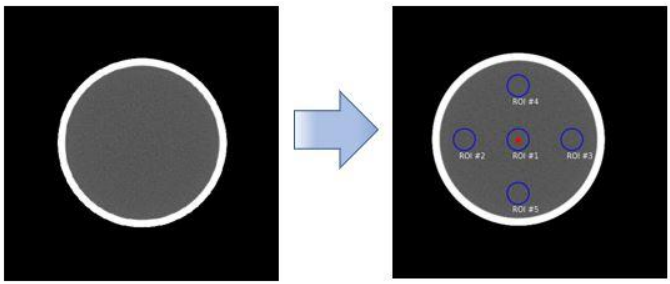

CT number homogeneity

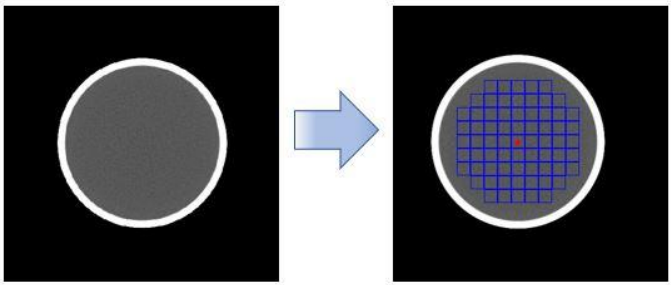

CT number histogram

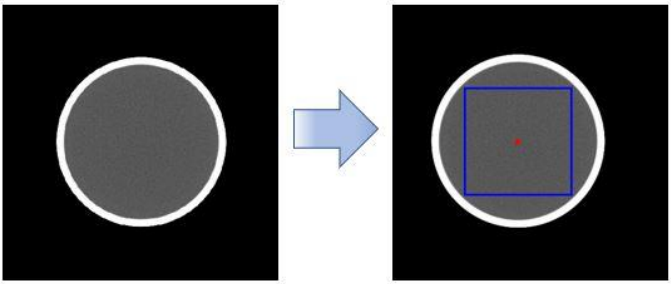

CT number profile

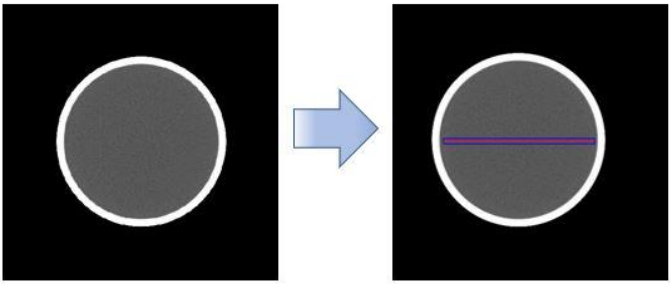

Noise accuracy

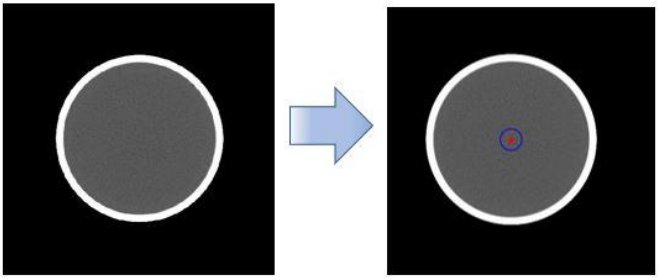

Noise uniformity

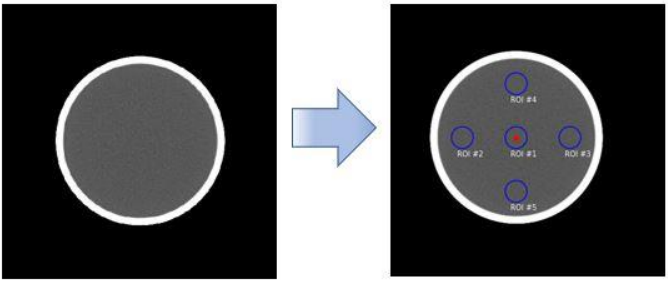

Noise power spectrum (NPS)

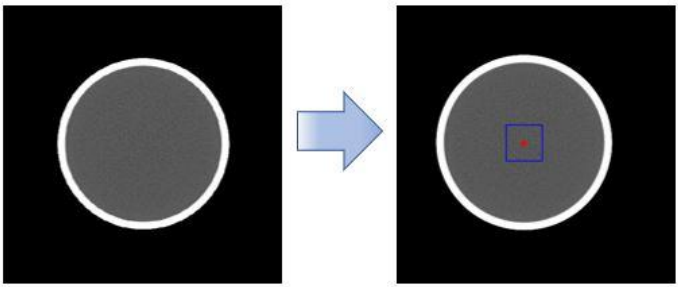

CT number linearity

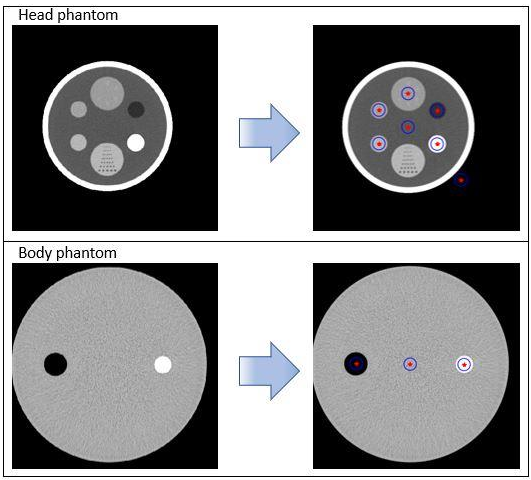

Spatial resolution
Visual resolution

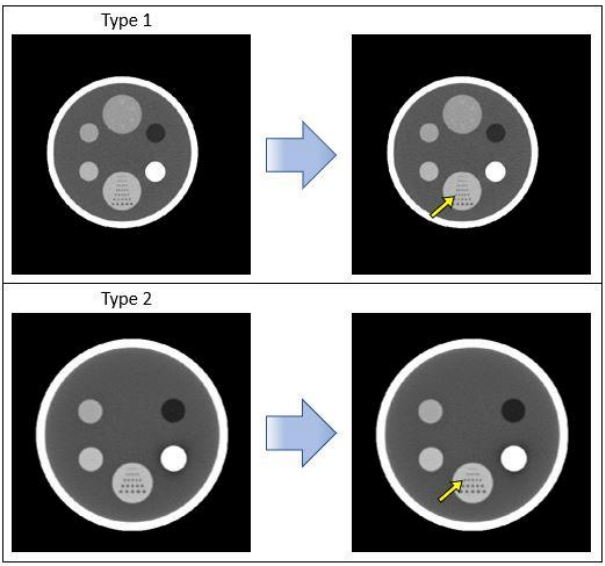

Point MTF

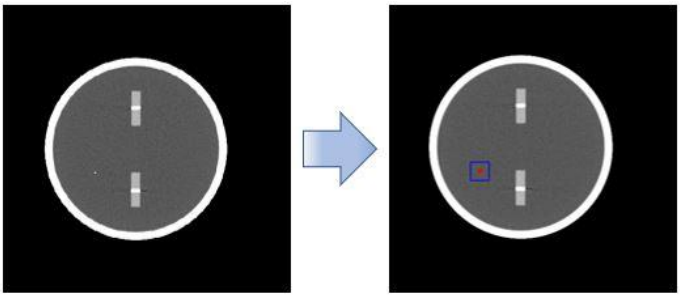

Edge MTF

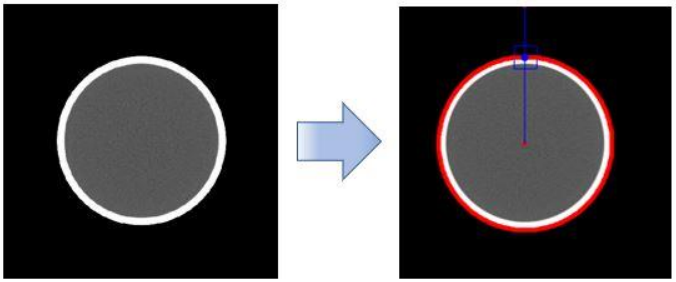

Task Transfer Function (TTF)

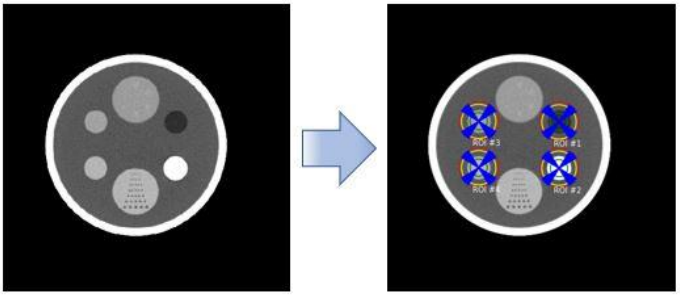

Slice thickness

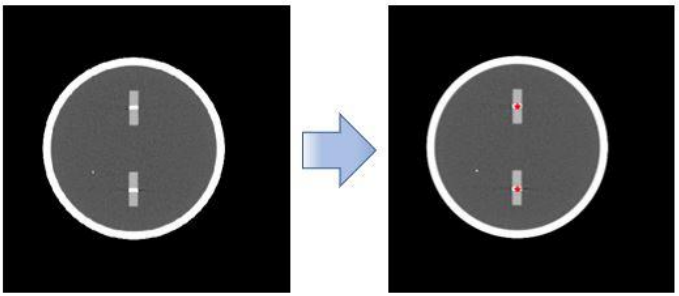

Low contrast
Smallest object

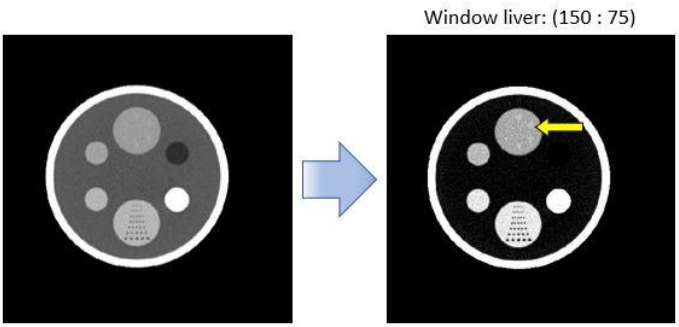

SD-LCD

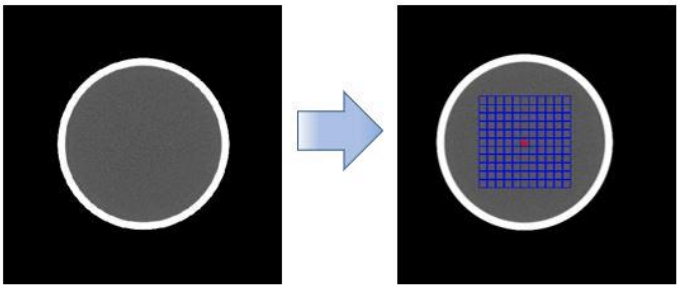

Alignment

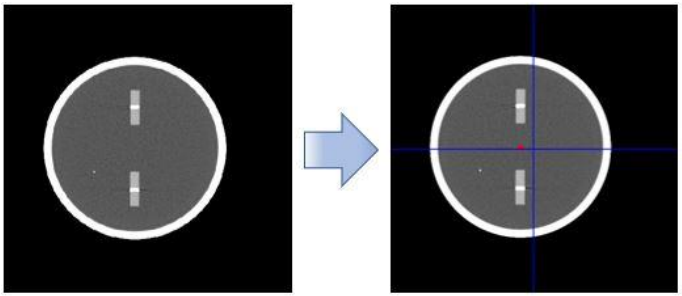

Gantry tilt

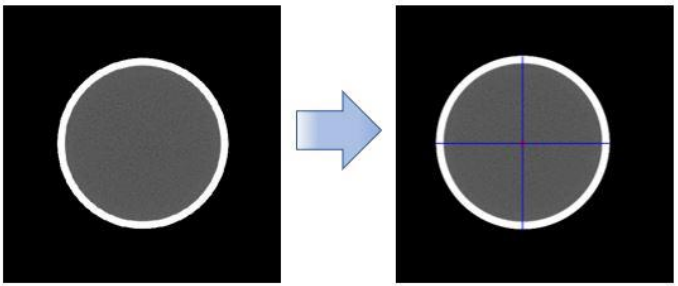

Diameter

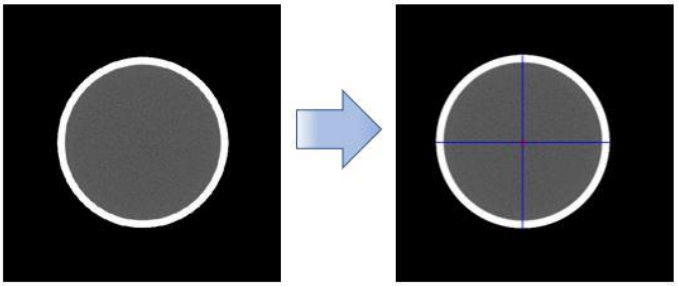

Distance between slices

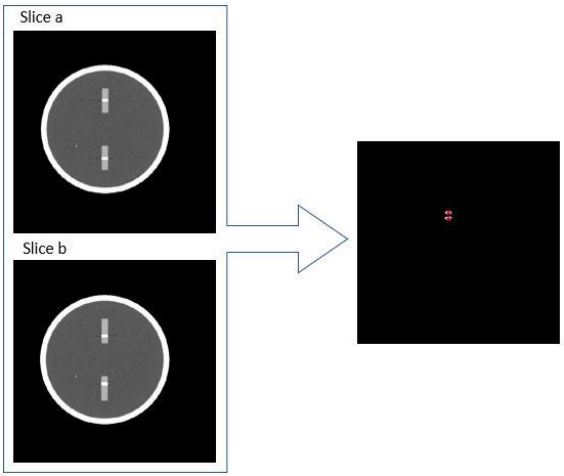

EXAMPLE MEASUREMENTS ON NEUSOFT PHANTOM

CT number accuracy

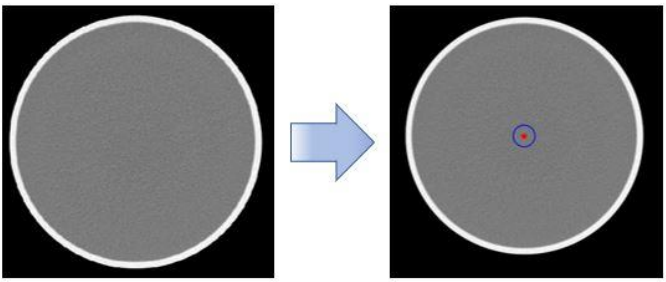

CT number uniformity

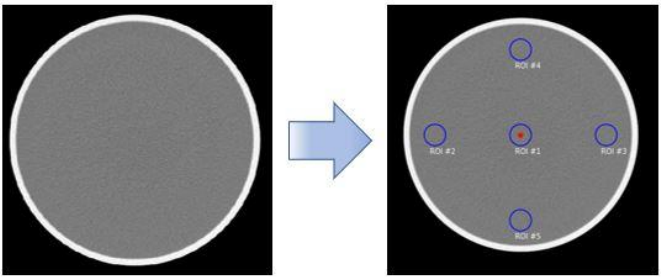

CT number homogeneity

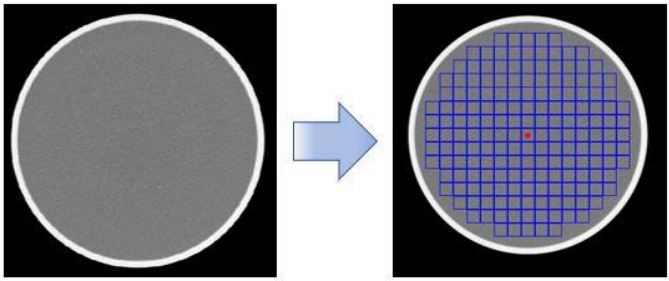

CT number histogram

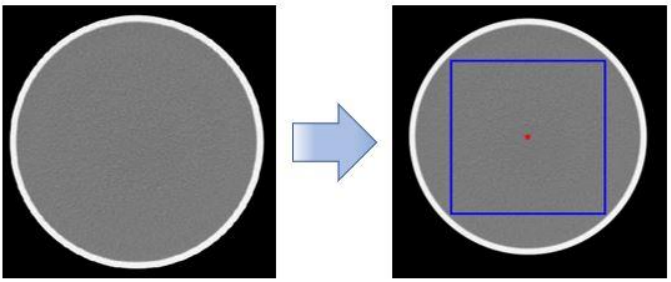

CT number profile

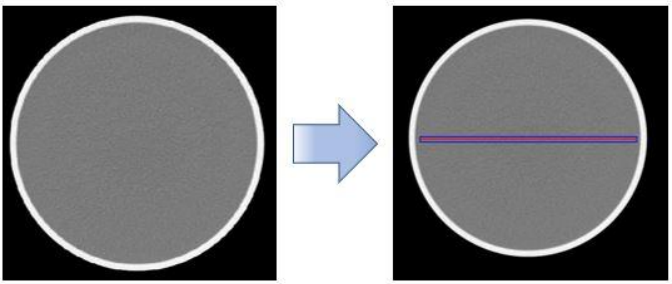

Noise accuracy

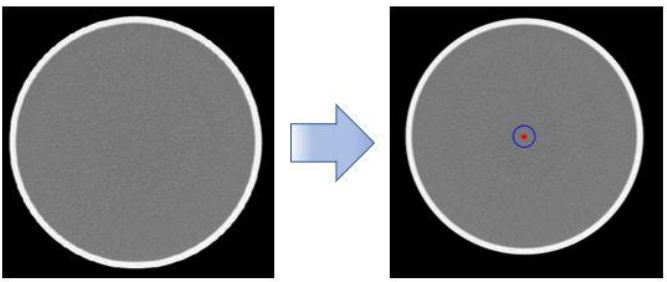

Noise uniformity

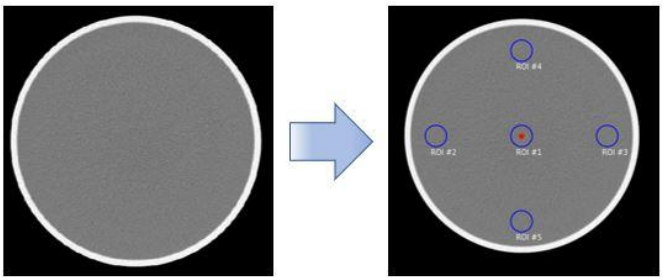

Noise Power Spectrum (NPS)

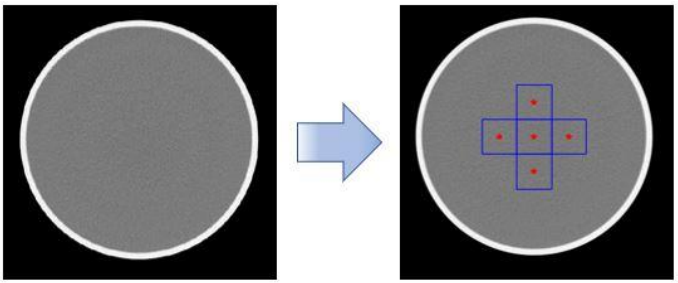

CT number linearity

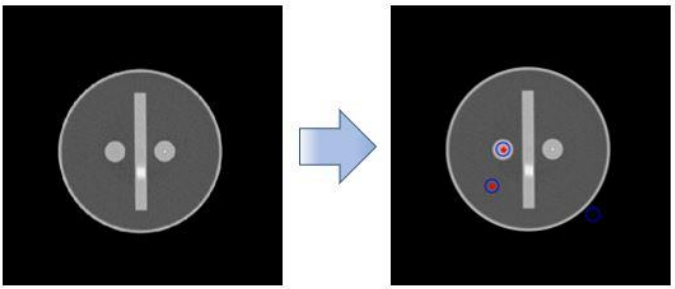

Spatial resolution

Point MTF

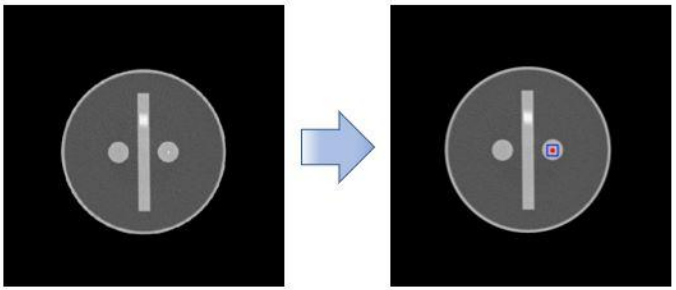

Edge MTF

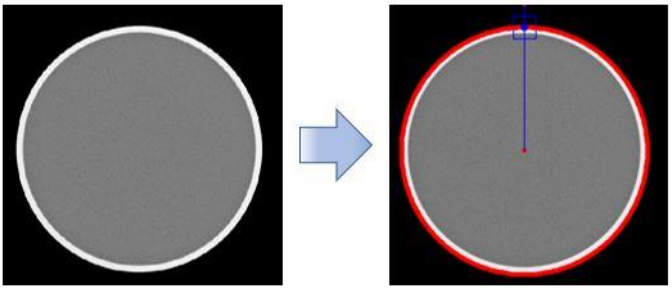

Slice thickness

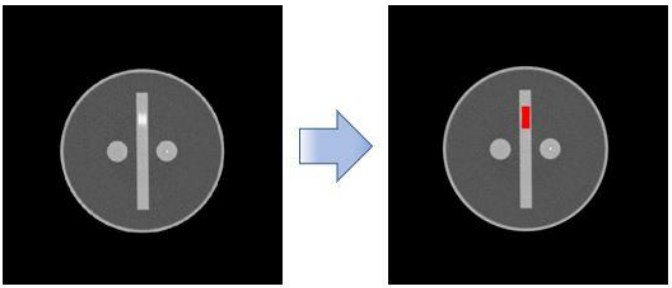

Low contrast
CNR

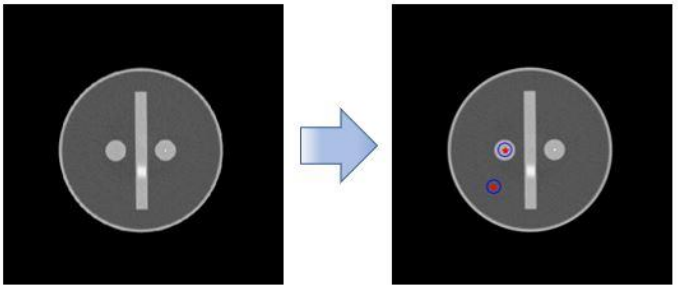

SD-LCD

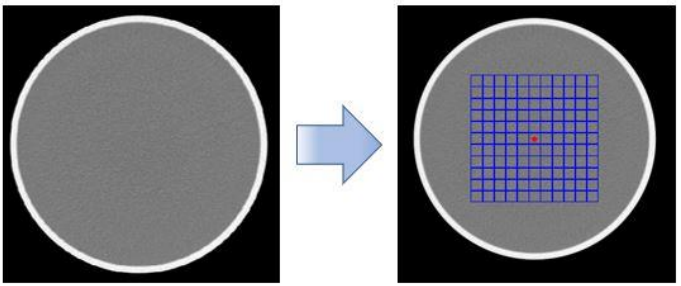

Alignment

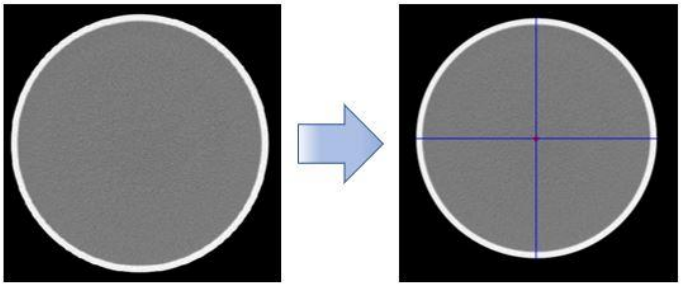

Gantry tilt

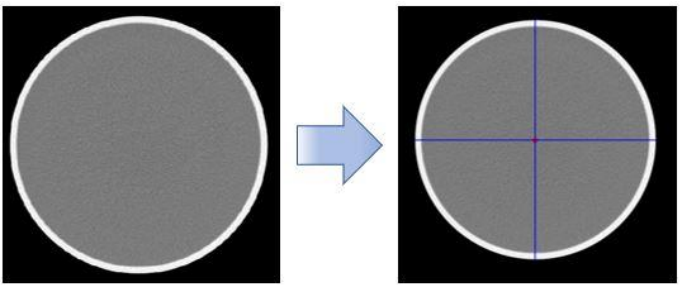

Diameter

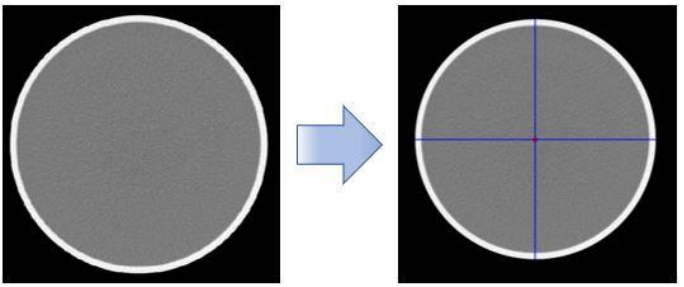

Distance between slices

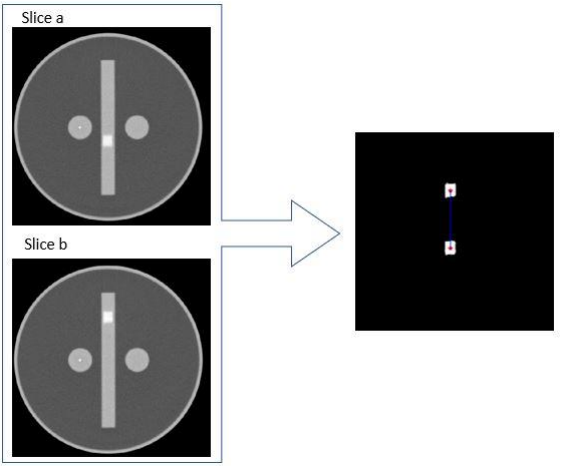

EXAMPLE MEASUREMENTS ON HITACHI PHANTOM

CT number accuracy

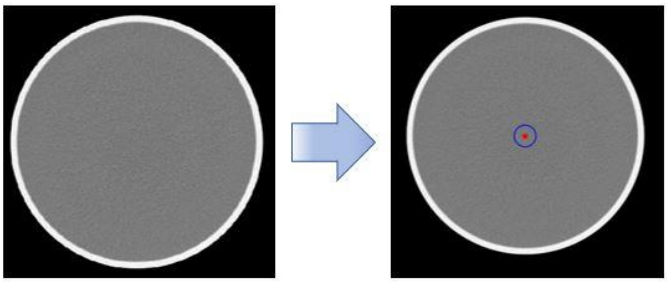

CT number uniformity

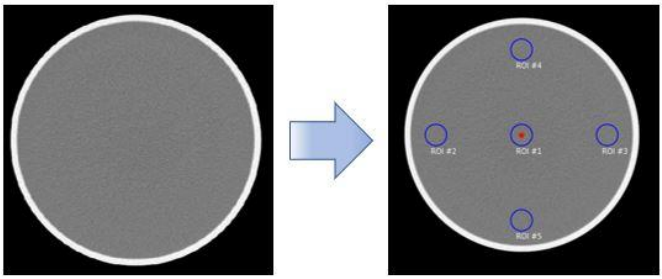

CT number homogeneity

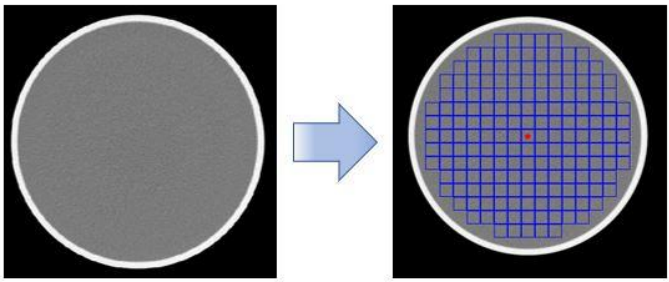

CT number histogram

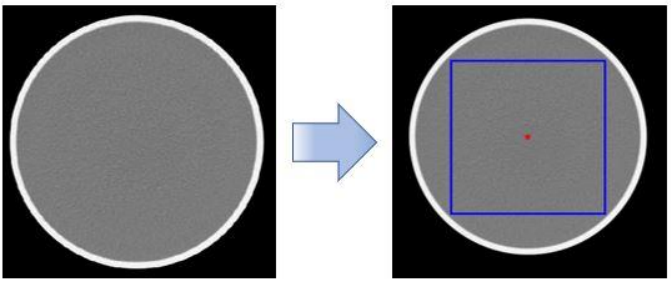

CT number profile

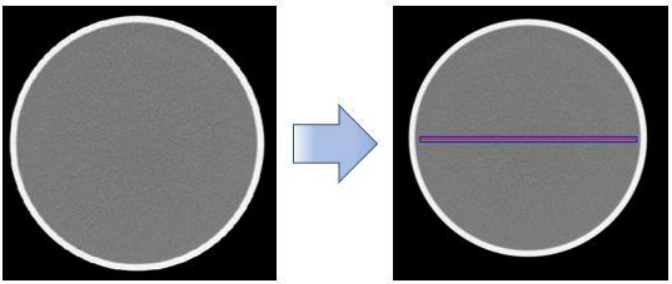

Noise accuracy

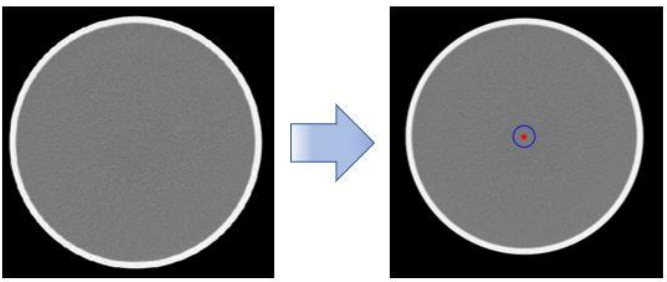

Noise uniformity

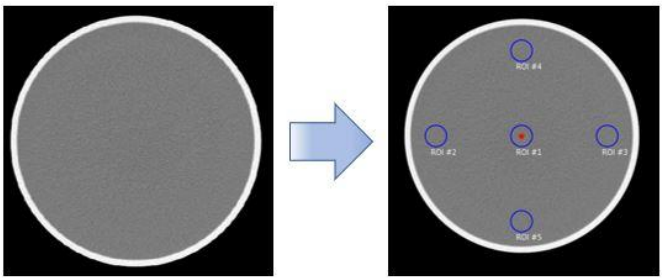

Noise Power Spectrum (NPS)

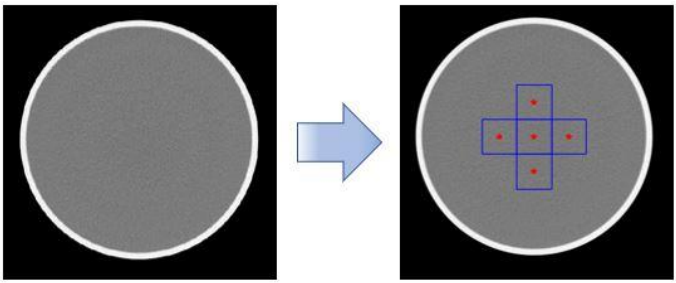

CT number linearity

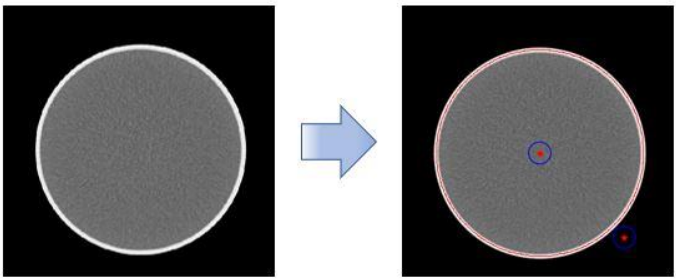

Spatial resolution
Edge MTF

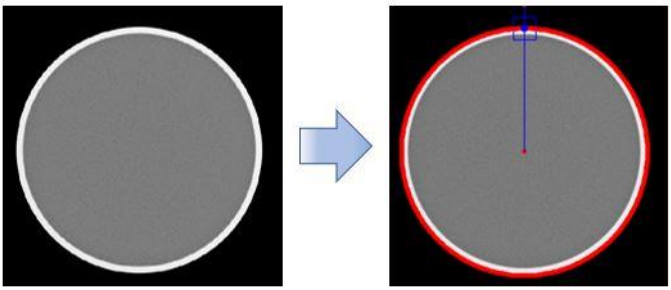

Low contrast
CNR

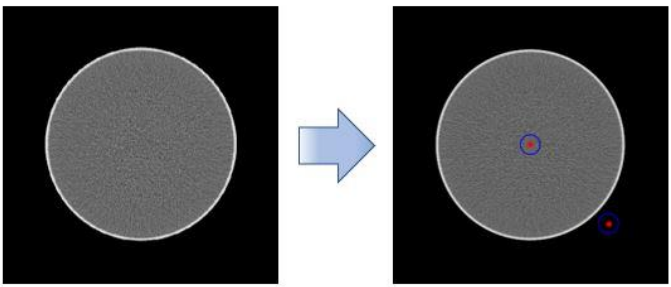

SD-LCD

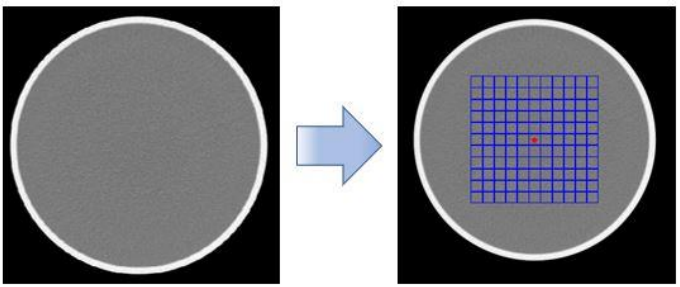

Alignment

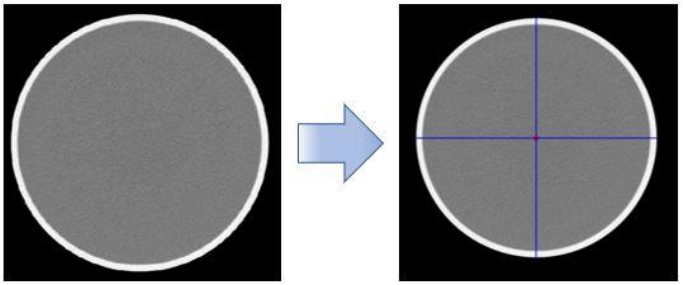

Gantry tilt

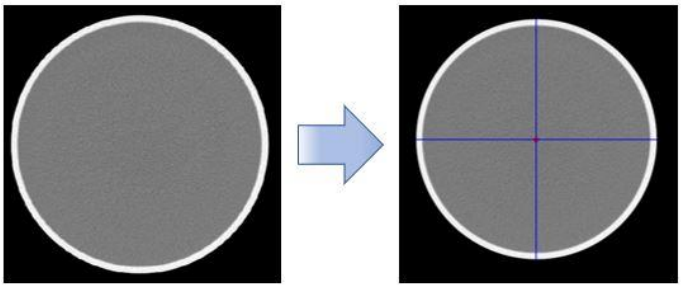

Diameter

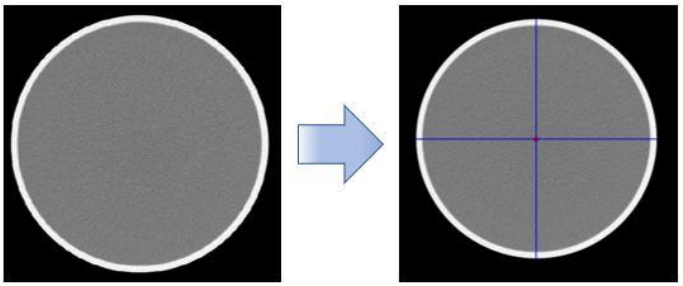

EXAMPLE MEASUREMENTS ON COMPUTATIONAL PHANTOM

CT number accuracy

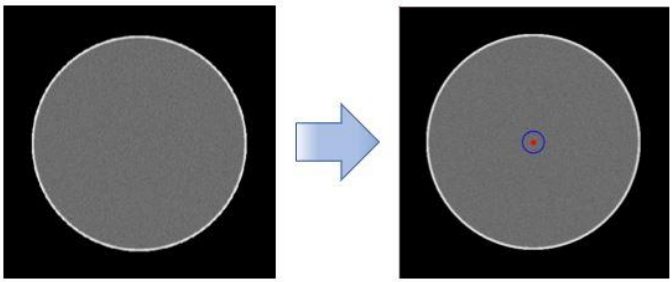

CT number uniformity

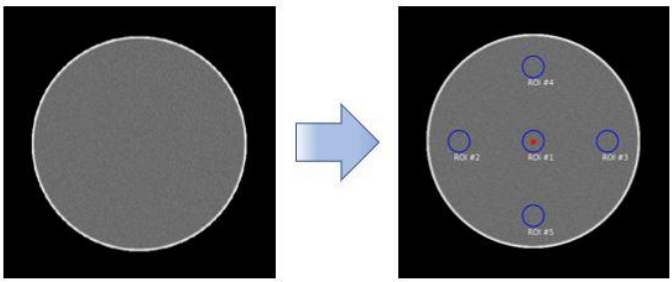

CT number homogeneity

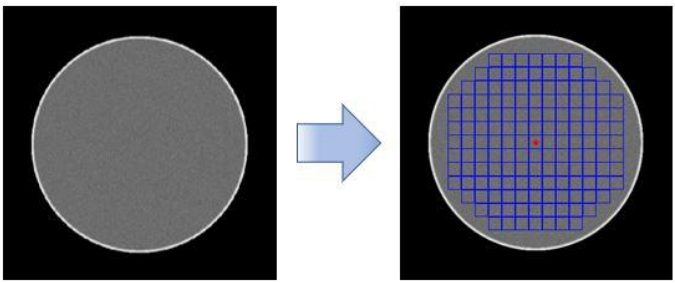

CT number histogram

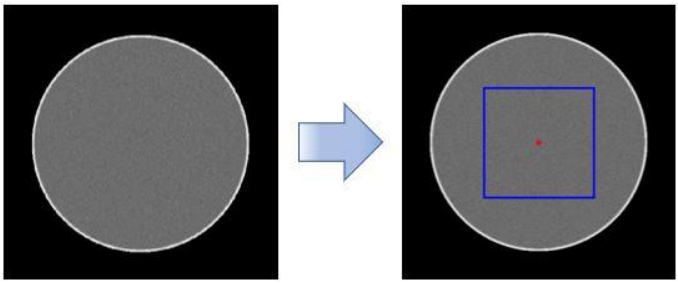

CT number profile

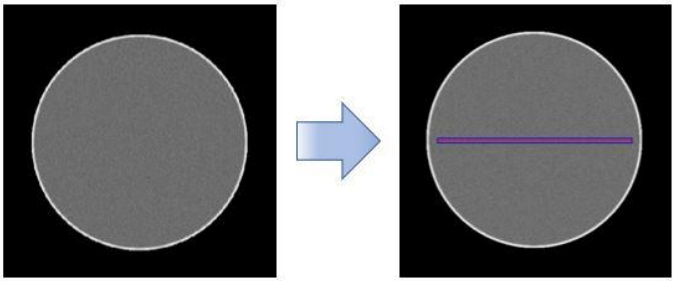

Noise accuracy

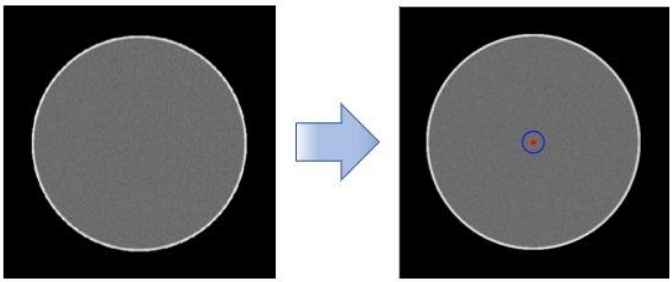

Noise uniformity

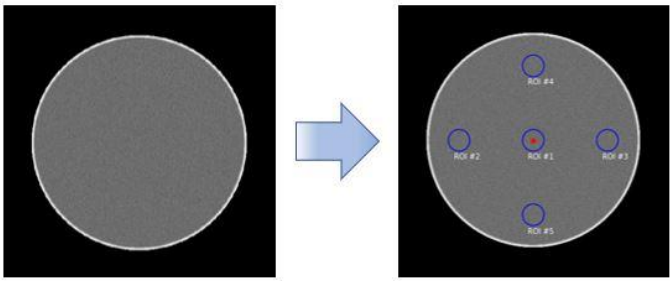

Noise Power Spectrum (NPS)

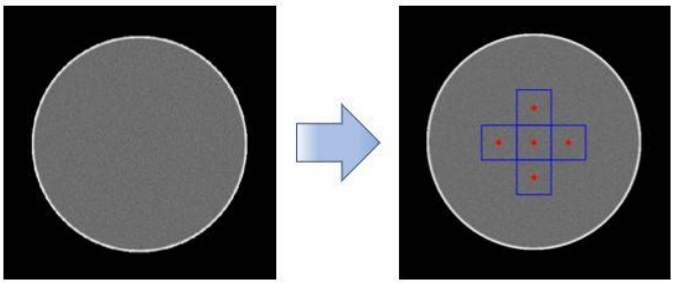

Spatial resolution
Point MTF

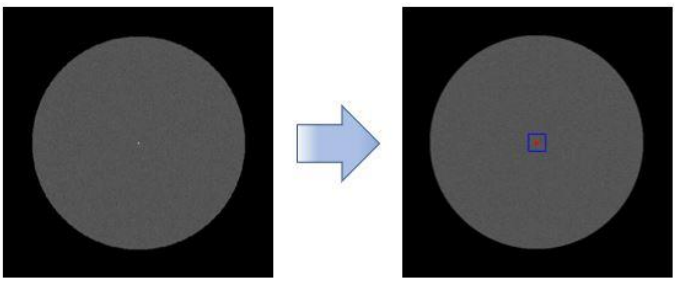

Edge MTF

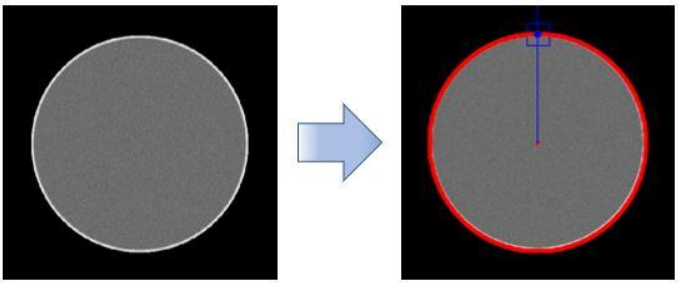

Low contrast
SD-LCD

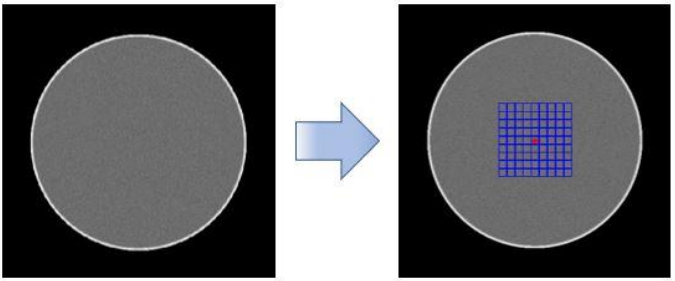

Alignment

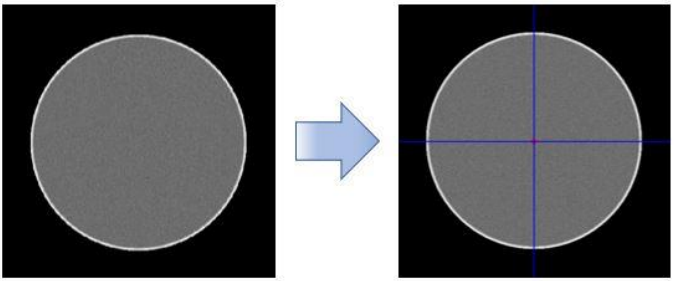

Gantry tilt

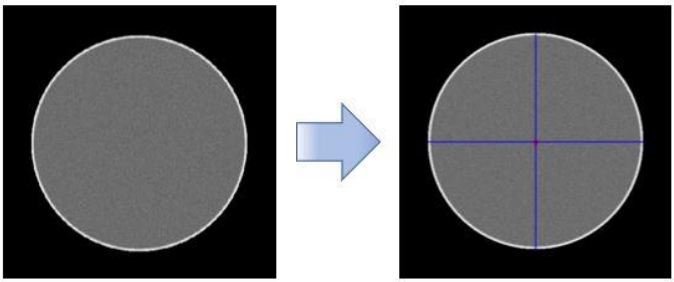

Diameter

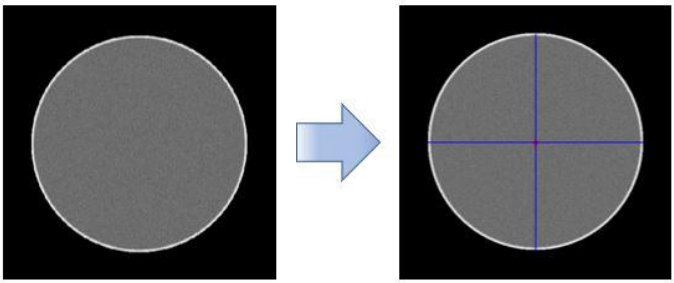

EXAMPLE MEASUREMENTS
ON ANTHROPOMORPHIC PHANTOM / PATIENT

CT number

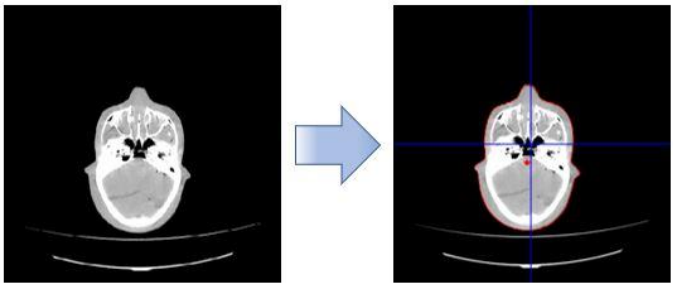

Noise

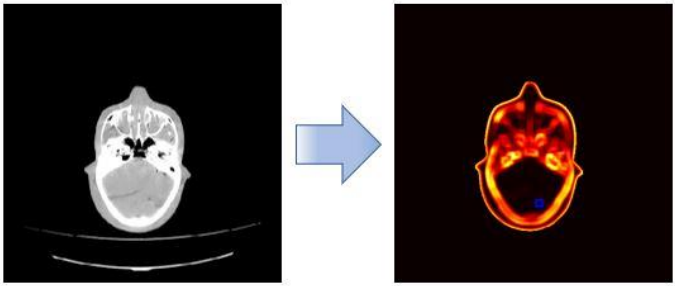

Low contrast

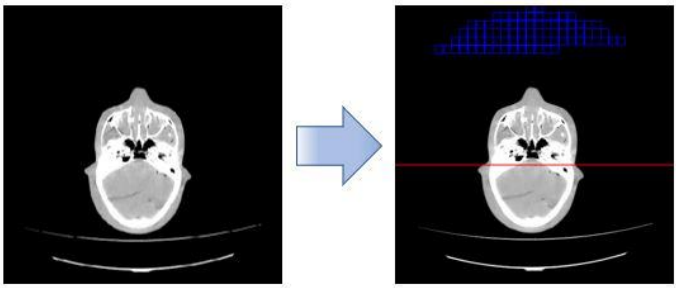

Alignment

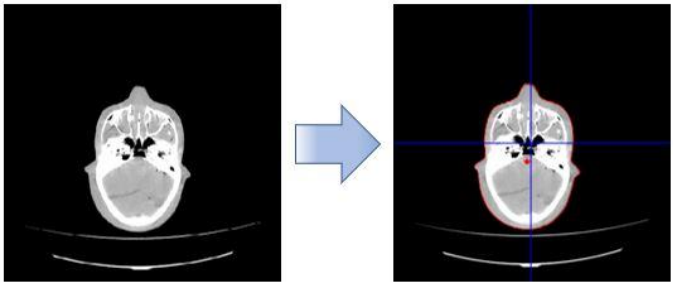

Diameter

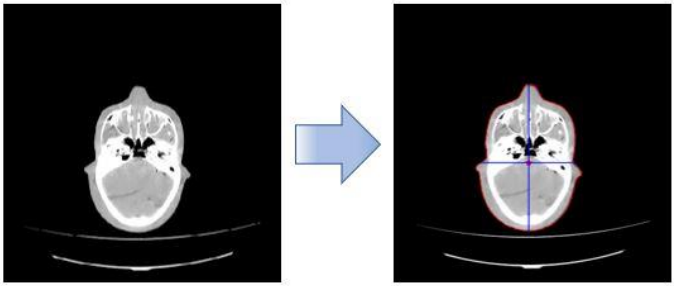

Author Biographies

Dr. Choirul Anam, M.Si completed his Ph.D in Physics Department, Bandung Institute of Technology (ITB) in 2018. He received Master degree from University of Indonesia (UI) in 2010 and the B.Sc degree in physics from Diponegoro University (UNDIP) in 2001. In 2016, he conducted research on Computed Tomography (CT) dosimetry at Kyushu University (KU). He is currently working as a lecturer and researcher in UNDIP. His research interests are medical image reconstruction, medical image processing, and dosimetry for diagnostic radiology, particularly in CT. He has authored and co-authored over 180 papers. In the last ten years, he was the first author over 50 papers in peer reviewed scientific journals. He is a reviewer in many reputable medical physics journals, such as Medical Physics (Med Phys), Physics in Medicine and Biology (PMB), Journal of Applied Clinical Medical Physics (JACMP), Physica Medica: European Journal of Medical Physics (EJMP), and so on. He is a member of the Editorial Board for Journal of Medical Physics and Biophysics (JMPB) and Journal of Physics and Its Application (JPA). One of his paper published in the Journal of Applied Clinical Medical Physics (JACMP) had been awarded as the Best Medical Imaging Physics Article in 2016. He received the Best Paper Award during 15th South East Asian Congress of Medical Physics (SEACOMP). He was also recognised as an Outstanding Reviewer for Physics in Medicine and Biology (PMB) in 2018 and for Biomedical Physics and Engineering Express (BPEX) in 2019. He was also awarded as the SEAFOMP Young Leader Awards 2019 for his contribution in CT

dosimetry and image quality from the South East Asian Federation of Organizations for Medical Physics (SEAFOMP). In 2022, he was 3rd Best Author in the Science and Engineering category of SINTA, at UNDIP. He is developer of two software, i.e. IndoseCT (A software for measuring and managing radiation dose of computed tomography for an individual patient) and IndoQCT (A software for measuring CT image quality). The software can be downloaded through the website of www.indosect.com. Anam is a member of Indonesian Association of Physicist in Medicine (AFISMI).

Ariij Naufal, M.Si was born in Brebes, June 24 1995. He completed his undergraduate in Physics Education, Faculty of Mathematics and Natural Sciences, Semarang State University (UNNES). He continued his Masters degree at the Department of Physics, Faculty of Science and Mathematics Diponegoro University (UNDIP) in the field of Medical Physics. While pursuing a master's degree, he investigated the use of the Kinect camera in determining the height and area of the patient on CT examination. The framework that he develop uses the MatLab programming language. This study has published two papers in reputable international journals. In 2021, he learn Python programming language to develop IndoQCT with Dr. Choirul Anam. While developing IndoQCT, he also led laboratory activities in the field of CT image quality research on quality control procedures. For about 1.5 years, he developed IndoQCT to its current version. Several articles in this research interest have been published in reputable journals.

Prof. Dr. Wahyu Setia Budi was born in Magelang on June 15, 1958. He is a professor of Radiation Physics and X-ray imaging in the Department of Physics, Faculty of Science and Mathematics, Diponegoro University. He completed his Bachelor of Physics at FMIPA Gadjah Mada University in 1983, Master of Optoelectrotechnics and Laser Applications at the University of Indonesia in 1992, and Doctor of Optoelectrotechnics and Laser Applications at the University of Indonesia in 1999. Together with Dr. Choirul Anam and Prof. Heri Sutanto, he has contributed a lot to medical physics research.

Prof. Dr. Heri Sutanto, M.Si was born in Pati, February 15, 1975. He studied for his Bachelor's degree at the Department of Physics, FMIPA-UNDIP (1992-1997), followed by his Masters degree at ITB (2000-2002) and Doctoral degree at the Physics Department of ITB (2003- 2008) in the field of Material Physics. Since 1998, he has been a lecturer at the Department of Physics, Diponegoro University, Semarang. After completing his doctoral degree, he founded the Smart Material Research Center (SMARC) UNDIP research group as well as becoming Chair of the SMARC UNDIP in 2008 with a focus on developing zinc oxide (ZnO) and Titania (TiO2) photocatalyst semiconductor materials. Various research findings on semiconductor materials have been successfully applied to waste treatment of synthetic and antibacterial dyes in water treatment and agriculture processes. Several research

results regarding ZnO and TiO2 have been registered as Patent No. P00201100715, S09201300330, and P00201406488. In mid-2017, he and his students started to conduct research on initial medical materials, namely boluses using silicone rubber (SR) material and in early 2018 using natural rubber (NR) material. The results of this research were published in the Scopus-indexed journal, Material Research Express. In addition to developing boluses, he and members of the SMARC UNDIP Medical Materials division team are developing SR-based X-ray protective materials with metal composite materials.

Dr. rer. nat. Freddy Haryanto, M.Si completed his undergraduate education at the Bandung Institute of Technology (ITB) in 1994, and continued his master's degree at the same campus in 1996. His doctoral education was taken at Eberhard Karls Universität Tübingen, Germany, and finished in 2003. His research field revolves around Monte Carlo-based simulation that is applied to many things, such as treatment planning systems and CT dosimetry. He has written more than 130 papers in reputable international journals. In 2021, together with Dr. Choirul Anam, he developed IndoseCT, software to calculate and manage CT doses in patients.

Prof. Geoff Dougherty graduated with First Class in Physics at Manchester University, did a post-baccalaureate teaching certificate at Leeds University, taught at a community college and then completed a PhD on DNA-

drug interactions at Keele University. This was followed by a post-doc period investigating closed-circular DNA at the Swiss Federal Institute of Technology, Zurich. He taught at the Science University of Malaysia; did research on DNA-drug binding using electron spin resonance at Monash University, Australia; and taught at the University of the South Pacific, Fiji and Oxford Brookes University. After that he moved to Kuwait as Professor of Radiologic Sciences (1992-2002). He moved to California in 2002, where he is currently Professor of Applied Physics and Medical Imaging. His research interests are integrative and interdisciplinary. He applies image analysis and pattern recognition techniques to medical images from a variety of modalities in an effort to extract the maximum quantifiable diagnostic and prognostic information from them. This has led him into work on osteoporosis, scoliosis, retinal diseases, breast cancer, arteriosclerosis, hepatocellular cancer, and even the removal of tattoos and unwanted hair by laser light. He has also written papers on CT, SPECT and MRI imaging. His three Fulbright experiences (two as Senior Scholar and one as a Specialist) have resulted in many new collaborations, including work on the automated measurement of CT dose, improved noise reduction and filtering strategies, and the automated classification of covid-19 images.

ISBN 978-623-417-106-8